Phylogeny and Evolution of *Lerista* (Lygosominae, Scincidae, Squamata)

Adam Skinner

A thesis submitted in fulfilment of the

requirements for the degree of

Doctor of Philosophy

Department of Environmental Biology

The University of Adelaide

November, 2007

This work contains no material that has been accepted for the award of any other degree or diploma in any university or other tertiary institution and, to the best of my knowledge and belief, contains no material previously published or written by another person, except where due reference has been made in the text.

I give consent to this copy of my thesis, when deposited in the University Library, being available for loan and photocopying.

Adam Skinner

November, 2007

Abstract

In this thesis, I investigate the phylogeny and evolution of *Lerista*, a clade of more than 75 species of scincid lizards, distributed in arid, semi-arid, and seasonally dry habitats throughout Australia. Among extant tetrapods, *Lerista* is exceptional in comprising a large number of closely-related species displaying prodigious variability of body form; several species possessing well-developed, pentadactyl limbs resemble typical non-fossorial scincids in body proportions, while many other species exhibit varying degrees of limb reduction and body elongation, including two that are highly elongate and entirely limbless. The extensive variation in limb morphology observed among species, incorporating at least 20 distinct phalangeal configurations, has prompted some authors to identify *Lerista* as the best available model for studying limb reduction in squamates. Nonetheless, lack of a well-resolved phylogeny has impeded investigation of the pattern and mode of limb reduction and loss within the clade. The primary goal of my research was to furnish a comprehensive phylogenetic hypothesis for *Lerista*, enabling more sophisticated study of the evolution of limb morphology and body form in this clade than has previously been possible.

A recent phylogenetic analysis of mitochondrial DNA sequences for a series of Australian *Sphenomorphus* group scincids (including two species of *Lerista*) recovered several well-supported, major clades, although these were generally separated by relatively short branches associated with low support values. Applying a recently described methodology for inferring lineage-level polytomies, I use ATP synthetase-β subunit intron sequences and the existing mitochondrial DNA data set (with sequences for additional taxa) to assess the hypothesis that the poorly resolved basal relationships within the Australian *Sphenomorphus* group are a consequence of the major clades having originated essentially simultaneously. Phylogenetic analyses of the separate mitochondrial DNA and intron sequence data reveal a number of congruent clades, however, the relationships among these

clades indicated by the two data sets are generally incongruent. Although this may be partly ascribed in to error in estimating phylogenetic relationships due to insufficient data, some incongruence is evident when uncertainty in inferred relationships is allowed for. Moreover, the congruent clades are typically separated by very short branches, several having a length insignificantly different from zero. These results suggest that initial diversification of Australian *Sphenomorphus* group scincids was rapid relative to the substitution rates of the mitochondrial DNA and intron fragments considered, if not essentially simultaneous.

The pattern and rate of limb reduction in *Lerista* are investigated, employing a nearly complete phylogeny inferred from nucleotide sequences for a nuclear intron and six mitochondrial genes. Ancestral digit configurations reconstructed assuming this phylogeny indicate at least ten independent reductions in the number of digits from a pentadactyl condition, including four independent losses of all digits, three from pentadactyl or tetradactyl conditions. At the highest rate, complete loss of digits from a pentadactyl condition is estimated to have occurred within no more than 3.6 million years. Patterns of digit loss for the manus and pes are consistent with selection for preserving hindlimb utility as the limbs are reduced, and suggest that intermediate digit configurations exhibited by extant species do not represent transitory stages in a continuing process of limb reduction. An increase in the relative length of the body is demonstrated to precede digit loss in lineages experiencing substantial reduction of the limbs, supporting the hypothesis that limb reduction and loss is a consequence of the adoption of lateral undulation as a significant locomotory mode. However, less extensive limb reduction may proceed in the absence of body elongation, perhaps due to a decrease in absolute body size. The exceptionally high frequency and rate of limb reduction in *Lerista* emphasise the potential for rapid and dramatic evolutionary transformation of body form in squamates.

The substantial divergence of relative limb and body length evident within *Lerista* is more readily explained by the correlated progression model of phenotypic transformation than

the independent blocks model. At each step in the attainment of a limb-reduced, elongate body form, alterations to the relative length of the limbs are accompanied by changes in relative snout-vent length (or vice versa) enabling the maintenance of locomotory ability. Nonetheless, some dissociation of hindlimb reduction and body elongation is possible, emphasising the potentially variable intensity of functional constraints and, accordingly, that the independent blocks model and correlated progression are extremes of a continuum of models (each invoking a different degree of functional integration) and do not describe discrete categories of phenotypic change. An increase in the extent of seasonally dry and arid habitats coincident with the origination of *Lerista* would have facilitated limb reduction and body elongation by furnishing an environment conducive to the adoption of fossorial habits, however, trends toward a limbless, highly elongate body form may be attributed primarily to the very low probability of re-elaborating reduced limbs. Such asymmetry in the probabilities of possible phenotypic changes may be a significant cause of evolutionary trends resulting in the emergence of higher taxa.

Acknowledgements

The research presented in this thesis was conducted at the South Australian Museum under the supervision of Mike Lee and Mark Hutchinson, to whom I am extremely grateful for their advice, encouragement, and patience; I could not have hoped for better advisors. Paul Doughty and Brad Maryan (Western Australian Museum) kindly permitted access to tissues and specimens in their care. Matt Brandley, Steve Donnellan, Mark Hutchinson, Mike Lee, and Dan Rabosky provided thoughtful comments on one or more chapters. Many thanks to Andrew Hugall, Carolyn Kovach, Paul Oliver, and Kate Sanders for helpful discussion of my work and their own. And finally, a special thank you to Alison Fitch for her companionship and support over the past four years.

My research was supported financially by a grant from the Hermon Slade Foundation awarded to Mike Lee and Mark Hutchinson.

Table of Contents

Chapter 1

General Introduction

Phylogenetics has become an integral part of evolutionary biology, and is assuming an increasingly significant role in disciplines traditionally considered far removed from the study of evolution. As Felsenstein (1985) and others (e.g., Harvey and Pagel, 1991) have discussed, values for any heritable variable recorded for a set of species can not be regarded as statistically independent; closely-related species will typically exhibit more similar phenotypes than distantly-related species due to their more recent derivation from a shared ancestor. Consequently, attempts to elucidate the causes of evolutionary change by searching for statistically significant associations between variables have to allow for varying degrees of phylogenetic propinquity among species if they are to avoid potentially serious difficulties resulting from non-independence. Aside from their indispensable role in comparative evolutionary study, phylogenetic trees have been employed in testing macroevolutionary models of phenotypic change (e.g., Mooers *et al*., 1999), estimating rates of speciation and extinction (e.g., Harvey *et al*., 1994), inferring modes of speciation (e.g., Barraclough and Vogler, 2000), and reconstructing biogeographic histories (see Lomolino *et al*., 2006). Moreover, phylogenies have relatively recently proved an invaluable tool in such fields as community ecology (see Webb *et al*., 2002), conservation biology (see Purvis *et al*., 2005), and epidemiology (Harvey and Nee, 1994).

In this thesis, I investigate the phylogeny and evolution of *Lerista*, a clade of more than 75 species of scincid lizards, distributed in arid, semi-arid, and seasonally dry habitats throughout Australia (Greer, 1989; Cogger, 2000). Among extant tetrapods, *Lerista* is exceptional in comprising a large number of closely-related species displaying prodigious variability of body form; several species possessing well-developed, pentadactyl limbs resemble typical non-fossorial scincids in body proportions, while many other species exhibit

varying degrees of limb reduction and body elongation, including two that are highly elongate and entirely limbless (Greer, 1987, 1989, 1990a). The extensive variation in limb morphology observed among species, incorporating at least 20 distinct phalangeal configurations, has prompted some authors to identify *Lerista* as the best available model for studying limb reduction in squamates (Greer, 1987, 1990a; Greer *et al*., 1983). Nonetheless, lack of a well-resolved phylogeny has impeded investigation of the pattern and mode of limb reduction and loss within the clade. Thus, the primary goal of my research was to furnish a comprehensive phylogenetic hypothesis for *Lerista*, enabling more sophisticated study of the evolution of limb morphology and body form in this clade than has previously been possible.

The thesis consists of five chapters (including this introductory chapter). Chapter 2 presents a phylogenetic analysis of Australian *Sphenomorphus* group scincids; this analysis places *Lerista* within a broader phylogenetic context, minimally allowing the identification of suitable outgroup taxa for subsequent analyses. In Chapter 3, I employ a nearly complete phylogeny for *Lerista*, based on nucleotide sequences for a nuclear intron and six mitochondrial genes, to infer the pattern and rate of limb reduction within the clade and test the hypothesis, proposed by Gans (1975), that the reduction and loss of limbs in squamates is a consequence of the adoption of lateral undulation as a primary locomotory mode. A more thorough examination of phylogenetic relationships within *Lerista* is presented in Chapter 4. Finally, in Chapter 5, I evaluate the ability of two distinct macroevolutionary models to account for the substantial divergence of body form within *Lerista*. Hopefully, I have managed, in Chapters 3 and 5 particularly, to demonstrate at least some of the enormous potential phylogenetic methods have for advancing our knowledge of evolutionary patterns and processes.

All chapters were prepared such that they could be submitted for publication with minimal alteration. As a consequence, repetition of some material will be evident, particularly in the introductory sections; hopefully this does not seriously detract from the

cohesion of the thesis. Chapter 2 has recently been published in the Biological Journal of the Linnean Society, while a slightly modified version of Chapter 3 is presently being reviewed; both papers are cited elsewhere in the thesis as they would be if the chapters were published in the order they are presented (e.g., the published version of Chapter 2 [Skinner, 2007] is cited in Chapter 3, while the submitted version of Chapter 3 [Skinner *et al*., 2007] is cited in Chapter 4). This indirect cross-referencing of chapters, while perhaps awkward, reflects their preparation as prospective journal papers.

Chapter 2

Phylogenetic Relationships and Rate of Early Diversification of Australian *Sphenomorphus* Group Scincids

2.1. Introduction

Australian scincid lizards represent three major clades within the cosmopolitan Lygosominae, the *Egernia*, *Eugongylus*, and *Sphenomorphus* groups (Greer, 1979a). The *Sphenomorphus* group is the most speciose of these clades in Australia (*c*. 235 species), composing more than half of the Australian scincid fauna (Cogger, 2000). Moreover, Australian *Sphenomorphus* group scincids are morphologically and ecologically diverse, including diurnal and nocturnal, arboreal, terrestrial, and fossorial, and oviparous and viviparous species, exhibiting varying body sizes and degrees of body elongation and limb reduction. Although monophyly of the *Sphenomorphus* group is well supported by several morphological apomorphies (see Greer, 1979a) and recent phylogenetic analyses of mitochondrial DNA sequences (Honda *et al*., 2000; Reeder, 2003), evidence for monophyly of Australian *Sphenomorphus* group scincids has until recently been lacking. Reeder (2003) presented a combined analysis of mitochondrial 12S and 16S rRNA, and ND4 and adjacent tRNA sequences for a series of lygosomines, including representatives of all except one Australian *Sphenomorphus* group genus, indicating that the Australian *Sphenomorphus* group constitutes a clade. Nonetheless, as Reeder (2003) noted, few non-Australian *Sphenomorphus* group taxa were included in this analysis, so that further study incorporating additional material is needed to confirm this conclusion.

Phylogenetic relationships among Australian *Sphenomorphus* group scincids, as for those within the more inclusive *Sphenomorphus* group, have been the focus of few studies. Reeder's (2003) was the first comprehensive higher-level phylogeny for the Australian

Sphenomorphus group, prior phylogenetic hypotheses being limited to smaller, reputedly monophyletic groups of species (e.g., *Calyptotis* [Greer, 1983a]; *Anomalopus* [Greer and Cogger, 1985]). His analysis recovered several well-supported clades, many coinciding with genera and other putative monophyletic groups identified previously on the basis of morphology (e.g., *Anomalopus*, *Ctenotus*, *Lerista*, *Glaphyromorphus gracilipes* + *Hemiergis*). However, these clades are generally separated by relatively short branches associated with low support values and, accordingly, many basal relationships within the Australian *Sphenomorphus* group are poorly resolved.

Many authors observing relatively short, poorly-supported internal branches in molecular phylogenies have ascribed this pattern to very rapid or simultaneous origination of several lineages from an ancestral species in the history of the study clade (e.g., Kraus and Miyamoto, 1991; Helm-Bychowski and Cracraft, 1993; Lessa and Cook, 1998). Jackman *et al*. (1999) and Walsh *et al*. (1999) formalised such interpretations, describing and applying methods for distinguishing true (or 'hard') polytomies from those constituting artefacts of the data and analyses employed ('soft' polytomies; Maddison, 1989). These methods were intended as means for discovering lineage-level polytomies (the consequence of essentially simultaneous origination of more than two species from an ancestor) using phylogenies derived from analyses of nucleotide sequences for a single locus or combined data for multiple loci. As Slowinski (2001, p. 114) noted, however, inferences of lineage-level polytomies from such phylogenies 'are at best only weak'. This is a consequence of the potentially tenuous connection between the phylogeny of (population) lineages and that of alleles within those lineages. Polytomies in molecular phylogenies, even if they are 'hard' (and it is not evident that this is possible), may be observed where the pattern of relationship among lineages is strictly dichotomous if three or more alleles descended independently from a single ancestral allele and present in an ancestral lineage are maintained in separate descendant lineages (see Slowinski, 2001, his Fig. 1B). Slowinski (2001) outlined an alternative method for inferring lineage-level polytomies founded on the expectation that

under simultaneous separation of more than two population lineages, phylogenies for independent (i.e., unlinked) gene segments should be no more congruent than expected by chance (since alleles in the ancestral lineage are sorted randomly among the descendant lineages).

Recently, Poe and Chubb (2004) described a methodology for detecting lineage-level polytomies using multiple independent data sets, elaborating on the approach proposed by Slowinski (2001). Their methodology consists initially in testing two predictions for independent gene trees under the hypothesis of a lineage-level polytomy. Firstly, as noted by Slowinski (2001), relationships among lineages composing a polytomy should be no more congruent across such trees than chance expectation. Secondly, internal branches separating such lineages should be extremely short in all trees, indicating 'that speciation happened extremely rapidly' (Poe and Chubb, 2004, p. 406). Poe and Chubb (2004) presented a series of tests for detecting zero-length (i.e., extremely short) branches and non-random congruence in a set of molecular phylogenies. Assuming these predictions are confirmed, Poe and Chubb (2004) noted that several alternative hypotheses must be eliminated before accepting the presence of a lineage-level polytomy as a cogent explanation. These include insufficient data to resolve relatively short branches, taxonomic sampling artefacts (see Jackman *et al*., 1999), and use of genes that are evolving at unsuitable rates for inferring the relationships of concern (e.g., the value of mitochondrial genes for recovering ancient relationships may be limited by severe saturation). Following Poe and Chubb (2004), the sufficiency of the amount of available data for resolving short branches can be assessed by calculating the power of tests for zero-length branches, the effect of taxonomic sampling may be investigated by performing taxon subsampling experiments, and the usefulness of the genes employed may be assessed according to their ability to resolve relationships above and below the putative polytomy.

The poorly resolved basal relationships within the Australian *Sphenomorphus* group evident in Reeder's (2003) phylogeny might tentatively be explained by rapid diversification

early in the group's history. Nonetheless, testing this hypothesis requires data for genes that are independent of those Reeder (2003) employed. Here, I present a phylogenetic analysis of nuclear ATP synthetase-β subunit intron sequences for a selection of Australian *Sphenomorphus* group scincids, including nearly all species considered by Reeder (2003) plus several additional taxa. I also reanalyse Reeder's (2003) mitochondrial DNA data set, which has been expanded to include the additional species. Applying the methodology of Poe and Chubb (2004), I use the two independent data sets to evaluate the hypothesis that at least some of the major clades of Australian *Sphenomorphus* group scincids identified in Reeder's (2003) analysis (the support for which is reassessed considering the novel data) originated essentially simultaneously. An additional goal, peripheral (although not unrelated) to that of examining the phylogenetic relationships and rate of diversification of Australian *Sphenomorphus* group scincids, is to further investigate support for Australian *Sphenomorphus* group monophyly. Hence, I have included a limited number of non-Australian *Sphenomorphus* group scincids in the analyses not represented in Reeder's (2003) study.

2.2. Materials and Methods

2.2.1. Data and phylogenetic analyses

Fifty species of lygosomines, including all *Sphenomorphus* group scincids considered by Reeder (2003), an additional 21 *Sphenomorphus* group species, and four outgroup taxa, were included in the analyses (see Appendix 1). Additional Australian *Sphenomorphus* group species were selected on the basis that they allowed the monophyly of putative clades represented by single species in Reeder's (2003) analysis (e.g., *Calyptotis*, *Hemiergis*, the *Eulamprus quoyii* group) to be tested. As noted above (see Section 2.1), I also included additional non-Australian *Sphenomorphus* group taxa to further test the monophyly of the Australian *Sphenomorphus* group; these consisted of representatives of *Sphenomorphus* from New Guinea and *Papuascincus*. An attempt was made to acquire ATP synthestase-β subunit

intron sequences for the specimens in Reeder's (2003) data set where possible; otherwise, I selected specimens collected from localities as near as possible to those from which Reeder's (2003) specimens were collected. *Anomalopus mackayi* (one of the two species of *Anomalopus* represented in Reeder's [2003] data set) is absent from the intron data set, as material for this species was unavailable. *Egernia whitii*, *Eugongylus rufescens*, *Lamprolepis smaragdina*, and *Mabuya longicaudata* were employed as outgroup taxa based on Reeder (2003).

Total cellular DNA was extracted from liver using DNAzol (Life Technologies). ATP synthetase-β subunit intron and (for the additional taxa) mitochondrial 12S and 16S rRNA, and ND4 and adjacent tRNA-His, tRNA-Ser, and tRNA-Leu fragments were amplified by means of the polymerase chain reaction (PCR). Primer sequences and PCR conditions are presented in Table 2.1. PCR products were purified using UltraClean PCR clean-up columns (Mo Bio Laboratories) and sequenced using the ABI PRISM BigDye Terminator Cylce Sequencing Ready Reaction Kit and an ABI 3700 automated sequencer.

Alignment of ND4 sequences did not require the insertion of internal gaps and was straightforward. 12S and 16S rRNA, and tRNA sequences were initially aligned with Clustal X (Thompson *et al*., 1997) assuming the default pairwise and multiple alignment parameter values. Adjustments to alignments were made with the aid of secondary structure models (Wuyts *et al*., 2001, 2002; Macey and Verma, 1997). The exclusion of highly variable loop regions from the 12S and 16S rRNA alignments did not significantly alter tree topologies or posterior probabilities for nodes, and I present only those analyses including all sites. ATP synthetase-β subunit intron sequences were aligned with Clustal X using the default settings.

Bayesian phylogenetic analyses were performed for the mitochondrial and intron sequences separately and for the combined data using MrBayes (Ronquist and Huelsenbeck,

Table 2.1

Primers and PCR conditions.

Gene(s)	Primers	$MgCl_2$ $conc^n$ (mM)	Annealing temperature (°C)
12S rRNA	tPhe 5´-AAA GCA CRG CAC TGA AGA TGC-3´ (Wiens *et al*., 1999) 12e 5´-GTR CGC TTA CCW TGT TAC GAC T-3´ (Wiens et al., 1999)	2	48
16S rRNA	16aR2 5´-CCC GMC TGT TTA CCA AAA ACA-3´ (Reeder, 2003) 16d 5´-CTC CGG TCT GAA CTC AGA TCA CGT AG-3´ (Reeder, 1995)	2	50
ND4, tRNA-His, tRNA-Ser, tRNA-Leu	ND4 5´-TGA CTA CCA AAA GCT CAT GTA GAA GC-3´ (Forstner *et al*., 1995) M246 5´-TTT TAC TTG GAT TTG CAC CA-3´ (Skinner *et al*., 2005)	4	55
	ND4 5´-CAC CTA TGA CTA CCA AAA GCT CAT GTA GAA GC-3´ (Arévalo et al., 1994) M541 5´-CCA GGG AAA GGA GTT AGC-3´	2	55-58
ATP synthetase-β subunit intron	ATPSβf1 5´-CGT GAG GGH AAY GAT TTH TAC CAT GAG ATG AT-3´ (Jarman *et al*., 2002) G613 5´-TCT GTC CAT AAA CTA GCG-3´	4	48

2003). For the mitochondrial and combined analyses, I partitioned the sequence data according to locus and (for ND4 sequences) codon position (the tRNAs were combined in a single partition due to their short length and functional similarity), specifying nucleotide substitution models for partitions separately. An appropriate substitution model for each partition was selected on the basis of hierarchical likelihood-ratio tests, performed using Modeltest (Posada and Crandall, 1998). For all tests, I assumed a tree topology derived from parsimony analysis of either the combined mitochondrial or intron sequences; the former topology (i.e., that derived from the combined mitochondrial sequences) was assumed in selecting models for the mitochondrial genes, whilst the latter was assumed in selecting a model for the intron. Parsimony analyses were implemented in PAUP* (Swofford, 1999), employing a heuristic search strategy with random stepwise sequence addition (100 replicates) and tree bisection and reconnection branch swapping (a limit of 10^6 rearrangements per addition sequence replicate was imposed for the analysis of intron sequences to reduce computation time). All Bayesian analyses consisted in running four incrementally-heated Markov chains (with the default temperature parameter value, 0.2), initiated with random starting trees and default priors, for 10^7 generations, sampling every 1000^{th} generation. The number of generations required to attain stationarity was estimated by examining cumulative posterior probabilities for clades, plotted using AWTY (Wilgenbusch *et al*., 2004). All trees sampled prior to attaining stationarity were discarded and the remaining trees used to compute posterior probabilities for clades present in the most probable tree (i.e., the topology with the highest frequency in the post-stationarity sample of trees).

2.2.2. Assessment of congruence and tests for zero-length branches

Considering the limited number of independent data sets (i.e., two) and the lack of a specific hypothesis identifying lineages putatively composing one or more polytomies, I employed a method of assessing congruence among gene trees differing from that of Poe and Chubb (2004), who compared the number of taxon bipartitions shared across a set of

independent gene trees with that observed for sets of trees generated according to a pure-birth Markov process (Poe and Chubb's gene trees contained single representatives of clades for which simultaneous origination had been proposed and, accordingly, only lineages involved in the putative polytomy). Adopting an approach similar to that described by Buckley *et al*. (2002; see also Reeder, 2003), I constructed 95% credible sets of unique trees for the two data sets from trees sampled after attaining stationarity in the Bayesian analyses and determined whether the most probable topology, or specific components of that topology (i.e., clades), for each data set were consistent with one or more trees of the credible set for the other data set; if so, any incongruence between the data sets was considered insignificant.

An approach similar to that described by Poe and Chubb (2004) was employed in testing for zero-length branches in the two independent gene trees (all tests were performed assuming the most probable topologies). Firstly, maximum likelihood branch lengths were calculated for each gene tree using PAUP*, assuming a nucleotide substitution model chosen on the basis of hierarchical likelihood-ratio tests as described above (for the intron data set, this was the same model employed in the Bayesian analysis, however, it was necessary to reselect a model for the mitochondrial DNA data set using the combined [i.e., unpartitioned] data, as PAUP* does not support mixed-model analyses). All model parameter values were optimised in calculating branch lengths. A likelihood-ratio test was then employed to identify internal branches having a length insignificantly different from zero. Each test consisted in collapsing the branch to be tested (i.e., setting its length to zero), recalculating maximum likelihood branch lengths for all (uncollapsed) branches in the tree (simultaneously optimising model parameter values), comparing the likelihoods for the trees with and without the branch collapsed, and assessing the significance of the difference in likelihoods assuming that, under the hypothesis that the branch has a length of zero, the likelihood-ratio test statistic exhibits a mixed chi-square distribution (this procedure and its implementation are described in detail by Slowinski, 2001).

As Poe and Chubb (2004) noted, the above approach is useful for assessing whether a gene tree includes zero-length branches, however, it does not allow the hypothesis of multiple zero-length branches to be tested (as only a single branch is collapsed in each likelihood-ratio test). Thus, following Poe and Chubb (2004), I performed a further series of likelihood-ratio tests to identify, for each gene tree, the largest set of branches that could be simultaneously collapsed without producing a significant decrease in likelihood. I began by collapsing all internal branches found to have a length insignificantly different from zero when considered alone (see above) and compared the likelihood of the resulting tree (with optimised branch lengths [i.e., for uncollapsed branches] and model parameter values) with that of the uncollapsed tree. If the likelihood of the collapsed tree was significantly lower than that of the uncollapsed tree, I rejected the hypothesis that all collapsed branches were of zero-length and repeated the test collapsing all except one of the initial set of collapsed branches (specifically, the branch producing the highest likelihood-ratio test statistic when collapsed alone). This procedure continued until an insignificant difference between the likelihoods of the collapsed and uncollapsed trees was observed, when it was concluded that all collapsed branches had a length indistinguishable from zero.

For the latter series of likelihood-ratio tests (i.e., those in which multiple branches were collapsed simultaneously), null distributions for the test statistic, which might be expected to deviate significantly from a chi-square distribution (see Goldman and Whelan, 2000; Poe and Chubb, 2004), were generated by simulation. For each test, I used Mesquite (Maddison and Maddison, 2003) to simulate 100 data sets (of the same size as the data set being considered) on the collapsed tree assuming maximum likelihood branch lengths (for uncollapsed branches) and model parameter values, and for each simulated data set calculated the likelihoods of the collapsed (i.e., null) and uncollapsed trees, optimising branch lengths (again, for uncollapsed branches) and parameter values. The difference between these likelihoods served as the test statistic. The proportion of data sets for which the test statistic exceeded the observed value (i.e., that for the actual data) was interpreted as the *P*-value for

the test, and the hypothesis that all collapsed branches were of zero-length was rejected where this was less than 0.05.

Adopting the approach of Poe and Chubb (2004), the sufficiency of the amount of available data for recovering short branches was evaluated by computing power curves for the likelihood-ratio tests for zero-length branches (specifically, those yielding the largest insignificant test statistic when multiple branches are collapsed). Power curves were generated by firstly simulating 100 data sets on trees with those branches that could be simultaneously collapsed (i.e., without a significant decrease in likelihood; see above) set to a length of zero, assuming maximum likelihood estimates for the remaining branch lengths and model parameter values. For each simulated data set, I calculated the likelihoods of the null tree (i.e., the tree on which the data were simulated) and a tree with unconstrained branch lengths. All model parameter values and unconstrained branch lengths were optimised in calculating likelihoods. The sixth largest difference between these likelihoods provided an estimate of the critical value for the test statistic employed in the likelihood-ratio tests accepting a probability of type I error of 0.05. I then simulated 100 data sets on each of a series of trees with those branches that could be simultaneously collapsed set to various lengths (all collapsable branches were assigned the same length in any particular tree), assuming maximum likelihood estimates for the remaining branch lengths and model parameter values. For each data set, the likelihoods of a tree with all branches that could be simultaneously collapsed set to a length of zero and a tree with unconstrained branch lengths were calculated, optimising branch lengths (where these were unconstrained) and model parameter values. The proportion of data sets for each imposed branch length for which the difference between these likelihoods (i.e., the test statistic for the likelihood-ratio tests) exceeded the critical value (see above) afforded an estimate of the probability of type II error from which I calculated power (i.e., the probability of rejecting the null hypothesis of zero-length branches assuming the constrained branches are of the imposed length). Power was

calculated for simulated data sets having the same number of sites as the aligned sequences and for data sets with 5000 sites.

2.3. Results

ATP synthetase-β subunit intron sequences could not be obtained for *Glaphyromorphus douglasi*, *Glaphyromorphus isolepis*, *Glaphyromorphus pardalis*, and *Scincella lateralis*. An initial alignment of intron sequences for the remaining available taxa was considered highly ambiguous, due primarily to substantial length differences between ingroup and outgroup sequences, so that sequences for the outgroup taxa were excluded from the data set before realigning those for the ingroup taxa. The numbers of aligned sites, variable sites, and unique site patterns for all partitions employed in the Bayesian analyses are presented in Table 2.2. Table 2.3 presents the selected nucleotide substitution model and model parameter estimates (means, with 95% credible intervals, of values sampled after attaining stationarity; see below) for each partition.

Due to the exclusion of ATP synthetase-β subunit intron sequences for the outgroup taxa, two nested sets of taxa were used in the Bayesian analyses. All taxa were included in the analysis of the mitochondrial DNA sequence data, the result of which afforded a basis for identifying a set of suitable outgroup taxa for the analysis of the pared intron data set. The latter set of taxa (i.e., those included in the intron data set) was also employed in the combined analysis (this analysis included mitochondrial DNA sequences for those taxa for which I was unable to obtain intron sequences; see above). An examination of cumulative posterior probabilities for nodes indicated that in all analyses, stationarity had been attained by 4×10^6 generations. Figures 2.1, 2.2, and 2.3 present the most probable trees, with posterior probabilities for clades, sampled after attaining stationarity in the analyses of the mitochondrial and intron sequence data and the combined data, respectively.

Table 2.2

Numbers of aligned sites, variable sites, and unique site patterns for partitions employed in the Bayesian analyses. 'Variable sites' and 'Unique site patterns' values for the 12S and 16S rRNA, ND4, and tRNAs partitions are for the mitochondrial DNA sequence analysis, with those for the combined analysis (which included fewer taxa; see text) in parentheses.

Partition	Aligned sites	Variable sites	Unique site patterns
12S rRNA	898	471 (439)	508 (481)
16S rRNA	544	228 (208)	255 (238)
ND4, 1st codon position	235	121 (109)	137 (126)
ND4, 2nd codon position	236	48 (41)	66 (60)
ND4, 3rd codon position	236	235 (234)	236 (236)
tRNAs	181	116 (107)	157 (153)
ATP synthetase-β subunit	646	290	406

Australian *Sphenomorphus* group monophyly is strongly supported by the mitochondrial DNA sequence data (Fig. 2.1). Among the non-Australian *Sphenomorphus* group scincids, the three included species of *Sphenomorphus* compose a well-supported clade, as do *Papuascincus* and *Prasinohaema virens*. *Notoscincus ornatus* is placed as the sister lineage to the remaining Australian *Sphenomorphus* group species, which compose a strongly-supported monophyletic group. *Anomalopus*, *Calyptotis*, *Ctenotus*, and *Lerista* constitute well-supported clades within this more restricted group. There is strong support for a clade including *Eremiascincus richardsonii* and species representing the *Glaphyromorphus isolepis* group (*G. douglasi*, *G. isolepis*, and *G. pardalis*), and for a clade containing *G. gracilipes* and species of *Hemiergis*. The remaining species of *Glaphyromorphus*

Table 2.3

Selected nucleotide substitution model and parameter estimates (mean values followed by 95% credible intervals in parentheses) for partitions employed in the Bayesian analyses (parameter estimate values for the 12S and 16S rRNA, ND4, and tRNAs partitions are for the mitochondrial DNA sequence analysis).

Model selected

12S rRNA	GTR + I + Γ
16S rRNA	GTR + I + Γ
ND4, 1st codon position	GTR + Γ
ND4, 2nd codon position	GTR + I + Γ
ND4, 3rd codon position	GTR + Γ
tRNAs	K80 + Γ
ATP synthetase-β subunit	HKY85 + Γ

Parameter estimates

Nucleotide frequencies

	π_A	π_C	π_G	π_T
12S rRNA	0.401 (0.376-0.427)	0.272 (0.250-0.295)	0.135 (0.117-0.153)	0.192 (0.175-0.210)
16S rRNA	0.396 (0.358-0.432)	0.281 (0.254-0.309)	0.153 (0.126-0.181)	0.170 (0.149-0.196)
ND4, 1st codon position	0.426 (0.376-0.475)	0.340 (0.297-0.384)	0.141 (0.112-0.174)	0.093 (0.080-0.107)
ND4, 2nd codon position	0.157 (0.114-0.205)	0.320 (0.267-0.372)	0.130 (0.092-0.173)	0.393 (0.338-0.450)
ND4, 3rd codon position	0.365 (0.318-0.414)	0.389 (0.345-0.434)	0.056 (0.047-0.065)	0.191 (0.167-0.216)
tRNAs	Equal nucleotide frequencies			
ATP synthetase-β subunit	0.288 (0.262-0.315)	0.149 (0.192-0.239)	0.215 (0.192-0.239)	0.349 (0.320-0.376)

Substitution rates

	A↔C	A↔G	A↔T	C↔G	C↔T
12S rRNA	2.484 (1.395-4.116)	11.053 (6.733-17.833)	2.731 (1.545-4.629)	0.473 (0.135-1.071)	20.647 (11.996-34.001)
16S rRNA	1.885 (0.823-3.896)	5.203 (2.586-10.085)	3.071 (1.443-6.163)	0.187 (0.014-0.599)	25.479 (11.396-48.973)
ND4, 1st codon position	0.032 (0.011-0.087)	1.047 (0.649-1.679)	0.983 (0.524-1.740)	0.021 (0.010-0.054)	12.082 (7.159-19.923)
ND4, 2nd codon position	6.393 (0.723-17.916)	16.700 (1.982-49.043)	0.712 (0.013-3.286)	4.822 (0.455-15.818)	48.329 (11.045-96.276)
ND4, 3rd codon position	1.555 (0.472-6.170)	19.799 (5.664-80.798)	1.969 (0.518-8.219)	1.370 (0.058-6.187)	9.414 (2.870-36.756)
tRNAs			κ = 9.676 (7.757-11.954)		
ATP synthetase-β subunit			κ = 3.619 (2.977-4.345)		

Among-site rate heterogeneity

	I	α
12S rRNA	0.367 (0.326-0.404)	0.547 (0.488-0.607)
16S rRNA	0.403 (0.345-0.467)	0.399 (0.338-0.477)
ND4, 1st codon position	-	0.282 (0.246-0.320)
ND4, 2nd codon position	0.625 (0.497-0.704)	0.222 (0.122-0.266)
ND4, 3rd codon position	-	1.160 (0.879-1.525)
tRNAs	-	0.360 (0.301-0.427)
ATP synthetase-β subunit	-	1.794 (1.186-2.799)

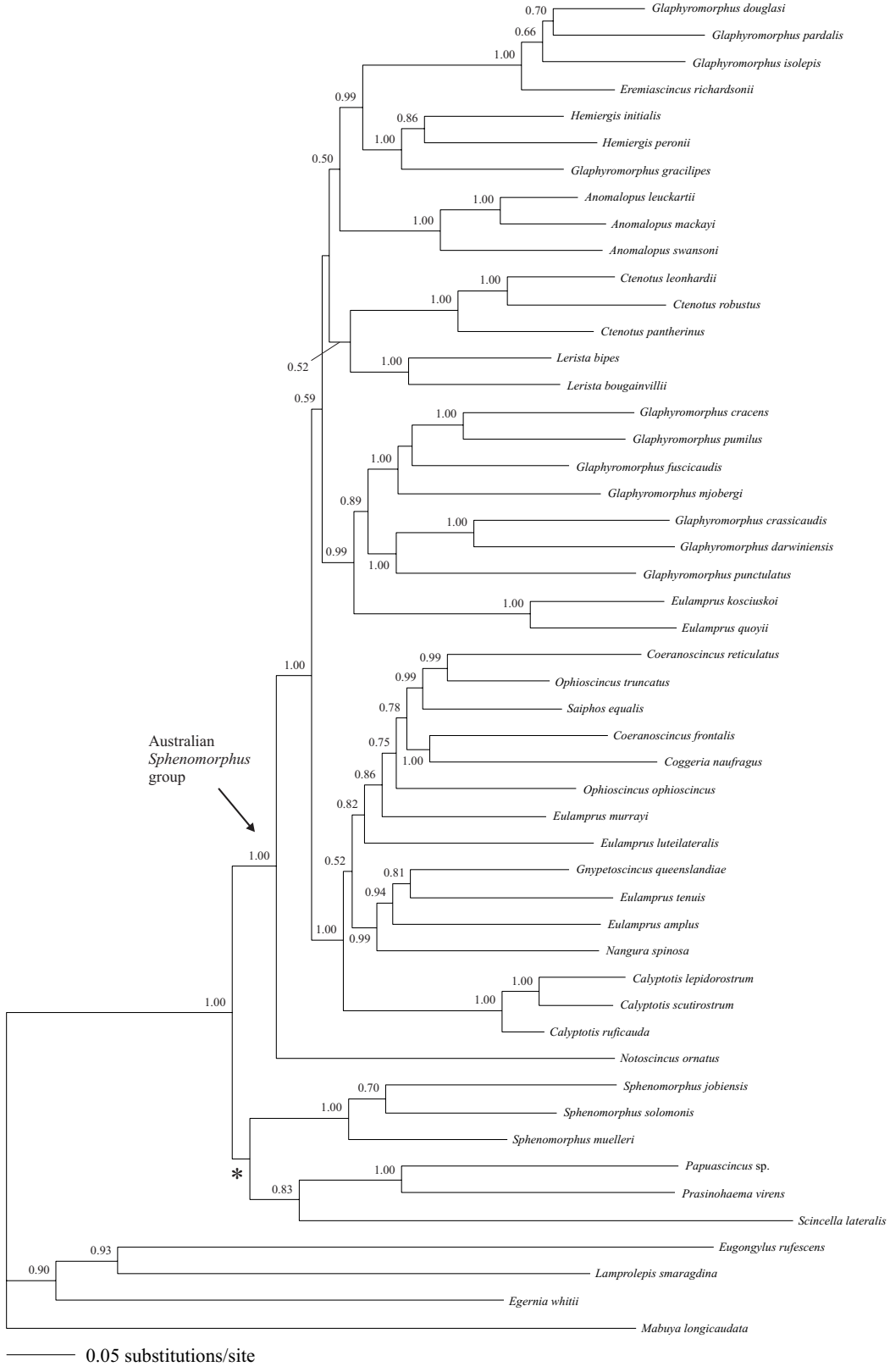

Figure 2.1. Most probable tree for the mitochondrial DNA sequence data with maximum likelihood branch lengths. Branches that can be collapsed without producing a significant decrease in likelihood are marked with an asterisk. Posterior probabilities ≥0.50 are shown adjacent to nodes.

Figure 2.2. Most probable tree for the ATP synthetase-β subunit intron sequence data with maximum likelihood branch lengths. Branches that can be simultaneously collapsed without producing a significant decrease in likelihood are marked with an asterisk. Note that several (unmarked) branches have a maximum likelihood length of zero. Posterior probabilities ≥0.50 are shown adjacent to nodes.

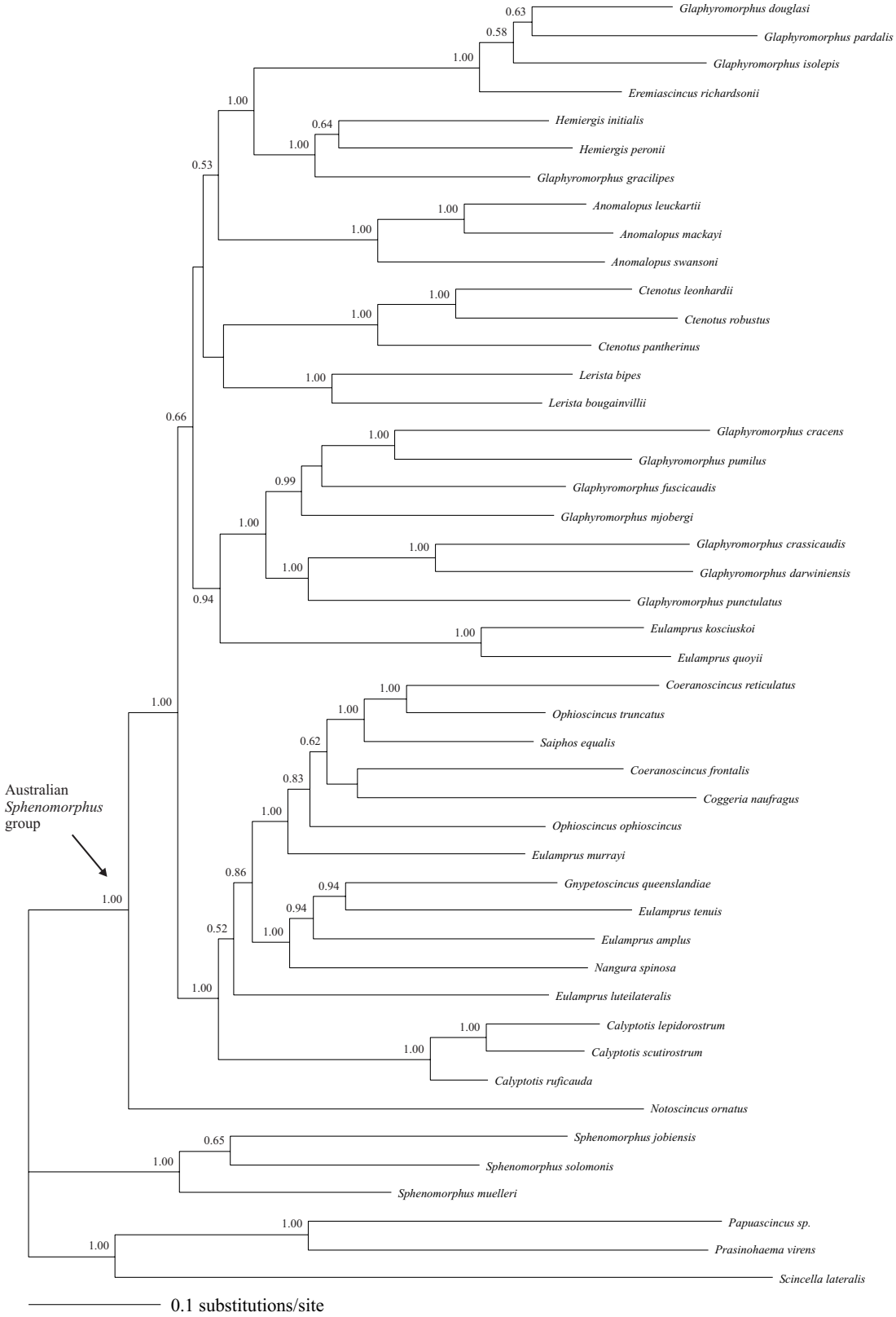

Figure 2.3. Most probable tree for the combined mitochondrial DNA and ATP synthetase-β subunit intron sequence data with mean branch lengths (derived from the post-stationarity sample of trees). Posterior probabilities ≥0.50 are shown adjacent to nodes.

(*Glaphyromorphus cracens*, *Glaphyromorphus crassicaudis*, *Glaphyromorphus darwiniensis*, *Glaphyromorphus fuscicaudis*, *Glaphyromorphus mjobergi*, *Glaphyromorphus pumilus*, and *Glaphyromorphus punctulatus*) compose a clade (hereafter referred to as the *G. crassicaudis* group; see Section 2.4.1), however, this is poorly supported. The *E. quoyii* group (represented by *Eulamprus kosciuskoi* and *E. quoyii*) is strongly supported, as is a clade including *Eulamprus amplus*, *Eulamprus tenuis*, *Gnypetoscincus queenslandiae*, and *Nangura spinosa*. *Coeranoscincus reticulatus*, *Ophioscincus truncatus*, and *Saiphos equalis* compose a well-supported monophyletic group, and there is strong support for a sister group relationship between *Coeranoscincus frontalis* and *Coggeria naufragus*. A relatively large clade distributed in mesic eastern Australia and including *Calyptotis*, the *E. amplus* + *E. tenuis* + *Gnypetoscincus* + *Nangura*, *C. reticulatus* + *O. truncatus* + *Saiphos*, and *C. frontalis* + *Coggeria* clades, *Eulamprus luteilateralis*, *Eulamprus murrayi*, and *Ophioscincus ophioscincus* is strongly supported, as are sister group relationships between the *E. quoyii* group and the *G. crassicaudis* group, and the *Eremiascincus* + *G. isolepis* group and *G. gracilipes* + *Hemiergis* clades. The remaining relationships within the Australian *Sphenomorphus* group are predominantly weakly supported.

Papuascincus, *P. virens*, and the three species of *Sphenomorphus* were employed as outgroup taxa in the analysis of the ATP synthetase-β subunit intron sequences (Fig. 2.2). As for the mitochondrial DNA sequence data (see Fig. 2.1), the intron sequence data strongly support monophyly of *Anomalopus*, *Calyptotis*, *Ctenotus*, and *Lerista*. Additionally, the *E. quoyii* group, the *G. crassicaudis* group, and the *G. gracilipes* + *Hemiergis* and *C. reticulatus* + *O. truncatus* + *Saiphos* clades are well supported. There is strong support for a clade including *C. frontalis*, *E. amplus*, *E. murrayi*, *E. tenuis*, *Gnypetoscincus*, *Nangura*, and *O. ophioscincus*. The remaining relationships are generally poorly supported and incongruent with those inferred in the mitochondrial DNA sequence analysis (see Fig. 2.1), and the topology of the most probable tree (i.e., for the intron sequence data) is inconsistent with all trees of the 95% credible set for the mitochondrial DNA sequence data (and vice versa). A

number of relationships supported by the mitochondrial DNA sequence data, although conflicting with the most probable tree for the intron sequence data, appear in the 95% credible set of trees, however, this is not the case for several other relationships (Table 2.4).

The most probable tree for the combined analysis (Fig. 2.3; note that *S. lateralis*, for which I was unable to obtain ATP synthetase-β subunit intron sequences, but for which mitochondrial DNA sequences were available, was included as an outgroup taxon in this analysis) is similar to that for the mitochondrial DNA sequence data (as might be expected, considering the numbers of aligned and variable sites for the mitochondrial DNA and intron data sets; see Table 2.2). Posterior probabilities are generally higher than those in the most probable tree for the mitochondrial DNA sequence data (where these are lower than unity) for clades recovered in both the mitochondrial DNA and intron sequence analyses (e.g., the *G. crassicaudis* group), or in some cases are slightly lower where the topologies for the mitochondrial DNA and intron sequence data are incongruent (e.g., the sister group relationship of the *E. quoyii* group and the *G. crassicaudis* group). Interestingly, support for the sister group relationship between the *Eremiascincus* + *G. isolepis* group and *G. gracilipes* + *Hemiergis* clades is (slightly) higher in the most probable tree for the combined data than in that for the mitochondrial DNA sequence data, despite this relationship not being supported by the intron sequence data (however, see Table 2.4).

Accepting a probability of type I error of 0.05, with a Bonferroni correction for the number of tests performed (see Slowinski, 2001; Poe and Chubb, 2004), 14 of 44 internal ingroup branches in the most probable tree for the mitochondrial DNA sequence data have a maximum likelihood length insignificantly different from zero when considered independently (i.e., in the initial series of likelihood-ratio tests, in which a single branch was collapsed for each test; see Section 2.2.2). Nonetheless, simultaneously collapsing more than one of these branches produces a significant decrease in likelihood, so that (according to the criterion adopted here) only a single branch may be considered to have a length

Table 2.4

Assessment of congruence for selected clades (see text). Posterior probabilities are for the analysis in which the clade was recovered (see Figs 2.1 and 2.2). For clades recovered in the mitochondrial DNA sequence analysis, 'Number of consistent trees' is the number of trees of the 95% credible set for the ATP synthetase-β subunit intron sequence analysis in which the clade is present, and vice versa.

	Posterior probability	Number of consistent trees
Clades present in most probable tree for mitochondrial DNA sequence data (see Fig. 2.1)		
Australian *Sphenomorphus* group scincids excluding *Notoscincus ornatus*	1.00	143
Coeranoscincus frontalis + *Coggeria naufragus*	1.00	0
Eulamprus amplus + *E. tenuis* + *Gnypetoscincus* + *Nangura*	1.00	3822
Mesic eastern Australian clade	1.00	10
Eulamprus quoyii group + *Glaphyromorphus crassicaudis* group	0.99	58
Glaphyromorphus gracilipes + *Hemiergis* + *Eremiascincus* + *Glaphyromorphus isolepis* group	0.99	35
Coeranoscincus + *Coggeria* + *Ophioscincus* + *Saiphos* + *Eulamprus murrayi*	0.86	4
Coeranoscincus + *Coggeria* + *Ophioscincus* + *Saiphos* + *Eulamprus murrayi* + *E. luteilateralis*	0.82	0
Coeranoscincus + *Coggeria* + *Saiphos* + *Ophioscincus truncatus*	0.78	0
Coeranoscincus + *Coggeria* + *Ophioscincus* + *Saiphos*	0.75	0
Australian *Sphenomorphus* group scincids excluding *Notoscincus ornatus* and mesic eastern Australian clade	0.59	1
Ctenotus + *Lerista*	0.52	42
Mesic eastern Australian clade excluding *Calyptotis*	0.52	7
Anomalopus + *Glaphyromorphus gracilipes* + *Hemiergis* + *Eremiascincus* + *Glaphyromorphus isolepis* group	0.50	0
Clades present in most probable tree for ATP synthetase-β subunit intron sequence data (see Fig. 2.2)		
Eulamprus amplus + *E. murrayi* + *E. tenuis* + *Gnypetoscincus* + *Nangura* + *Coeranoscincus frontalis* + *Ophioscincus ophioscincus*	1.00	0

indistinguishable from zero (Fig. 2.1). A substantial proportion of internal ingroup branches (12 of 34) in the most probable tree for the ATP synthetase-β subunit intron sequence data

have a maximum likelihood length of zero (Fig. 2.2), while nine of the remaining 22 branches have a length insignificantly different from zero when considered alone. Two of these latter branches can be collapsed simultaneously without a significant reduction in likelihood and, accordingly, are regarded as having lengths indistinguishable from zero (Fig. 2.2).

As no zero-length branches were identified within the Australian *Sphenomorphus* group in the most probable tree for the mitochondrial DNA sequence data (see Fig. 2.1), power curves were generated only for the ATP synthetase-β subunit intron data set (Fig. 2.4). For the range of lengths estimated (by maximum likelihood) for those branches that could be simultaneously collapsed without producing a significant decrease in likelihood (0.00150-0.00186 substitutions per site), power varies approximately from 0.44 (calculated for a branch length of 0.001 substitutions per site) to 0.67 (calculated for a branch length of 0.002 substitutions per site) for simulated data sets of the same size as the aligned sequence data (i.e., 646 sites). These values are notably lower than for simulated data sets having 5000 sites, particularly for shorter branch lengths.

2.4. Discussion

2.4.1. Phylogenetic relationships

The phylogenetic analyses of the mitochondrial and ATP synthetase-β subunit intron data sets indicate several firm conclusions regarding the relationships of Australian *Sphenomorphus* group scincids. As Miyamoto and Fitch (1995; see also Swofford, 1991) have discussed, congruence among trees for data partitions that may be considered subject to substantially different modes or patterns of evolution due, for example, to differing phylogenetic histories (as may be the case for unlinked gene segments), nucleotide substitution rates, or functions, affords among the most cogent evidence for inferred phylogenetic relationships. Where such congruence is observed, the explanation of a shared underlying history may be far more probable than that of other causes (e.g., lineage sorting of

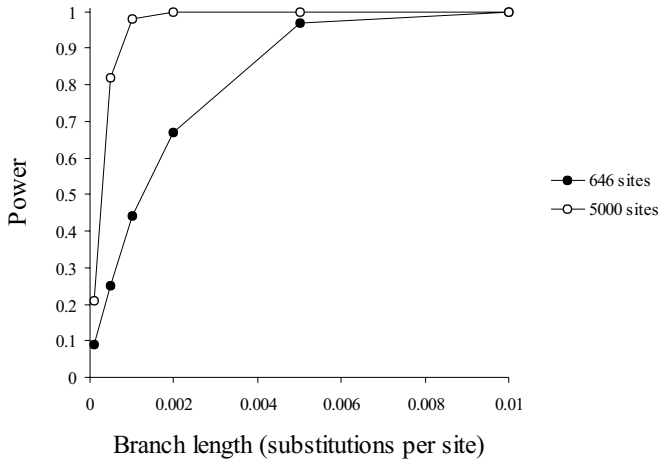

Figure 2.4. Power curves for the ATP synthetase-β subunit intron sequence data. Closed circles represent simulated data sets of the same size as the aligned sequence data (i.e., 646 sites); open circles represent simulated data sets having 5000 sites.

ancestral polymorphism, horizontal gene transfer, stochastic or systematic error in estimating phylogenetic relationships) independently producing similar topologies. Thus, there is considerable support for those clades recovered in both analyses, including *Anomalopus*, *Calyptotis*, *Ctenotus*, *Lerista*, the *E. quoyii* group, the *G. crassicaudis* group, and the *G. gracilipes* + *Hemiergis* and *C. reticulatus* + *O. truncatus* + *Saiphos* clades.

Greer and Cogger (1985) presented a list of morphological apomorphies diagnosing the seven species of *Anomalopus* (*Anomalopus brevicollis*, *Anomalopus gowi*, *Anomalopus leuckartii*, *A. mackayi*, *Anomalopus pluto*, *Anomalopus swansoni*, and *Anomalopus verreauxii*). Although they noted that many of these proposed apomorphies are presumably associated with fossorial habits and, accordingly, perhaps especially liable to convergence, their list included several 'not so obviously burrowing-associated features' (Greer and Cogger,

1985, p. 13). These character states, which include partial separation of the last two supraoculars by a supraciliary, seven or fewer premaxillary teeth, presence of an ectopterygoid process, and absence of a postorbital, are observed elsewhere within the Australian *Sphenomorphus* group (character states were polarised with respect to a hypothetical ancestral *Sphenomorphus* group scincid), however, Greer and Cogger (1985) considered at least the first as having potentially originated independently in the ancestor of the extant species of *Anomalopus*. Their conclusion that *Anomalopus* constitutes a monophyletic group is confirmed by Reeder's (2003) analysis and the analyses presented here. Additionally, the mitochondrial DNA sequence analysis (see Fig. 2.1) supports Greer and Cogger's (1985, p. 14) proposal that those species of *Anomalopus* possessing limbs (*A. leuckartii*, *A. mackayi*, and *A. verreauxii*) compose 'a distinct lineage'.

Calyptotis is presently considered to include five species (*Calyptotis lepidorostrum*, *Calyptotis ruficauda*, *Calyptotis scutirostrum*, *Calyptotis temporalis*, and *Calyptotis thorntonensis*) exhibiting a series of morphological character states considered by Greer (1983a) to be apomorphic within the *Sphenomorphus* group, including palatal rami of the pterygoids that are approximately triangular in shape and separated anteriorly by processes extending posteriorly from the palatines, four phalanges in the fourth toe of the manus, the postmental contacting only the first infralabial, a single loreal, and the fourth supralabial positioned below the eye. These shared character states, in conjunction with several other 'more difficult-to-interpret features' (Greer, 1983a, p. 30), similar ecological traits, and a nearly continuous distribution, prompted Greer (1983a) to propose that *Calyptotis* is a monophyletic group, a conclusion supported by my analyses. Greer (1983a) considered that *S. equalis* is the sister lineage of, or is perhaps nested within, *Calyptotis*, citing a number of shared, reputedly apomorphic character states as evidence for this relationship (including many of those regarded as supporting monophyly of *Calyptotis* mentioned above). However, Reeder (2003, p. 393), whose analysis failed to support a sister group relationship of *Calyptotis* and *Saiphos*, regarded a single loreal as 'the only potentially convincing

morphological apomorphy provided by Greer (1983a) for a *Calyptotis* + *Saiphos* clade'. The recovery of the *C. reticulatus* + *O. truncatus* + *Saiphos* clade in both the mitochondrial DNA and intron sequence analyses confirms Reeder's (2003) finding that *Calyptotis* and *Saiphos* are not sister taxa, although a sister group relationship between *Calyptotis* and this more inclusive clade (i.e., the *C. reticulatus* + *O. truncatus* + *Saiphos* clade) is consistent with a number of trees of the 95% credible set for the intron sequence data (but not the mitochondrial DNA sequence data).

The *C. reticulatus* + *O. truncatus* + *Saiphos* clade, aside from contradicting a sister group relationship of *Calptotis* and *Saiphos*, is inconsistent with monophyly of *Coeranoscincus* and *Ophioscincus*. Greer and Cogger (1985, p. 41) listed several putative morphological apomorphies diagnosing the two species of *Coeranoscincus* (*C. frontalis* and *C. reticulatus*), including four — large size, eight or fewer premaxillary teeth, pointed and recurved teeth, and medially separated palatal rami of the pterygoids — that 'are not necessarily associated with burrowing and therefore provide the primary reason for hypothesizing the monophyly of the group'. Similarly, they presented a list of reputedly apomorphic character states shared by the three species of *Ophioscincus* (*Ophioscincus cooloolensis*, *O. ophioscincus*, and *O. truncatus*), including at least one not evidently related to fossorial habits, specifically, squared off tooth crowns that are rotated slightly posteromedially and exhibit a distinct apical groove. Although the exact relationships of *C. frontalis*, *O. ophioscincus*, and the *C. reticulatus* + *O. truncatus* + *Saiphos* clade should perhaps be considered unresolved (considering the conflict between the mitochondrial and intron data sets; compare Figs 2.1 and 2.2, and see Table 2.4), my analyses indicate that at least some of these character states originated more than once in the history of Australian *Sphenomorphus* group scincids. Reeder's (2003) analysis, which did not include *O. truncatus*, supported a sister group relationship of *C. reticulatus* and *Saiphos*, a result he noted is corroborated by identical phalangeal formulas in these taxa (0.2.3.3.0 for both the manus and pes, shared only with *C. naufragus*, which is absent from Reeder's data set). Nonetheless, the

mitochondrial DNA and intron sequence data presented here indicate a sister group relationship of *C. reticulatus* and *O. truncatus* (while the phylogenetic position of *Coggeria* is uncertain), implying at least that this character state has been modified in *O. truncatus* (which lacks all elements distal to a single proximal carpal and a single proximal tarsal in the forelimb and hindlimb, respectively) or attained independently in *C. reticulatus* and *Saiphos*.

As intimated by Greer (1989, 1992) and demonstrated by Reeder (2003), *Eulamprus* and *Glaphyromorphus* do not constitute monophyletic groups. Greer (1989) divided *Eulamprus* into three species groups, the *E. murrayi* group (including *E. luteilateralis*, *E. murrayi*, and *Eulamprus tryoni*; see also Sadlier, 1998), the *E. quoyii* group (including *Eulamprus heatwolei*, *E. kosciuskoi*, *Eulamprus leuraensis*, *E. quoyii*, and *Eulamprus tympanum*), and the *E. tenuis* group (including *E. amplus*, *Eulamprus brachysoma*, *Eulamprus frerei*, *Eulamprus martini*, *Eulamprus sokosoma*, *E. tenuis*, and *Eulamprus tigrinus*; see also Greer, 1992). Although unable to identify any apomorphic character states diagnosing the *E. tenuis* group, Greer (1989) proposed that species of the *E. murrayi* group exhibit at least one distinctive apomorphy, the postmental contacting only a single infralabial, while those of the *E. quoyii* group are differentiable on the basis of at least two apomorphies, dorsal scales of the digits that are arranged in a single row distally and longitudinally grooved subdigital lamellae. Furthermore, Greer (1989) noted that species of the *E. murrayi* group and the *E. quoyii* group have the third pair of chin scales separated by five (as opposed to three) longitudinal scale rows, a character state otherwise exhibited among Australian *Sphenomorphus* group scincids only by *G. queenslandiae* and *N. spinosa* (see O'Connor and Moritz, 2003), and lack inguinal fat bodies, and consequently suggested that the two species groups compose a clade. However, only a single apomorphic character state, ovoviviparity, was identified as possibly uniting the three species groups of *Eulamprus*, prompting Greer (1989, p. 150) to consider that 'their association together as an evolutionary lineage is only tentative'. According to O'Connor and Moritz's (2003) preferred phylogenetic hypothesis for *Eulamprus*, *Gnypetoscincus*, and *Nangura* (based on parsimony and Bayesian analyses of mitochondrial

16S rRNA and ND4 sequences and presented in their Fig. 3), the three species groups of *Eulamprus* discussed by Greer (1989) are each monophyletic, with *Nangura*, *Gnypetoscincus*, the *E. murrayi* group, and the *E. quoyii* group being placed as successive sister lineages (or clades) of the *E. tenuis* group (it should be noted, however, that O'Connor and Moritz included no other Australian *Sphenomorphus* group scincids as ingroup taxa in their analyses). Reeder's (2003) analysis recovered a clade including *E. amplus*, *Gnypetoscincus*, and *Nangura*, but did not support a close relationship between this clade and either *E. murrayi* or *E. quoyii*, or between the latter two taxa. The analyses presented here indicate that the *E. quoyii* group and the *E. tenuis* group, *Gnypetoscincus*, and *Nangura* (see below) constitute clades, however, monophyly of both the *E. murrayi* group and the *E. tenuis* group is not supported (although the *E. murrayi* group is consistent with a number of trees of the 95% credible set for the mitochondrial sequence data, whilst the *E. tenuis* group is present in the 95% credible sets of trees for the mitochondrial DNA and intron sequence data), while *Eulamprus* is polyphyletic, as Reeder (2003) concluded.

Greer (1989, p. 157) noted that species of *Glaphyromorphus* 'lack traits distinctive enough to ally them either with each other or with other genera in the *Sphenomorphus* group', and considered that 'the group is not monophyletic'. Choquenot and Greer (1989; see also Greer, 1989) proposed that *G. gracilipes* is the sister lineage of *Hemiergis*, a conclusion supported by Reeder's (2003) analysis (although with some conflict between protein-encoding and structural RNA partitions) and the analyses presented here (interestingly, however, *G. gracilipes* is nested within *Hemiergis* in the most probable tree for the intron data set; see Fig. 2.2), and corroborated by viviparity and yellowish-orange ventral colouration in both taxa (Reeder, 2003). Among the remaining species of *Glaphyromorphus*, Greer (1989, 1990b) recognised two species groups, the *G. crassicaudis* group (including *G. crassicaudis*, *G. mjobergi*, *G. pumilus*, and *G. punctulatus*) and the *G. isolepis* group (including *Glaphyromorphus antoniorum*, *Glaphyromorphus brongersmai*, *G. douglasi*, *Glaphyromorphus emigrans*, *G. isolepis*, *G. pardalis*, and *Glaphyromorphus timorensis*). The

G. crassicaudis group was considered to be supported by two morphological apomorphies, a phalangeal formula for the pes of 2.3.4.5.3 and the postmental contacting a single infralabial. Additionally, Greer (1989) identified at least one apomorphic character state shared by the *G. crassicaudis* group, *G. arnhemicus*, *G. cracens*, *G. darwiniensis*, *G. fuscicaudis*, *G. gracilipes*, and *G. nigricaudis*, specifically, an elevated number of presacral vertebrae (28 or more). Although my analyses failed to recover the *G. crassicaudis* group as conceived of by Greer (1989), the mitochondrial DNA and intron sequence data indicate that the latter, more inclusive group, excluding *G. gracilipes*, constitutes a clade, to which I propose the name *G. crassicaudis* group could be ascribed (pending a formal revision of the higher taxonomy of the Australian *Sphenomorphus* group). A series of seven putative apomorphies was regarded by Greer (1990b) as diagnosing the *G. isolepis* group, including auricular lobules that are reduced or absent, five infralabials, the postmental contacting a single infralabial, relatively short limbs, absence of pterygoid teeth, squared off palatal rami of the pterygoids that are in medial contact, and presence of an ectopterygoid process. All of these character states occur elsewhere within the Australian *Sphenomorphus* group, however, the mitochondrial DNA sequence data indicate that the *G. isolepis* group constitutes a clade (although the associated posterior probability is low). Greer (1989, p. 157) suggested that '*Eremiascincus* is probably derived from an ancestor like *Glaphyromorphus nigricaudis* or *G. isolepis*', implying a close relationship among these taxa (see also Greer, 1979b). Both Reeder's (2003) analysis and the mitochondrial DNA sequence analysis presented here indicate that *Eremiascincus* and the *G. isolepis* group compose a clade, although they do not support a close relationship of this clade and the *G. crassicaudis* group (of which *G. nigricaudis* is presumably a part; see above and Figs 2.1, 2.2, and 2.3).

A substantial proportion (more than 70%) of Australian *Sphenomorphus* group scincids are referred to *Ctenotus* and *Lerista*, which include more than 90 and more than 75 species, respectively (Cogger, 2000). Storr (1964) described a suite of morphological attributes characterising species of *Ctenotus* (see also Cogger, 2000), including prominent

auricular lobules, which are highly reduced or absent in all other Australian *Sphenomorphus* group scincids (Storr, 1964; Reeder, 2003), and a dorsal pattern of longitudinal stripes or series of spots. Nonetheless, Storr (1964) did not consider the polarity of the character states he mentioned and, accordingly, made no explicit attempt to demonstrate that *Ctenotus* is monophyletic. Although including only a limited number of species, both Reeder's (2003) and my analyses substantiate Storr's (1964, p. 84) recognition of this 'sharply definable group of species', indicating that *Ctenotus* constitutes a clade. Greer (1986) presented an extensive list of character states shared by species of *Lerista* that he regarded as apomorphic (with respect to a hypothetical ancestral *Sphenomorphus* group scincid) and hence as evidence for monophyly. Reeder's (2003) analysis and the analyses presented here confirm that *Lerista* is a clade, although taxon sampling is again limited.

Aside from those clades recovered in both the mitochondrial DNA and intron sequence analyses, there are several monophyletic groups that are strongly supported by the mitochondrial and combined data sets and consistent with a number of trees of the 95% credible set for the intron data set (despite not being present in the most probable tree). These monophyletic groups, which, following Wiens (1998), may be considered well supported, include a clade composed of all Australian *Sphenomorphus* group scincids except *N. ornatus*, the relatively large mesic eastern Australian clade (including *Calyptotis*, the *C. reticulatus* + *O. truncatus* + *Saiphos* clade, *C. frontalis*, *C. naufragus*, *E. amplus*, *E. luteilateralis*, *E. murrayi*, *E. tenuis*, *G. queenslandiae*, *N. spinosa*, and *O. ophioscincus*), a clade including *E. amplus*, *E. tenuis*, *Gnypetoscincus*, and *Nangura* (discussed above), a clade containing the *E. quoyii* group and the *G. crassicaudis* group, and a clade including the *G. gracilipes* + *Hemiergis* and *Eremiascincus* + *G. isolepis* group clades (the latter clade represented by *Eremiascincus* in the intron sequence analysis). The placement of *Notoscincus* as the sister lineage of the remaining Australian *Sphenomorphus* group scincids is consistent with Reeder's (2003) preferred phylogenetic hypothesis (his Fig. 3), as are sister group relationships between the *E. quoyii* group and the *G. crassicaudis* group and the *G. gracilipes* + *Hemiergis*

and *Eremiascincus* + *G. isolepis* group clades. The mesic eastern Australian clade largely coincides with Reeder's (2003) Clade A, differing only in excluding *Anomalopus*.

The mitochondrial DNA sequence data indicate that the Australian *Sphenomorphus* group (presumably including *G. antoniorum*, *G. emigrans*, and *G. timorensis*, distributed in the Lesser Sunda Islands; see Greer, 1990b) constitutes a clade, however, the number of non-Australian *Sphenomorphus* group scincids included in the analysis remains limited. Reeder (2003, p. 392) suggested that species of the *Sphenomorphus fasciatus* group in particular should be added to his data set 'to more rigorously test the monophyly of the Australian clade'. Recently, Greer and Shea (2004) diagnosed a group of 22 species of *Sphenomorphus* distributed in the southern Philippines, the Palaus, New Guinea and the Bismarck Archipelago, and the Solomon Islands on the basis of a single putative apomorphy, the possession of a previously unnamed scale posterior to the supraoculars designated the postsupraocular. These species, referred to collectively as the *Sphenomorphus maindroni* group, constitute a large subset of those included by Greer and Parker (1967, 1974) in the *fasciatus* group of *Sphenomorphus*, which Greer and Shea (2004, p. 85) proposed 'is not a monophyletic group and hence has little residual value as a taxonomic concept'. Assuming the *S. maindroni* group is a clade (Greer and Shea [2004] were disinclined to conclude this from the distribution of a single character state), the placement of *Sphenomorphus solomonis* (a part of the *S. maindroni* group) with the two other included species of *Sphenomorphus* (see Fig. 2.1) entails that at least a significant proportion of those species Reeder (2003) presumably considered are possibly nested within the Australian *Sphenomorphus* group have a closer relationship with non-Australian taxa.

2.4.2. Topological incongruence, branch lengths, and rate of diversification

Although there is substantial support for a number of clades within the Australian *Sphenomorphus* group, the relationships among these clades inferred in the mitochondrial DNA and ATP synthetase-β subunit intron sequence analyses are generally poorly supported

and incongruent (compare Figs 2.1 and 2.2). At least some of the observed incongruence assuredly may be ascribed to error in estimating phylogenetic relationships due to limited data, considering the low posterior probabilities associated with nearly all of the conflicting nodes. However, even when uncertainty in inferred relationships is allowed for (by examining 95% credible sets of trees), some incongruence is evident (see Table 2.4). Thus, the placement of *Anomalopus* as the sister lineage of the *G. gracilipes* + *Hemiergis* and *Eremiascincus* + *G. isolepis* group clades is inconsistent with all trees of the 95% credible set for the intron sequence data. Similarly, few of the relationships among *Calyptotis*, the *C. reticulatus* + *O. truncatus* + *Saiphos* and *E. amplus* + *E. tenuis* + *Gnypetoscincus* + *Nangura* clades, *C. frontalis*, *C. naufragus*, *E. murrayi*, *E. luteilateralis*, and *O. ophioscincus* indicated by the most probable tree for the mitochondrial DNA sequence data are present in the 95% credible set of trees for the intron data set, while a clade including the *E. amplus* + *E. tenuis* + *Gnypetoscincus* + *Nangura* clade, *C. frontalis*, *E. murrayi*, and *O. ophioscincus*, recovered in the intron sequence analysis, is inconsistent with all trees of the 95% credible set for the mitochondrial DNA sequence data. Accordingly, it may be tentatively (considering the poor support for many of the nodes concerned) concluded that at least some of the relationships among the well-supported clades of Australian *Sphenomorphus* group scincids indicated by the mitochondrial and intron sequence data conflict, consistent with Poe and Chubb's (2004) first prediction for independent gene trees assuming a lineage-level polytomy (see Section 2.1).

A considerable proportion of internal ingroup branches (12 of 34) in the most probable tree for the intron sequence data have a length indistinguishable from zero. Several of these branches separate the well-supported clades recovered in the mitochondrial DNA and intron sequence analyses, the relationships of which are generally incongruent with those indicated by the most probable tree for the mitochondrial data set (e.g., *Ctenotus*, *Lerista*, the *G. gracilipes* + *Hemiergis* clade). As discussed above, however, at least some of the incongruence apparent when comparing topologies for the mitochondrial DNA and intron

sequence data may be attributable to stochastic error in inferring phylogenetic relationships, and it should be noted that nearly all of the conflicting relationships associated with zero-length branches are poorly supported. Additionally, a number branches separating clades that are not present in the most probable tree for the mitochondrial DNA sequence data have a length significantly greater than zero (e.g., the *C. frontalis* + *E. amplus* + *E. murrayi* + *E. tenuis* + *Gnypetoscincus* + *Nangura* + *O. ophioscincus* clade, which is inconsistent with all trees of the 95% credible set for the mitochondrial data set; see above). There is, accordingly, limited evidence for an association of zero-length branches and significant incongruence (with respect to the relationships inferred in the mitochondrial DNA sequence analysis) in the most probable tree for the intron data set. Indeed, the distribution of zero-length branches is consistent with much of the observed incongruence resulting from error in estimating relationships (i.e., in the intron sequence analysis) due to insufficient data (see below). Furthermore, all branches within the Australian *Sphenomorphus* group in the most probable tree for the mitochondrial DNA sequence data are of non-zero length. Thus, Poe and Chubb's (2004) second prediction for independent gene trees under the hypothesis of a lineage-level polytomy (i.e., that branches separating lineages composing the polytomy should have a length insignificantly different from zero in all trees) is not confirmed.

Poe and Chubb (2004) regarded significant incongruence and concordant zero-length branches among independent gene trees as primary lines of evidence in establishing the presence of a lineage-level polytomy, however, they did not consider both lines of evidence necessary. Thus, according to their Figure 2, which depicts the steps involved in applying their methodology for detecting lineage-level polytomies, it is possible to proceed from the observation of either incongruent gene trees in which branches are of non-zero length or congruent gene-level polytomies to the inference of a lineage-level polytomy. Although it might be expected that branches separating lineages composing a polytomy will be short in some sense, in many instances an ancestral lineage will contain multiple alleles for particular loci and, accordingly, potentially recoverable gene trees in which at least some branches have

lengths greater than zero. This is especially probable where an ancestral lineage is geographically widespread (permitting phylogeographic structure), exhibits a large effective population size (increasing the mean persistence time of alleles; see Avise, 2000), or both (a widespread geographical distribution may additionally increase the probability of an ancestral lineage simultaneously producing three or more descendant lineages; see Poe and Chubb, 2004, p. 405). As a consequence, even where three or more lineages originate simultaneously from an ancestral lineage, the relationships of alleles randomly sorted among those lineages may be accurately represented as a bifurcating tree in which all branches are of non-zero length (see Slowinski, 2001, his Fig. 1A). Poe and Chubb (2004) noted that in the absence of persisting ancestral polymorphism estimated branch lengths are likely to be zero regardless of the lineage-level topology, although they proposed that in this instance 'hard lineage-level polytomies are indicated by … congruent zero-length branches across the gene trees' (Poe and Chubb, 2004, p. 409). There are, however, plausible circumstances in which concordant gene-level polytomies may be expected assuming strictly dichotomous relationships among lineages (e.g., where successive speciation events over a relatively brief period produce multiple lineages descended from an initial ancestral lineage with a small effective population size and, consequently, exhibiting limited polymorphism for many independent loci).

The significance of congruent zero-length branches across independent gene trees in inferring lineage-level polytomies is, I believe, not evident. Assuming that 'hard' gene-level polytomies (if they are possible) are rare (see Slowinski, 2001; Poe and Chubb, 2004), many zero-length branches will result from insufficient data or lack of persisting ancestral polymorphism (these two explanations are not unrelated, as the probability of detecting ancestral polymorphism will depend on the amount of available data). It is unclear that concordance of gene-level polytomies deriving from either cause is more probable under the hypothesis of a lineage-level polytomy than if rapid (relative to the substitution rates of the genes considered), but strictly dichotomous, origination of lineages is assumed. Adopting Poe and Chubb's (2004, p. 404) perspective that a lineage-level polytomy obtains 'when rapid

evolutionary splitting has caused a lack of central tendency in the constituent gene trees [of three or more lineages]', differentiating these two hypotheses requires that such a 'lack of central tendency' or, conversely, non-random topological congruence is demonstrated. However, this will not be possible where, due to insufficient data or an absence of persisting ancestral polymorphism, we are unable to provide resolved bifurcating trees for independent (i.e., unlinked) genes (nonetheless, replication ensures that such trees exist). Poe and Chubb (2004) proposed that, although concordance of short internal branches is expected under the hypothesis of a lineage-level polytomy, it is not predicted where incongruence among gene trees is a consequence of horizontal gene transfer or paralogy and, accordingly, may afford a basis for discounting these alternative explanations. Here, however, the condition that branches have a length indistinguishable from zero becomes an arbitrary criterion for deciding that a branch should be considered 'short'. Aside from being overly restrictive (considering the potential for ancestral polymorphism), this criterion is problematic, as branches having lengths insignificantly different from zero will in many instances be poorly supported, so that associated incongruence may plausibly be ascribed to estimation error.

In accordance with the above discussion, the power curves for the intron data sets indicate that the probability of rejecting the hypothesis that the inferred zero-length branches have a length of zero is low, and hence that the results of the tests for zero-length branches may reflect insufficient data (as opposed to the presence of actual zero-length branches). Moreover, all of these branches are poorly supported, so that associated incongruence might be considered a consequence of stochastic error in estimating phylogenetic relationships. However, as noted above, at least some incongruence is evident when uncertainty in inferred relationships is allowed for. Although many branches separating the well-supported clades recovered in the mitochondrial DNA and intron sequence analyses exhibit a length significantly greater than zero (particularly in the most probable tree for the mitochondrial DNA sequence data; see Fig. 2.1), an appreciable proportion may be regarded as very short, having lengths comparable to (in some instances less than) those estimated for the inferred

zero-length branches. Thus, following Poe and Chubb (2004), horizontal gene transfer or paralogy, for which concordance of short internal branches among independent trees is not predicted, may perhaps be considered less probable than the presence of a lineage-level polytomy as an explanation for the observed incongruence (see above). Alternative hypotheses invoking taxon sampling artefacts and the use of genes that are evolving at unsuitable rates (see Section 2.1) were regarded by Poe and Chubb (2004) as potentially explaining gene-level polytomies rather than topological incongruence (see, for example, their Fig. 2; see also Jackman *et al*., 1999), however, it may be noted that for the mitochondrial DNA sequence data at least, the topology and relative branch lengths obtained in Reeder's (2003) analysis (which included considerably fewer *Sphenomorphus* group scincids) are similar to those recovered in the analyses presented here, while there are well-supported nodes above and below the short, conflicting branches in the most probable tree (see Fig. 2.1). Nonetheless, I refrain from proposing that the phylogeny of Australian *Sphenomorphus* group scincids includes one or more lineage-level polytomies, as the limited number of independent gene trees considered does not permit the possibility of observing a '"majority" signal' (Poe and Chubb, 2004, p. 406) among topologies (this would necessitate that at least three trees are compared). However, the very short internal branches and associated incongruence suggest that initial diversification of the Australian *Sphenomorphus* group was at least rapid relative to the substitution rates of the mitochondrial DNA and intron fragments employed in the analyses.

Traditionally, rapid diversification of particular clades has been regarded as a consequence of multiple 'prospective adaptive zones [being] opened more or less simultaneously' when either 'a rather distinctive new adaptive type has developed' or 'a group spreads to new and, for it, ecologically open territory' (Simpson, 1953, pp. 222-223). Nonetheless, as Simpson (1953) discussed, the occupation of several 'prospective adaptive zones' may be progressive, as opposed to simultaneous: 'Progressive occupation of such [adaptive] zones is not simultaneous and usually involves in any one period of time the

change of only one or a few lines from one zone to another, with each transition involving a distinctly different ancestral type' (Simpson, 1953, p. 223). Thus, the availability of a number of 'adaptive zones' does not entail that a clade will diversify rapidly to occupy those zones. Rosenzweig (1975, 1995) presented a graphical model relating community species diversity on continents to rates of speciation and extinction according to which an increasing number of species is associated with a decreasing rate of increase in the rate of speciation and an increasing rate of increase in the rate of extinction (resulting primarily from successive reduction of population and geographical range sizes as an ancestral lineage is subdivided), so that species diversity attains an equilibrium. At equilibrium, the model predicts that extinction rate is increasing more rapidly than speciation rate and, accordingly, that a negative shift from the equilibrium number of species will depress extinction rate to a greater extent than speciation rate. Hence, Rosenzweig (1975) proposed that rapid diversification on continents may result from a very low extinction rate rather than a preternaturally high rate of speciation. More recently, Hubbell (2001) argued that (meta-) community species diversity will attain an equilibrium given a constant per capita speciation rate. Assuming a community is saturated with individuals, so that no available limiting resources are unused, increasing diversity will reduce the mean population size of species and, concomitantly, increase the rate of extinction; eventually, the extinction rate will increase to equal the constant (per capita) speciation rate and an equilibrium species diversity will obtain. In the event that a community is greatly desaturated (as effectively occurs where multiple 'prospective adaptive zones' simultaneously become available), populations will enlarge to exploit unused resources and, consequently, absolute (as opposed to per capita) speciation rate will increase without being offset by an increasing extinction rate. Accordingly, the apparent rapid diversification of Australian *Sphenomorphus* group scincids might be ascribed to a decreased rate of extinction (resulting from a non-equilibrium species diversity) subsequent to colonisation of the Australian continent. Alternatively, extrinsic events or processes, such as changing climate, may have induced an episode of extremely rapid speciation through, for example, the essentially simultaneous isolation of multiple subpopulations of a geographically widespread

ancestral species. Assessing these alternative hypotheses will necessitate comparing estimates of rates of speciation for recent lineages (which are less liable to distortion due to extinction; see, for example, Harvey *et al*., 1994) with those inferred for the period of initial rapid diversification, and considering patterns of diversification for co-distributed clades of similar age that may reveal an influence of extrinsic events or processes.

Chapter 3

Rapid and Repeated Limb Reduction in *Lerista*

3.1. Introduction

Limb reduction has occurred repeatedly during tetrapod evolution, with several major clades (e.g., Aves, Lissamphibia, Mammalia, Squamata) including limb-reduced species (Gans, 1975; Lande, 1978). Among these clades, Squamata (lizards and snakes) provides perhaps the finest models for studying modes and causes of limb reduction. At least 53 squamate lineages have been identified as having independently lost one or more bones of the fore- or hindlimb (Greer, 1991). Many of these lineages are closely related and, accordingly, offer excellent comparative material. More significantly, a number of squamate clades include extant species displaying a range of intermediate states between pentadactyl and limbless conditions, affording the possibility of reconstructing patterns and rates of limb reduction and loss. The Australian scincid clade *Lerista* is pre-eminent among these, comprising more than 75 species exhibiting at least 20 distinct limb bone configurations, from that considered plesiomorphic for squamates (phalangeal formulae of 2.3.4.5.3 and 2.3.4.5.4 for the manus and pes, respectively) to entirely limbless (Greer, 1987, 1990a).

Although *Lerista* has been considered the best available model for investigating squamate limb reduction (Greer, 1987, 1990a), lack of a well-resolved phylogeny has impeded study of the pattern and mode of limb reduction and loss within the clade. Greer (1987, 1990a), who examined intra- and interspecific variation in phalangeal configurations for more than half of the species of *Lerista* then described, relied on an arrangement of observed configurations entailing the minimum amount of change between each in reconstructing sequences of phalanx loss, while noting that 'it would be most desirable to be able to order variation on the basis of a hypothesis of intrageneric relationships for *Lerista* based on characters independent of those under study, but unfortunately, this is not yet

possible' (Greer, 1987, p. 267). Two decades later, the phylogeny of *Lerista* remains largely obscure. A modest number of species groups have been diagnosed explicitly on the basis of proposed apomorphic character states, implying monophyly (Greer *et al*., 1983; Greer, 1986, 1990c), however, relationships within and among these species groups are unknown. In this chapter, I present the first comprehensive phylogeny for *Lerista*, inferred from nucleotide sequences for a nuclear intron and six mitochondrial genes. This phylogeny is employed in reconstructing ancestral digit configurations, which, in conjunction with estimates of absolute ages for nodes, provide insight into the pattern, rate, and causes of limb reduction within the clade.

3.2. Materials and Methods

3.2.1. Phylogenetic analysis

Specimen registration and collection locality data are provided in Appendix 2. ATP synthetase-β subunit intron, 12S rRNA, 16S rRNA, and ND4 and adjacent tRNA-His, tRNA-Ser, and tRNA-Leu fragments were amplified and sequenced as described by Skinner (2007). Alignment of ND4 sequences did not require the insertion of gaps and was straightforward. 12S, 16S, and tRNA sequences were initially aligned with Clustal X (Thompson *et al*., 1997) assuming the default pairwise and multiple alignment parameter values. Adjustments to alignments were made with the aid of secondary-structure models (Wuyts *et al*., 2001, 2002; Macey and Verma, 1997). ATP synthetase-β subunit intron sequences were aligned with Clustal X using the default settings.

Aligned sequences were partitioned according to locus and, for protein-encoding (i.e., ND4) sequences, codon position (the tRNAs were considered as a single partition, resulting in seven partitions; Table 3.1). All partitions were analysed simultaneously using mixed-model Bayesian methods, implemented in MrBayes (Ronquist and Huelsenbeck, 2003). An appropriate nucleotide substitution model for each partition was selected on the basis of

Table 3.1

Numbers of aligned sites, variable sites, and unique site patterns for partitions employed in the Bayesian analysis.

Partition	Aligned sites	Variable sites	Unique site patterns
12S rRNA	902	425	501
16S rRNA	548	216	252
ND4, 1st codon position	228	110	131
ND4, 2nd codon position	229	33	60
ND4, 3rd codon position	229	226	229
tRNAs	142	79	110
ATP synthetase-β subunit	581	276	405

hierarchical likelihood-ratio tests, performed using Modeltest (Posada and Crandall, 1998). Four incrementally-heated Markov chains, initiated with random starting trees and default priors, were run for 10^7 generations, sampling every 1000^{th} generation. Parameter values for each specified model were estimated independently (i.e., parameter values were unlinked across partitions). The number of generations required to attain stationarity was estimated by examining cumulative posterior probabilities for clades, plotted using AWTY (Wilgenbusch *et al*., 2004). All trees sampled prior to attaining stationarity were discarded and the remaining trees used to compute a majority-rule consensus topology, branch lengths, and posterior probabilities for nodes.

Penalised likelihood rate smoothing (Sanderson, 2002), performed with r8s (Sanderson, 2003), was employed to produce an ultrametric tree from the Bayesian majority-rule consensus (with mean branch lengths and an arbitrary age of 1.0 specified for the root

node). This tree was assumed in inferring ancestral states and calculating absolute ages for nodes (see below).

3.2.2. Ancestral state reconstruction

Modal digit configurations for extant species of *Lerista* were collated from data in the literature, verified and augmented by my own observations of specimens in the South Australian Museum and Western Australian Museum. Maximum likelihood numbers of manual and pedal digits for internal nodes were determined independently using Mesquite (Maddison and Maddison, 2003), assuming the asymmetrical Markov k-state 2-parameter (AsymmMk) model of character evolution. The two parameters in this model describe instantaneous rates of forward and reverse transitions, corresponding in my analyses to rates of digit loss and gain. It should be noted that the inclusion of separate rate parameters for all possible transitions does not significantly improve model fit (the alternative models were compared by means of a likelihood-ratio test, performed using M. Pagel's program Multistate).

The extent to which the ancestral state reconstructions depend on assumed rates of character state transition was assessed by comparing ancestral states inferred for a range of rates with those reconstructed assuming the maximum likelihood estimates. Limb reduction is generally considered to be only exceedingly rarely (perhaps never) reversed (e.g., Presch, 1975; Greer, 1987, 1990a, 1991; see, however, Kohlsdorf and Wagner, 2006) and I therefore focussed on rates of digit gain (while ancestral states entailing no reversals of limb reduction for a limited range of rates of digit loss may be uncontentious, it is probable that ancestral states implying reversals for only a limited range of rates of digit gain would be more controversial). Ancestral states were reconstructed for rates of digit gain representing all values not significantly less likely than the maximum likelihood estimate (according to likelihood-ratio tests) assuming estimated rates of digit loss.

As a means of evaluating the influence of uncertainty in inferred phylogenetic relationships and branch lengths, I reconstructed ancestral states across 1000 trees (every fifth of 5000 trees) sampled after attaining stationarity in the Bayesian analysis using the 'Trace Character Over Trees' option in Mesquite (Maddison and Maddison, 2003). For each node in the Bayesian majority-rule consensus, numbers of manual and pedal digits were inferred for all trees containing that node; the variability of inferred states among trees provides a measure of the degree to which ancestral state reconstructions for the node concerned are affected by uncertainty in tree topology and branch lengths (see Lutzoni *et al*., 2001; Pagel *et al*., 2004). The proportion of trees for which reconstructed ancestral states imply one or more reversals of limb reduction was also determined. A reversal was inferred where the greatest number of digits (or a higher number) observed among the set of species defined by a node was significantly less probable than the maximum likelihood state for that node (alternative states were compared on the basis of their contribution to the total likelihood for a tree, with differences of less than two log-likelihood units being considered insignificant; see Schluter *et al*., 1997). Ancestral states were reconstructed across trees for a range of rates of digit gain as described above.

The reduction and loss of limbs in squamates has been considered a consequence of the adoption of lateral undulation as a significant mode of locomotion (Gans, 1975). The use of lateral undulation is consistently (and presumably functionally) associated with body elongation (Gans, 1975; Greer *et al*., 1998), so that where limb reduction may be ascribed to increased reliance on undulatory locomotion, it should be preceded by an increase in the relative length of the body. To test this prediction, I reconstructed relative snout-vent length (defined here as snout-vent length divided by head length) for internal nodes and plotted these values and inferred numbers of digits against node age for individual lineages (i.e., direct paths from the root to extant species). Mean relative snout-vent length was calculated for each species included in the phylogenetic analysis from measurements of snout-vent length and head length (measured from the snout tip to the anterior margin of the auricular opening)

recorded from series of 1-5 specimens (measurements were not obtained for *L. ingrami*, *L. emmotti*, and *L. karlschmidti*; see Appendix 3). As a means of reducing any influence of allometric growth, only the largest available specimens were measured. Ancestral states were reconstructed using weighted squared-change parsimony (Maddison, 1991), implemented in Mesquite (Maddison and Maddison, 2003).

3.3. Results and Discussion

The majority-rule consensus of trees sampled after attaining stationarity in the Bayesian analysis (Fig. 3.1) includes many strongly-supported clades (those associated with a posterior probability >0.95). Several of these clades correspond with putative monophyletic groups recognised previously on the basis of morphology, including the *bipes* species group (Greer, 1986), the *nichollsi* species group (including *L. lineopunctulata*; see Greer, 1986), and the *orientalis* species group (excluding *L. muelleri*; see Greer, 1990c), although the majority of recovered relationships have never been hypothesised by earlier authors (e.g., the sister group relationship of *L. apoda* and the *bipes* species group, and of *L. praepedita* + *L. humphriesi* and the *nichollsi* species group). The four species with well-developed, pentadactyl limbs (*L. arenicola*, *L. bougainvillii*, *L. microtis*, *L. viduata*) compose two distant clades, neither of which is positioned basally within *Lerista*. Those species in which limbs are greatly reduced (*L. carpentariae*, *L. cinerea*, *L. humphriesi*, *L. karlschmidti*, *L. praepedita*, *L. stylis*, *L. wilkinsi*) or absent (*L. ameles*, *L. apoda*) similarly are polyphyletic.

For the manus, the ratio of maximum likelihood rates of digit gain and loss (9.524×10^{-5}) indicates that increases in the number of digits are far less probable than reductions. Maximum likelihood reconstructions of ancestral states imply 19 instances of digit loss with no reversals to an increased number of digits (Fig. 3.1). All rates of digit gain not significantly less likely than the maximum likelihood estimate yield maximum likelihood ancestral states identical to or only insignificantly more probable than those reconstructed

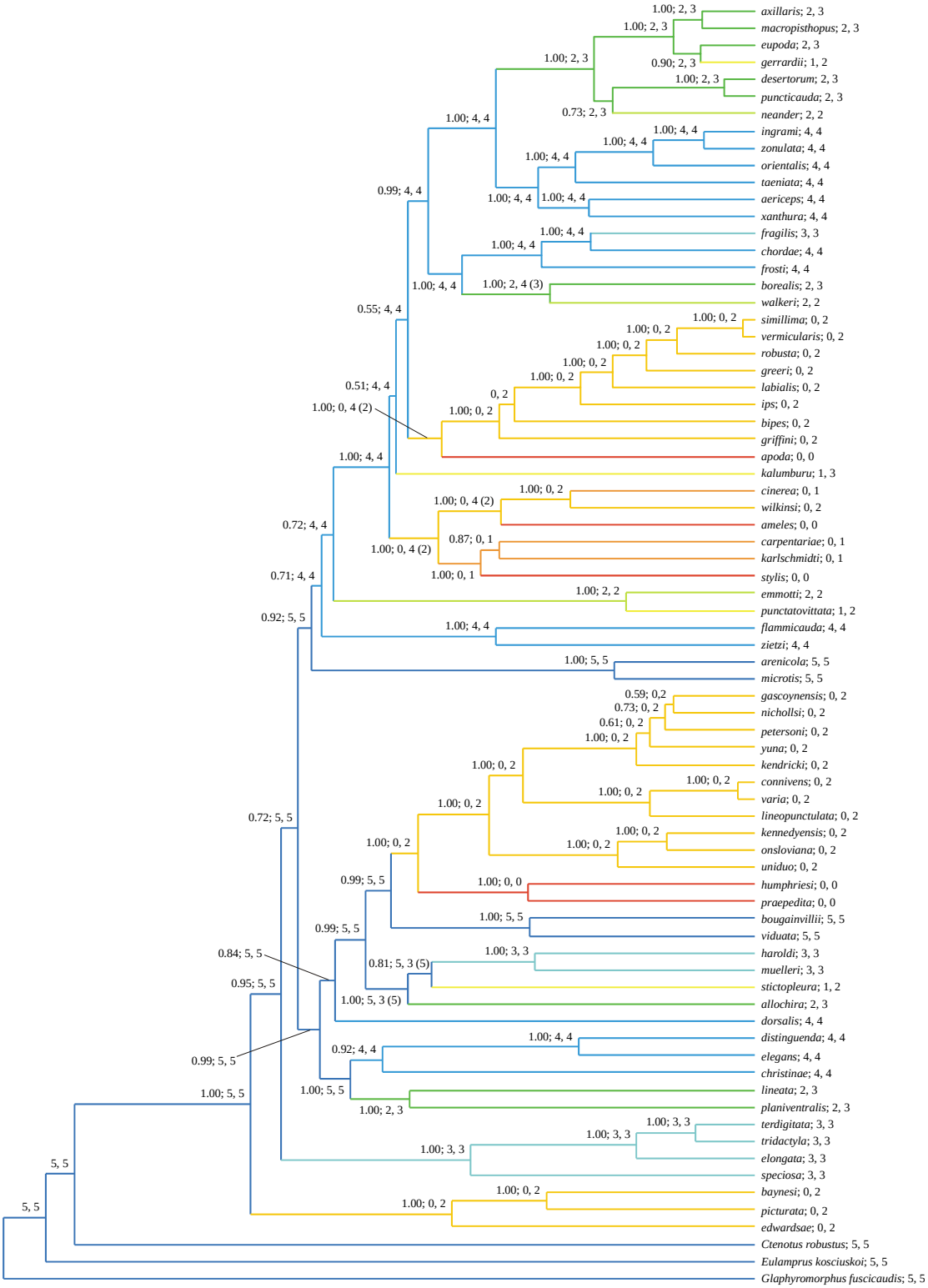
1.00; 2, 3
1.00; 2, 3
0.90; 2, 3
1.00; 2, 3
0.73; 2, 3
1.00; 2, 3
1.00; 4, 4
1.00; 4, 4
1.00; 4, 4
1.00; 4, 4
1.00; 4, 4
0.99; 4, 4
1.00; 4, 4
1.00; 4, 4
1.00; 4, 4
1.00; 4, 4
1.00; 4, 4
1.00; 2, 4 (3)
0.55; 4, 4
1.00; 0, 2
1.00; 0, 2
1.00; 0, 2
1.00; 0, 2
1.00; 0, 2
0.51; 4, 4
0, 2
1.00; 0, 4 (2)
1.00; 0, 2
1.00; 4, 4
1.00; 0, 2
1.00; 0, 4 (2)
0.72; 4, 4
0.87; 0, 1
1.00; 0, 4 (2)
1.00; 0, 1
0.71; 4, 4
1.00; 2, 2
0.92; 5, 5
1.00; 4, 4
1.00; 5, 5
0.59; 0,2
0.73; 0, 2
0.61; 0, 2
1.00; 0, 2
1.00; 0, 2
1.00; 0, 2
1.00; 0, 2
1.00; 0, 2
0.72; 5, 5
1.00; 0, 2
1.00; 0, 2
1.00; 0, 2
1.00; 0, 2
0.99; 5, 5
1.00; 0, 0
1.00; 5, 5
0.99; 5, 5
0.84; 5, 5
1.00; 3, 3
0.81; 5, 3 (5)
0.95; 5, 5
1.00; 5, 3 (5)
1.00; 4, 4
0.99; 5, 5
0.92; 4, 4
1.00; 5, 5
1.00; 5, 5
1.00; 2, 3
1.00; 3, 3
1.00; 3, 3
1.00; 3, 3
5, 5
1.00; 0, 2
5, 5
1.00; 0, 2
axillaris; 2, 3
macropisthopus; 2, 3
eupoda; 2, 3
gerrardii; 1, 2
desertorum; 2, 3
puncticauda; 2, 3
neander; 2, 2
ingrami; 4, 4
zonulata; 4, 4
orientalis; 4, 4
taeniata; 4, 4
aericeps; 4, 4
xanthura; 4, 4
fragilis; 3, 3
chordae; 4, 4
frosti; 4, 4
borealis; 2, 3
walkeri; 2, 2
simillima; 0, 2
vermicularis; 0, 2
robusta; 0, 2
greeri; 0, 2
labialis; 0, 2
ips; 0, 2
bipes; 0, 2
griffini; 0, 2
apoda; 0, 0
kalumburu; 1, 3
cinerea; 0, 1
wilkinsi; 0, 2
ameles; 0, 0
carpentariae; 0, 1
karlschmidti; 0, 1
stylis; 0, 0
emmotti; 2, 2
punctatovittata; 1, 2
flammicauda; 4, 4
zietzi; 4, 4
arenicola; 5, 5
microtis; 5, 5
gascoynensis; 0, 2
nichollsi; 0, 2
petersoni; 0, 2
yuna; 0, 2
kendricki; 0, 2
connivens; 0, 2
varia; 0, 2
lineopunctulata; 0, 2
kennedyensis; 0, 2
onsloviana; 0, 2
uniduo; 0, 2
humphriesi; 0, 0
praepedita; 0, 0
bougainvillii; 5, 5
viduata; 5, 5
haroldi; 3, 3
muelleri; 3, 3
stictopleura; 1, 2
allochira; 2, 3
dorsalis; 4, 4
distinguenda; 4, 4
elegans; 4, 4
christinae; 4, 4
lineata; 2, 3
planiventralis; 2, 3
terdigitata; 3, 3
tridactyla; 3, 3
elongata; 3, 3
speciosa; 3, 3
baynesi; 0, 2
picturata; 0, 2
edwardsae; 0, 2
Ctenotus robustus; 5, 5
Eulamprus kosciuskoi; 5, 5
Glaphyromorphus fuscicaudis; 5, 5

← Figure 3.1. Majority-rule consensus of 5000 trees sampled after attaining stationarity in a Bayesian analysis of nucleotide sequences for 72 species of *Lerista*. Mean branch lengths from the Bayesian analysis have been modified via penalised likelihood rate smoothing to produce an ultrametric tree. Posterior probabilities ≥0.50 followed by maximum likelihood numbers of digits for the manus and pes are shown adjacent to internal nodes. Ancestral states for the manus were reconstructed assuming maximum likelihood rates of digit gain and loss; for the pes, ancestral states are those inferred assuming the maximum likelihood rate of digit loss and rates of digit gain of 0.020-0.025 (see text). Alternative numbers of pedal digits yielding a log-likelihood within two units of the optimal value (i.e., that for the maximum likelihood estimate) are presented in parentheses for ancestral digit configurations not observed among nominal species of *Lerista*. Modal digit configurations follow species names. Branches are coloured according to digit configuration: dark blue, 5, 5; light blue, 4, 4; light blue-green, 3, 3; green, 2, 3; light yellow-green, 2, 2; yellow, 1, 3 and 1, 2; light orange, 0, 2; dark orange, 0, 1; red, 0, 0.

assuming the maximum likelihood rate (in comparing maximum likelihood and alternative states, log-likelihood differences of no more than two units were considered insignificant; see Section 3.2.2).

The estimated rate of digit gain for the pes exceeds that of digit loss (ratio of rates of gain and loss 2.056), with maximum likelihood reconstructions of ancestral states indicating 18 increases in the number of digits and 8 reductions (see Appendix 4). Although suggesting several reversals of limb reduction in *Lerista*, I regard this result as equivocal for two reasons. Firstly, a range of rates of digit gain for the pes are nearly as probable as the maximum likelihood estimate (0.394), and some of these rates yield ancestral state reconstructions implying no increases in the number of digits. Specifically, rates of 0.020-0.025 are not significantly less likely than the maximum likelihood rate and yield maximum likelihood ancestral states indicating 25 cases of digit loss but no instances in which digits are gained (Fig. 3.1). Secondly, when considered in conjunction with states inferred for the manus, reconstructions of numbers of pedal digits (i.e., for the maximum likelihood rate of digit gain) imply implausible digit configurations for many internal nodes. In particular, configurations of either five or four digits for the manus and two digits for the pes are implied for the majority of basal nodes, however, neither is represented among extant species of *Lerista* (which never exhibit fewer digits for the pes than the manus [Greer, 1987, 1990a]). Ancestral states reconstructed assuming rates of digit gain of 0.020-0.025, by contrast, imply implausible digit configurations for very few internal nodes. Moreover, in all instances, the ancestral states implying implausible digit configurations are not appreciably more probable than one or more states implying configurations observed among extant species of *Lerista* (see Fig. 3.1; this is not the case for ancestral states inferred under the maximum likelihood rate of digit gain). Thus, I am disinclined to conclude that limb reduction has been reversed in *Lerista*, preferring the ancestral states reconstructed assuming rates of pedal digit gain of 0.020-0.025.

An examination of ancestral state reconstructions across post-stationarity trees indicates that the above conclusions are largely insensitive to uncertainty in the inferred phylogeny. For all nodes, maximum likelihood numbers of manual digits reconstructed for more than 90% of trees are identical to or only insignificantly more probable than those inferred assuming the Bayesian majority-rule consensus (see Fig. 3.1), and reversals of limb reduction are inferred for only an insignificant proportion (less than 5%) of trees. Similar results are obtained when rates of digit gain considerably higher than those estimated by maximum likelihood are assumed. For example, a rate of 0.42, which is significantly less likely than the (nearly invariably lower) maximum likelihood rates for 90% of trees, yields maximum likelihood ancestral states for 69 of 74 internal nodes identical to or only insignificantly more probable than those reconstructed assuming the Bayesian majority-rule consensus in more than 92% of trees, with more than 62% of trees exhibiting no reversals of limb reduction (note that branch lengths for post-stationarity trees are unscaled, so that rates are not immediately comparable to those for the Bayesian majority-rule consensus). Thus, the inferred ancestral states for the manus in Figure 3.1 are not substantially affected by uncertainty in tree topology, branch lengths, and rates of character state transition.

Ancestral state reconstructions for the pes are similarly stable when uncertainty in the phylogeny is allowed for. Assuming estimated rates of digit gain, maximum likelihood numbers of pedal digits for all nodes are identical to or only insignificantly more probable than those for the Bayesian majority-rule consensus (see Appendix 4) in more than 90% of trees. As for the Bayesian majority-rule consensus (see above), ancestral state reconstructions for nearly all trees (more than 95%) imply one or more instances of reversed limb reduction. Nonetheless, a range of rates of pedal digit gain only insignificantly lower than those estimated for a considerable proportion of trees yield ancestral states reconstructions very similar to those obtained for the Bayesian majority-rule consensus assuming rates of digit gain of 0.020-0.025 (entailing no increases in the number of digits; see Fig. 3.1). A rate of 0.16, for example, is not significantly less likely than the estimated rates for 64% of trees and,

for all except a single node, yields maximum likelihood ancestral states for more than 97% of trees that are identical to or only insignificantly more probable than the preferred ancestral states in Figure 3.1. In almost all cases, numbers of pedal digits reconstructed for the single exceptional node (the most recent shared ancestor of *L. christinae*, *L. distinguenda*, *L. elegans*, *L. lineata*, and *L. planiventralis*) entail no increases in the number of digits, and reversed limb reduction is implied in less than 5% of trees.

Ancestral states reconstructed assuming the Bayesian majority-rule consensus, rates of digit gain of 0.020-0.025 for the pes, and maximum likelihood estimates for all other rates imply 11 independent reductions in the number of digits from a pentadactyl condition (ten if digit configurations for internal nodes observed among described species of *Lerista* are preferred; see Fig. 3.1). A further seven reductions are inferred to have proceeded independently from a tetradactyl condition derived from one of these reductions (that in the most recent shared ancestor of *L. flammicauda* and the *orientalis* species group). Four independent losses of all manual and pedal digits are inferred, three from pentadactyl or tetradactyl conditions. Assuming an age of 13.4 million years for *Lerista*, estimated using molecular dating methods (see Appendix 5), the loss of all digits from a pentadactyl condition in *L. ameles*, *L. apoda*, and *L. stylis* has occurred within a period of 11.8 million years. The most recent tetradactyl ancestor of *L. ameles* and *L. stylis* is no more than 9.7 million years old, while that of *L. apoda* is no more than 9.2 million years old. The highest rate of complete loss of digits from a pentadactyl or tetradactyl condition is inferred for *L. humphriesi* and *L. praepedita*; the most recent shared ancestor of these species (having a reconstructed digit configuration of no manual or pedal digits) is separated from an inferred pentadactyl ancestor by no more than 3.6 million years.

Almost invariably, species with greatly reduced limbs are separated from inferred pentadactyl or tetradactyl ancestors by very few nodes, so that, assuming limb reduction has not been saltational (i.e., that synchronous loss of several digits from the manus and pes has

not occurred), reconstruction of complete sequences of digit loss for individual lineages is not possible. Nonetheless, if digit loss is presumed to proceed similarly across all (or at least many) lineages, general conclusions concerning mode of limb reduction may be derived from a consideration of inferred losses for lineages exhibiting varying degrees of reduction. Thus, a plot of the numbers of manual and pedal digits lost in all reductions from a pentadactyl or tetradactyl condition versus the total number of (manual and pedal) digits lost (Fig. 3.2) may be considered to indicate that in the initial stages of limb reduction rates of digit loss are similar for the manus and pes, however, as limb reduction progresses, manual digits are lost more readily than pedal digits. This is consistent with a more significant role of the hindlimb in limb-mediated locomotion and selection for some ability to employ limb-mediated locomotion (as an adjunct to undulatory locomotion, which becomes increasingly important as limb reduction and body elongation proceed) in limb-reduced species. Particular intermediate digit configurations, most conspicuously that of no digits for the manus and two digits for the pes, generally originate relatively rapidly and persist for extended periods, suggesting that they do not represent transitory stages in a continuing process of limb reduction and providing further evidence for adaptive retention of digits in limb-reduced species.

In those lineages in which limbs are greatly reduced or lost, body elongation (i.e., an increase in relative snout-vent length) is typically observed prior to the loss of digits (Fig. 3.3), consistent with the hypothesis that limb reduction and loss is a consequence of increased reliance on undulatory locomotion. However, there is no apparent body elongation in other lineages exhibiting relatively minor limb reduction (the loss of one or two digits in the manus and pes), implying a cause other than transition to lateral undulation as a significant locomotory mode. A possible explanation for limb reduction in at least some of these lineages is small body size. Digit loss has been demonstrated to occur (at least in some instances) in association with a decrease in absolute size of the limb bud (Alberch and Gale, 1983, 1985; Raynaud, 1990), so that miniaturisation, involving diminution of the limb, may

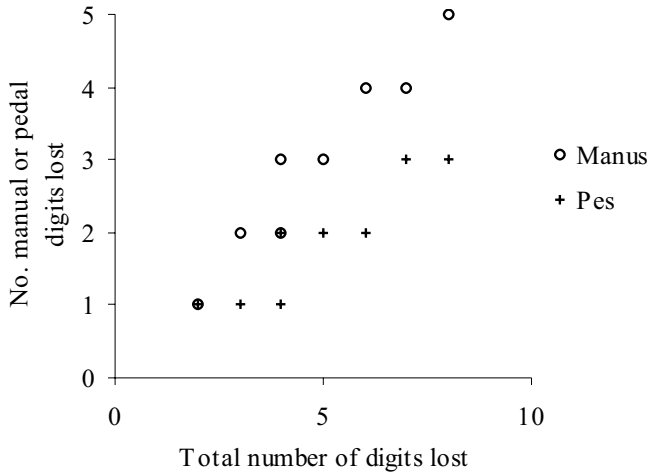

Figure 3.2. Numbers of manual and pedal digits lost in all inferred reductions from a pentadactyl or tetradactyl condition. Each point represents the number of manual or pedal digits initially lost by an inferred pentadactyl or tetradactyl ancestor; subsequent reductions (e.g., from a tridactyl condition produced as a consequence of the initial reduction) are not presented.

plausibly be proposed to account for the loss of digits (Alberch and Gale, 1985). Accordingly, it is perhaps significant that many of those lineages exhibiting digit loss in the absence of appreciable body elongation are represented by among the smallest extant species of *Lerista* (e.g., *L. christinae*, *L. distinguenda*, *L. elegans*, *L. haroldi*, *L. ingrami*, *L. taeniata*).

Many authors have noted the recurring evolution of a limb reduced, elongate body form in squamates, however, the frequency and rate of limb reduction inferred for *Lerista* in the present study are the highest recorded for a tetrapod clade, and emphasise the potential for substantial alteration of body form over (geologically) brief periods. An absence of cogent evidence for reversals of digit loss in *Lerista* contrasts with Kohlsdorf and Wagner's (2006)

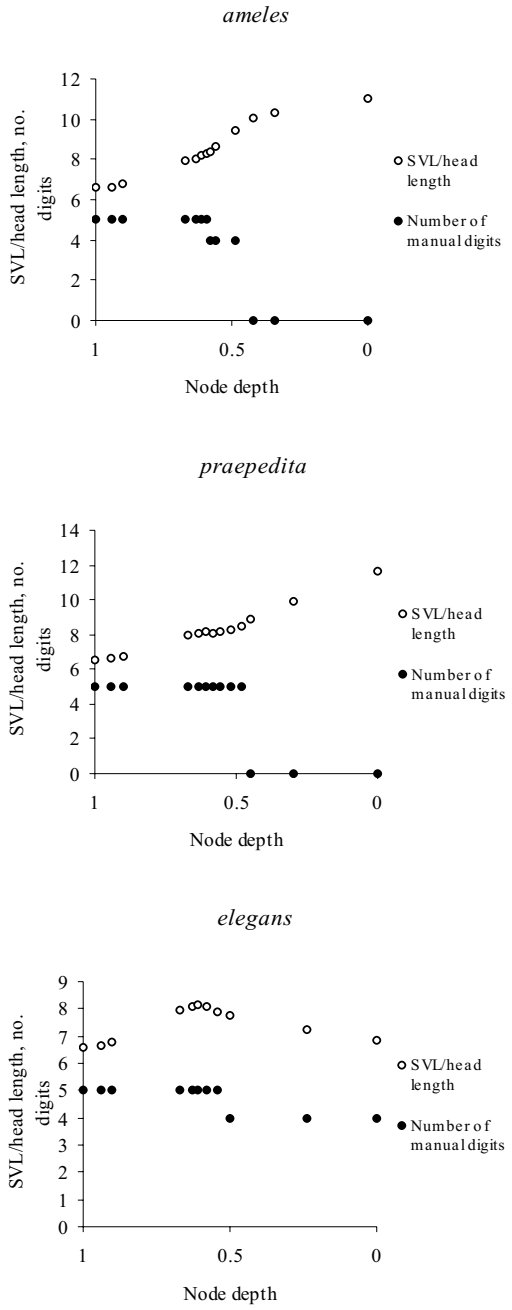

Figure 3.3. Plots of inferred relative snout-vent length and number of manual digits versus node depth for series of nodes defining selected lineages (i.e., direct paths from the root to extant species). Node depths are expressed as a proportion of the depth of the tree (extant species have a node depth of zero, with nodes closer to the root having higher values). Note that lineages in which limbs are greatly reduced (*ameles*, *praepedita*) exhibit an increase in relative snout-vent length prior to digit loss, however, there is no appreciable body elongation in lineages experiencing only minimal limb reduction (*elegans*). Plots for the number of pedal digits are similar.

recent proposal that digits have been regained in some species of the gymnophthalmid clade *Bachia*, assuredly reflecting a signficant influence of differing environmental and genetic contexts on the evolution of limb morphology in these clades. Future study of the genetic, developmental, and ecological bases of limb reduction and loss in *Lerista* and other relatively recent clades composed predominantly of limb-reduced species (e.g., *Bachia*, *Brachymeles*, *Chalcides*, *Scelotes*) promise not only elucidation of this phenomenon in squamates but also illumination of the mode and causes of dramatic morphological transformations in evolution generally.

Chapter 4

Phylogeny of *Lerista*

4.1. Introduction

Lerista is a clade of more than 75 species of scincid lizards, distributed in arid, semi-arid, and seasonally dry habitats throughout Australia (Greer, 1989; Cogger, 2000). Among extant tetrapods, *Lerista* is exceptional in comprising a large number of closely related species displaying prodigious variability of body form; several species possessing well-developed, pentadactyl limbs resemble typical non-fossorial scincids in body proportions, while many other species exhibit varying degrees of limb reduction and body elongation, including two that are highly elongate and entirely limbless (Greer, 1987, 1989, 1990a). The extensive variation in limb morphology observed within the clade, incorporating at least 20 distinct phalangeal configurations, has prompted some authors to identify *Lerista* as the best available model for studying modes and causes of limb reduction in squamates (Greer, 1987, 1990a; Greer *et al*., 1983).

Greer (1986) presented an extensive list of apomorphic character states collectively diagnosing species of *Lerista*, at least implicitly affording evidence that they compose a monophyletic group. Although none of the listed apomorphies occurs uniquely within *Lerista* (characters states were polarised with respect to a hypothetical ancestral *Sphenomorphus* group scincid), phylogenetic analyses of nucleotide sequences for a substantial proportion of Australian *Sphenomorphus* group scincids (Reeder, 2003; Skinner, 2007) provide additional evidence that *Lerista* constitutes a clade. The phylogenetic relationships among species of *Lerista* have received only limited attention, however, and, until recently, remained poorly resolved. Storr (1971; see also Storr *et al*., 1999) recognised a number of species groups within *Lerista* (Table 4.1), although these were delimited based on assessments of overall similarity, with no consideration of character state polarity, and apparently intended primarily

Table 4.1

Species groups recognised by previous authors.

bipes species group (Greer, 1986; Storr *et al*., 1999)
- *bipes*
- *greeri*
- *griffini*
- *ips*
- *labialis*
- *praefrontalis*
- *robusta*
- *simillima*
- *vermicularis*

bougainvillii species group (Storr *et al*., 1999)
- *arenicola*
- *bougainvillii*
- *microtis*
- *viduata*

elegans species group (Greer, 1990b)
- *christinae*
- *distinguenda*
- *elegans*
- *haroldi*
- *lineata*
- *separanda*
- *stictopleura*

frosti species group (Storr *et al*., 1999)
- *dorsalis*
- *flammicauda*
- *frosti*
- *quadrivincula*
- *zietzi*

lineopunctulata species group (Storr *et al*., 1999)
- *lineopunctulata*

macropisthopus species group (Storr *et al*., 1999)
- *axillaris*
- *baynesi*
- *bunglebungle*
- *desertorum*
- *edwardsae*
- *eupoda*
- *gerrardii*
- *macropisthopus*
- *neander*
- *picturata*
- *puncticauda*

nichollsi species group (Greer, 1986; Storr *et al*., 1999)
- *connivens*
- *gascoynensis*
- *kendricki*
- *kennedyensis*
- *maculosa*
- *nichollsi*
- *onsloviana*
- *petersoni*
- *talpina*
- *uniduo*
- *varia*
- *yuna*

orientalis species group (Greer, 1990b)
- *aericeps*
- *ingrami*
- *muelleri*
- *orientalis*
- *taeniata*
- *xanthura*
- *zonulata*

planiventralis species group (Storr et al., 1999)
- *planiventralis*

praepedita species group (Storr et al., 1999)
- *humphriesi*
- *praepedita*

stictopleura species group (Storr et al., 1999)
- *stictopleura*

terdigitata species group (Storr et al., 1999)
- *elongata*
- *speciosa*
- *terdigitata*
- *tridactyla*

walkeri species group (Storr et al., 1999)
- *borealis*
- *kalumburu*
- *walkeri*

wilkinsi species group (Greer *et al*., 1983)
- *ameles*
- *apoda*
- *cinerea*
- *storri*
- *stylis*
- *vittata*
- *wilkinsi*

Unassigned species
- *allanae*
- *carpentariae*
- *colliveri*
- *emmotti*
- *karlschmidti*
- *punctatovittata*

as aids for managing diversity rather than as phylogenetic hypotheses. Greer (1986, 1990b) and Greer *et al*. (1983), by contrast, relied explicitly on apomorphic character states in diagnosing species groups (see Table 4.1), which, accordingly, may be regarded as putative clades. Nonetheless, phylogenetic relationships among and within these species groups were either not discussed or noted to be unresolved. Moreover, many species of *Lerista* were not referred to any of the proposed species groups, and their phylogenetic relationships remained virtually unconsidered.

Recently, Skinner *et al*. (2007) presented a comprehensive phylogeny for *Lerista*, inferred from nuclear intron and mitochondrial nucleotide sequences, that included many significantly-supported clades, several corresponding with the species groups of Greer (1986, 1990b) and Greer *et al*. (1983). Ancestral digit configurations reconstructed assuming this phylogeny indicated a very high frequency of limb reduction, implying at least ten independent decreases in the number of digits from a pentadactyl condition, with four independent losses of all digits, three from pentadactyl or tetradactyl conditions. Although Skinner *et al*. (2007) considered the influence of phylogenetic uncertainty on inferred ancestral states (ancestral states were reconstructed across post-stationarity trees sampled in a Bayesian analysis of the combined sequence data), they were not concerned specifically with evaluating particular nodes in their phylogeny (inasmuch as ancestral state reconstructions were invariable across a substantial proportion of sampled trees). In the present chapter, I extend Skinner *et al*.'s (2007) phylogenetic analysis, assessing congruence among independent data partitions and considering different methods for estimating phylogeny. My primary concern is elucidating phylogenetic relationships (as opposed to the evolution of limb morphology), and the consistency of inferred clades with previous phylogenetic hypotheses is discussed at length. Additionally, I present preliminary evidence for unrecognised species within *Lerista*, indicating possible areas of future study.

4.2. Materials and Methods

The data employed in the phylogenetic analyses comprise ATP synthetase-β subunit intron, 12S rRNA, 16S rRNA, and ND4 and adjacent tRNA-His, tRNA-Ser, and tRNA-Leu nucleotide sequences for the 72 species of *Lerista* considered by Skinner *et al*. (2007), five subspecies not included in Skinner *et al*.'s (2007) analysis (*L. microtis intermedia*, *L. microtis schwaneri*, *L. macropisthopus galea*, *L. macropisthopus macropisthopus*, and *L. macropisthopus remota*), and six outgroup taxa (*Anomalopus leuckartii*, *Calyptotis lepidorostrum*, *Coggeria naufragus*, *Ctenotus robustus*, *Eulamprus kosciuskoi*, and *Glaphyromorphus fuscicaudis*) (see Appendix 6). Sequences for the additional subspecies were obtained as described by Skinner (2007). The outgroup taxa were selected based on Reeder (2003) and Skinner (2007).

Alignment of ND4 sequences did not require the insertion of internal gaps and was straightforward. 12S, 16S, and tRNA sequences were initially aligned with Clustal X (Thompson *et al*., 1997) assuming the default pairwise and multiple alignment parameter values. Adjustments to alignments were made with the aid of secondary-structure models (Wuyts *et al*., 2001, 2002; Macey and Verma, 1997). ATP synthetase-β subunit intron sequences were aligned with Clustal X using the default settings.

Parsimony and Bayesian phylogenetic analyses, implemented in PAUP* (Swofford, 1999) and MrBayes (Ronquist and Huelsenbeck, 2003), respectively, were performed for the mitochondrial DNA and intron sequences separately and for the combined data. A heuristic search strategy was adopted in the parsimony analyses, employing random stepwise sequence addition (100 replicates) and tree bisection and reconnection branch swapping. A limit of 2×10^6 rearrangements per addition sequence replicate was imposed for the intron sequence analysis to reduce computation time. Branch support (Bremer, 1988, 1994), calculated using TreeRot (Sorenson, 1999), and non-parametric bootstrapping (1000 replicates, each with 10

random stepwise sequence addition replicates), executed using PAUP*, were employed in assessing support for nodes. For the Bayesian analyses, I partitioned the sequence data according to locus and (for ND4 sequences) codon position (the tRNAs were combined in a single partition due to their short length and functional similarity), specifying nucleotide substitution models for partitions separately. An appropriate substitution model for each partition was selected on the basis of hierarchical likelihood-ratio tests, performed using MrModeltest (Nylander, 2002). All Bayesian analyses consisted in running four incrementally-heated Markov chains (with the default temperature parameter value, 0.2), initiated with random starting trees and default priors, for 10^7 generations, sampling every 1000^{th} generation. The number of generations required to attain stationarity was estimated by examining cumulative posterior probabilities for clades, plotted using AWTY (Wilgenbusch *et al*., 2004). All trees sampled prior to attaining stationarity were discarded and the remaining trees used to compute a majority-rule consensus topology, mean branch lengths, and posterior probabilities for nodes.

As a means of evaluating congruence (or incongruence) among data partitions, I used TreeRot (Sorenson, 1999) to calculate partitioned branch support (Baker and DeSalle, 1997) for clades retrieved in the parsimony analysis of the combined mitochondrial DNA and intron sequences. Additionally, I constructed 95% credible sets of unique trees for the mitochondrial DNA and intron data sets from trees sampled after attaining stationarity in the separate Bayesian analyses and determined whether clades supported by one data set were consistent with one or more trees of the credible set for the other data set; if so, the data sets were considered to exhibit no significant incongruence (see Buckley *et al*., 2002; Reeder, 2003).

4.3. Results

The combined sequence data consist of 2868 aligned sites, of which 1483 are invariable, 1018 are parsimony-informative, and 367 are variable but uninformative under parsimony. The numbers of aligned sites, variable and parsimony-informative sites, and unique site patterns for all data partitions are presented in Table 4.2. Table 4.3 presents the selected nucleotide substitution model and model parameter estimates for each partition. An examination of cumulative posterior probabilities for nodes indicated that in all Bayesian analyses, stationarity had been attained by 6×10^6 generations.

Parsimony analysis of the mitochondrial DNA sequence data yielded 22 equally parsimonious trees (length = 7670 steps), a strict consensus of which (not shown) differs only negligibly from the majority-rule consensus of trees sampled after attaining stationarity in the Bayesian analysis (Fig. 4.1). A number of clades are moderately to strongly supported and largely coincident with species groups recognised by previous authors (see Table 4.1 and Section 4.4): the *bipes* species group, composed of *L. bipes*, *L. greeri*, *L. griffini*, *L. ips*, *L. labialis*, *L. robusta*, *L. simillima*, and *L. vermicularis*; the *macropisthopus* species group, including *L. axillaris*, *L. desertorum*, *L. eupoda*, *L. gerrardii*, *L. macropisthopus fusciceps*, *L. m. galea*, *L. m. macropisthopus*, *L. m. remota*, *L. neander*, and *L. puncticauda*; the *nichollsi* species group, composed of *L. connivens*, *L. gascoynensis*, *L. kendricki*, *L. kennedyensis*, *L. lineopunctulata*, *L. nichollsi*, *L. onsloviana*, *L. petersoni*, *L. uniduo*, *L. varia*, and *L. yuna*; the *orientalis* species group, composed of *L. aericeps*, *L. ingrami*, *L. orientalis*, *L. taeniata*, *L. xanthura*, and *L. zonulata*; and the *terdigitata* species group, including *L. elongata*, *L. speciosa*, *L. terdigitata*, and *L. tridactyla*. Clades comprising *L. ameles*, *L. cinerea*, and *L. wilkinsi*, *L. arenicola*, *L. microtis intermedia*, *L. m. microtis*, and *L. m. schwaneri*, *L. baynesi*, *L. edwardsae*, and *L. picturata*, *L. borealis* and *L. walkeri*, *L. bougainvillii* and *L. viduata*, *L. chordae*, *L. fragilis*, and *L. frosti*, *L. distinguenda* and *L. elegans*, *L. emmotti* and *L. punctatovittata*, *L. flammicauda* and *L. zietzi*, *L. haroldi* and *L. muelleri*, and *L. humphriesi*

Table 4.2

Numbers of aligned sites, variable sites, parsimony-informative sites, and unique site patterns for partitions employed in the Bayesian analyses.

Partition	Aligned sites	Variable sites	Parsimony-informative sites	Unique site patterns
12S rRNA	903	432	342	506
16S rRNA	548	220	148	260
ND4, 1st codon position	228	110	84	131
ND4, 2nd codon position	229	33	19	60
ND4, 3rd codon position	229	226	219	229
tRNAs	142	82	60	112
ATP synthetase-β subunit	589	282	146	408

and *L. praepedita* are also well supported. There is moderate to strong support for sister group relationships of the *macropisthopus* and *orientalis* species groups, the *nichollsi* species group and the *L. humphriesi* + *L. praepedita* clade, and the *L. borealis* + *L. walkeri* and *L. chordae* + *L. fragilis* + *L. frosti* clades. A sister group relationship of the *bipes* species group and *L. apoda* is strongly supported in the Bayesian analysis, as are monophyletic groups composed of the *L. ameles* + *L. cinerea* + *L. wilkinsi* clade, *L. carpentariae*, *L. karlschmidtii*, and *L. stylis*, the *L. distinguenda* + *L. elegans* clade, *L. christinae*, *L. lineata*, and *L. planiventralis*, and the *L. haroldi* + *L. muelleri* clade, *L. allochira*, and *L. stictopleura*. A large clade incorporating the *bipes*, *macropisthopus*, and *orientalis* species groups, the *L. ameles* + *L. cinerea* + *L. wilkinsi*, *L. borealis* + *L. walkeri*, and *L. chordae* + *L. fragilis* + *L. frosti* clades, *L. apoda*, *L. carpentariae*, *L. kalumburu*, *L. karlschmidti*, and *L. stylis* is well supported in both analyses. The *macropisthopus* and *orientalis* species groups and the *L. borealis* + *L. walkeri* and *L. chordae* + *L. fragilis* + *L. frosti* clades compose a monophyletic group within this clade that is significantly supported in the Bayesian analysis. Posterior

Table 4.3

Selected nucleotide substitution model and parameter estimates (mean values followed by 95% credible intervals in parentheses) for partitions employed in the Bayesian analyses (parameter estimate values are for the combined analysis).

Model selected

12S rRNA	GTR + I + Γ
16S rRNA	GTR + I + Γ
ND4, 1st codon position	GTR + I + Γ
ND4, 2nd codon position	HKY85 + I + Γ
ND4, 3rd codon position	GTR + Γ
tRNAs	HKY85 + I + Γ
ATP synthetase-β subunit	HKY85 + Γ

Parameter estimates

Nucleotide frequencies

	π_A	π_C	π_G	π_T
12S rRNA	0.405 (0.378-0.431)	0.284 (0.263-0.312)	0.125 (0.109-0.142)	0.186 (0.148-0.207)
16S rRNA	0.421 (0.386-0.456)	0.254 (0.226-0.286)	0.142 (0.114-0.171)	0.182 (0.158-0.209)
ND4, 1st codon position	0.395 (0.344-0.449)	0.339 (0.293-0.388)	0.154 (0.117-0.194)	0.112 (0.089-0.137)
ND4, 2nd codon position	0.160 (0.117-0.208)	0.315 (0.264-0.369)	0.119 (0.085-0.156)	0.406 (0.352-0.461)
ND4, 3rd codon position	0.532 (0.483-0.581)	0.271 (0.236-0.310)	0.056 (0.048-0.067)	0.140 (0.118-0.167)
tRNAs	0.381 (0.320-0.439)	0.239 (0.197-0.283)	0.126 (0.098-0.157)	0.254 (0.211-0.300)
ATP synthetase-β subunit	0.277 (0.252-0.302)	0.180 (0.157-0.203)	0.227 (0.202-0.252)	0.317 (0.290-0.345)

Substitution rates

	A↔C	A↔G	A↔T	C↔G	C↔T
12S rRNA	4.709 (1.882-10.357)	32.021 (14.432-69.675)	4.646 (2.160-9.804)	1.054 (0.207-2.788)	36.329 (17.139-76.814)
16S rRNA	5.440 (1.942-11.884)	16.282 (6.575-34.397)	4.794 (1.709-10.454)	0.435 (0.016-1.466)	31.578 (11.624-67.464)
ND4, 1st codon position	0.252 (0.115-0.491)	1.579 (0.835-2.851)	0.335 (0.107-0.769)	0.024 (0.010-0.069)	13.650 (7.201-24.658)
ND4, 2nd codon position			κ = 23.192 (10.552-51.280)		
ND4, 3rd codon position	0.764 (0.258-2.411)	12.072 (4.437-37.154)	1.127 (0.361-3.610)	1.531 (0.485-5.120)	11.867 (4.587-35.564)
tRNAs			κ = 14.179 (10.758-18.274)		
ATP synthetase-β subunit			κ = 3.435 (2.854-4.121)		

Among-site rate heterogeneity

	I	α
12S rRNA	0.370 (0.324-0.421)	0.545 (0.468-0.631)
16S rRNA	0.475 (0.425-0.525)	0.525 (0.445-0.606)
ND4, 1st codon position	0.318 (0.235-0.393)	0.476 (0.374-0.590)
ND4, 2nd codon position	0.665 (0.583-0.741)	0.164 (0.133-0.213)
ND4, 3rd codon position	-	0.953 (0.714-1.401)
tRNAs	0.257 (0.118-0.367)	0.605 (0.420-0.810)
ATP synthetase-β subunit	-	0.152 (0.125-0.251)

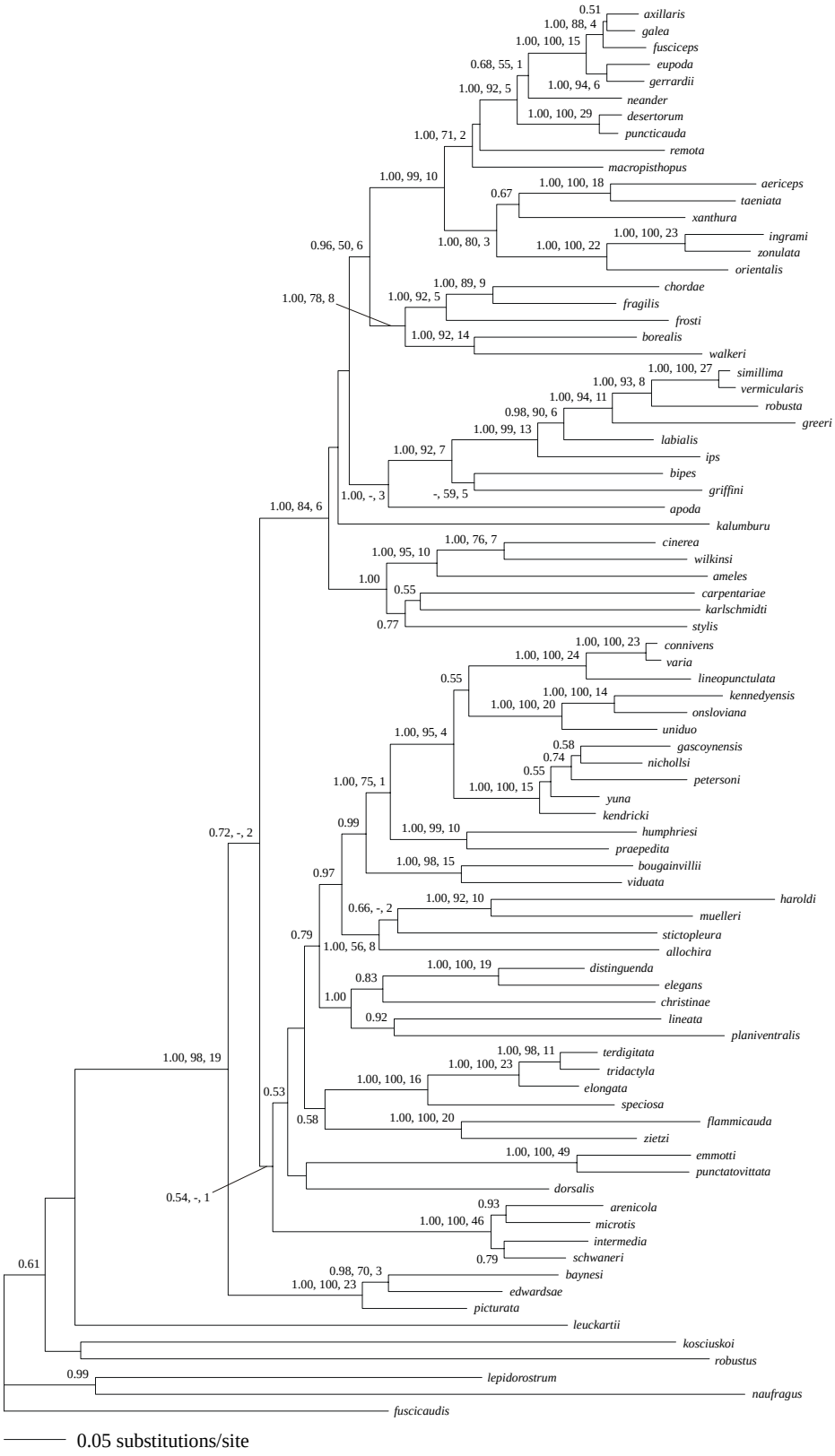

Figure 4.1. Bayesian majority-rule consensus for the mitochondrial DNA sequence data. Posterior probabilities ≥0.50 are shown adjacent to nodes; for nodes present in the parsimony strict consensus, posterior probabilities are followed by bootstrap values ≥50 and branch support values.

probabilities for a clade including the *nichollsi* species group and the *L. bougainvillii* + *L. viduata* and *L. humphriesi* + *L. praepedita* clades, and a sister group relationship of this clade and the *L. allochira* + *L. haroldi* + *L. muelleri* + *L. stictopleura* clade are also significant. *Lerista macropisthopus macropisthopus* and *L. m. remota* are separated from *L. m. fusciceps* and *L. m. galea* by two strongly-supported nodes, rendering *L. macropisthopus* non-monophyletic.

All clades appearing in a strict consensus of 169442 equally parsimonious trees (length = 493 steps) obtained in the parsimony analysis of the ATP synthetase-β subunit intron sequences (not shown) are also present in the Bayesian majority-rule consensus (Fig. 4.2). Several moderately- to strongly-supported clades are consistent with those recovered in the mitochondrial DNA sequence analyses (see Fig. 4.1) and include the *terdigitata* species group, a clade composed of all species of the *bipes* species group except *L. bipes* and *L. griffini*, a clade comprising all species and subspecies of the *macropisthopus* species group except *L. macropisthopus macropisthopus* and *L. m. remota*, a clade composed of all species of the *nichollsi* species group except *L. kennedyensis*, *L. onsloviana*, and *L. uniduo*, and clades comprising *L. ameles*, *L. cinerea*, and *L. wilkinsi*, *L. borealis* and *L. walkeri*, *L. bougainvillii* and *L. viduata*, *L. carpentariae* and *L. karlschmidtii*, *L. distinguenda* and *L. elegans*, *L. haroldi* and *L. muelleri*, *L. kennedyensis*, *L. onsloviana*, and *L. uniduo*, *L. microtis microtis* and *L. m. schwaneri*, and *L. macropisthopus macropisthopus* and *L. m. remota*. *Lerista chordae*, *L. fragilis*, *L. frosti*, *L. ingrami*, *L. orientalis*, *L. taeniata*, and *L. zonulata* compose a strongly-supported clade, contradicting monophyly of the *orientalis* species group and a sister group relationship of the *L. borealis* + *L. walkeri* and *L. chordae* + *L. fragilis* + *L. frosti* clades (cf. Fig. 4.1). A well-supported clade incorporating *L. arenicola* and *L. microtis intermedia* is inconsistent with monophyly of *L. microtis*. Monophyletic groups comprising *L. aericeps*, *L. flammicauda*, *L. planiventralis*, *L. xanthura*, and *L. zietzi*, *L. carpentariae*, *L. kalumburu*, *L. karlschmidtii*, and *L. stylis*, *L. emmotti* and *L. punctatovittata*, and *L.*

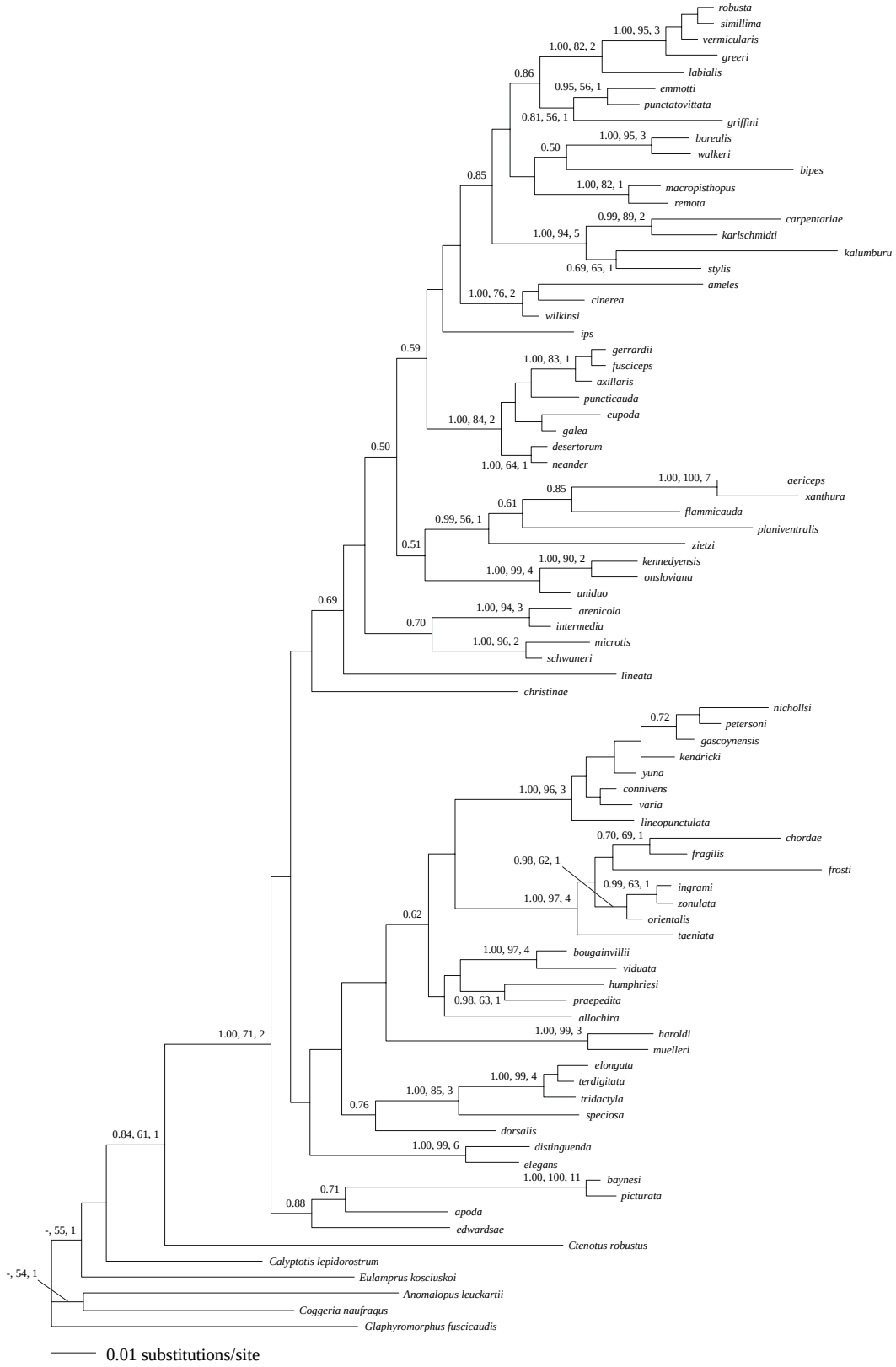

Figure 4.2. Bayesian majority-rule consensus for the ATP synthetase-β subunit intron sequence data. Posterior probabilities ≥0.50 are shown adjacent to nodes; for nodes present in the parsimony strict consensus, posterior probabilities are followed by bootstrap values ≥50 and branch support values.

humphriesi and *L. praepedita* are well supported in the Bayesian analysis. Although not present in the Bayesian majority-rule consensus, several clades indicated by the mitochondrial DNA sequence data appear in the 95% credible set of trees for the intron sequence data, including the *macropisthopus* species group and the *L. allochira* + *L. haroldi* + *L. muelleri* (+ *L. stictopleura*), *L. baynesi* + *L. edwardsae* + *L. picturata*, and *L. flammicauda* + *L. zietzi* clades; however, many other clades are absent from the 95% credible set of trees (Table 4.4). A number of clades strongly supported by the intron sequence data do not appear in the 95% credible set of trees for the mitochondrial DNA sequence data (Table 4.4).

As for the separate analyses, a strict consensus of three equally parsimonious trees (length = 8255 steps) obtained in the parsimony analysis of the combined sequence data (Fig. 4.3) does not differ significantly from the Bayesian majority-rule consensus (Fig. 4.4). All clades moderately to strongly supported in the mitochondrial DNA sequence analyses are also well supported by the combined sequence data. Moreover, there is significant support in the Bayesian analysis for a clade composed of *L. carpentariae*, *L. karlschmidti*, and *L. stylis*, and sister group relationships of *L. lineata* and *L. planiventralis*, *L. arenicola* and *L. microtis intermedia*, and *L. microtis microtis* and *L. m. schwaneri*. A clade including the *nichollsi* species group, the *L. allochira* + *L. haroldi* + *L. muelleri* + *L. stictopleura*, *L. bougainvillii* + *L. viduata*, *L. distinguenda* + *L. elegans*, *L. humphriesi* + *L. praepedita*, and *L. lineata* + *L. planiventralis* clades, *L. christinae*, and *L. dorsalis* is also significantly supported in the Bayesian analysis. Partitioned branch support values indicate minimal incongruence between the mitochondrial DNA and intron sequence data (Table 4.5), and branch support and bootstrap values are generally higher than those derived from the mitochondrial DNA sequence data alone (see Fig. 4.1). Notably, the *orientalis* species group and a monophyletic group composed of the *L. borealis* + *L. walkeri* and *L. chordae* + *L. fragilis* + *L. frosti* clades exhibit positive partitioned branch support values for the intron sequence data, despite being inconsistent with the results of the intron sequence analysis (see Fig. 4.2 and above).

Table 4.4

Assessment of congruence for selected clades (see text). For clades recovered in the mitochondrial DNA sequence analysis, 'Number of consistent trees' is the number of trees of the 95% credible set for the ATP synthetase-β subunit intron sequence analysis in which the clade is present, and vice versa.

	Number of consistent trees
Clades present in Bayesian majority-rule consensus for mitochondrial DNA sequence data (see Fig. 4.1)	
allochira + *haroldi* + *muelleri*	12
ameles + *carpentariae* + *cinerea* + *karlschmidti* + *stylis* + *wilkinsi*	0
baynesi+ *edwardsae* + *picturata*	473
bipes species group	0
bipes species group + *apoda*	0
bipes species group + *orientalis* species group + *macropisthopus* species group + *ameles* + *apoda* + *borealis* + *carpentariae* + *chordae* + *cinerea* + *fragilis* + *frosti* + *kalumburu* + *karlschmidti* + *stylis* + *walkeri* + *wilkinsi*	0
borealis + *chordae* + *fragilis* + *frosti* + *walkeri*	0
christinae + *distinguenda* + *elegans* + *lineata* + *planiventralis*	0
flammicauda + *zietzi*	388
macropisthopus species group	11
nichollsi species group	0
nichollsi species group + *humphriesi* + *praepedita*	0
orientalis species group	0
orientalis species group + *macropisthopus* species group	0
Clades present in Bayesian majority-rule consensus for ATP synthetase-β subunit intron sequence data (see Fig. 4.2)	
carpentariae + *kalumburu* + *karlschmidti* + *stylis*	0
chordae + *fragilis* + *frosti* + *ingrami* + *orientalis* + *taeniata* + *zonulata*	0

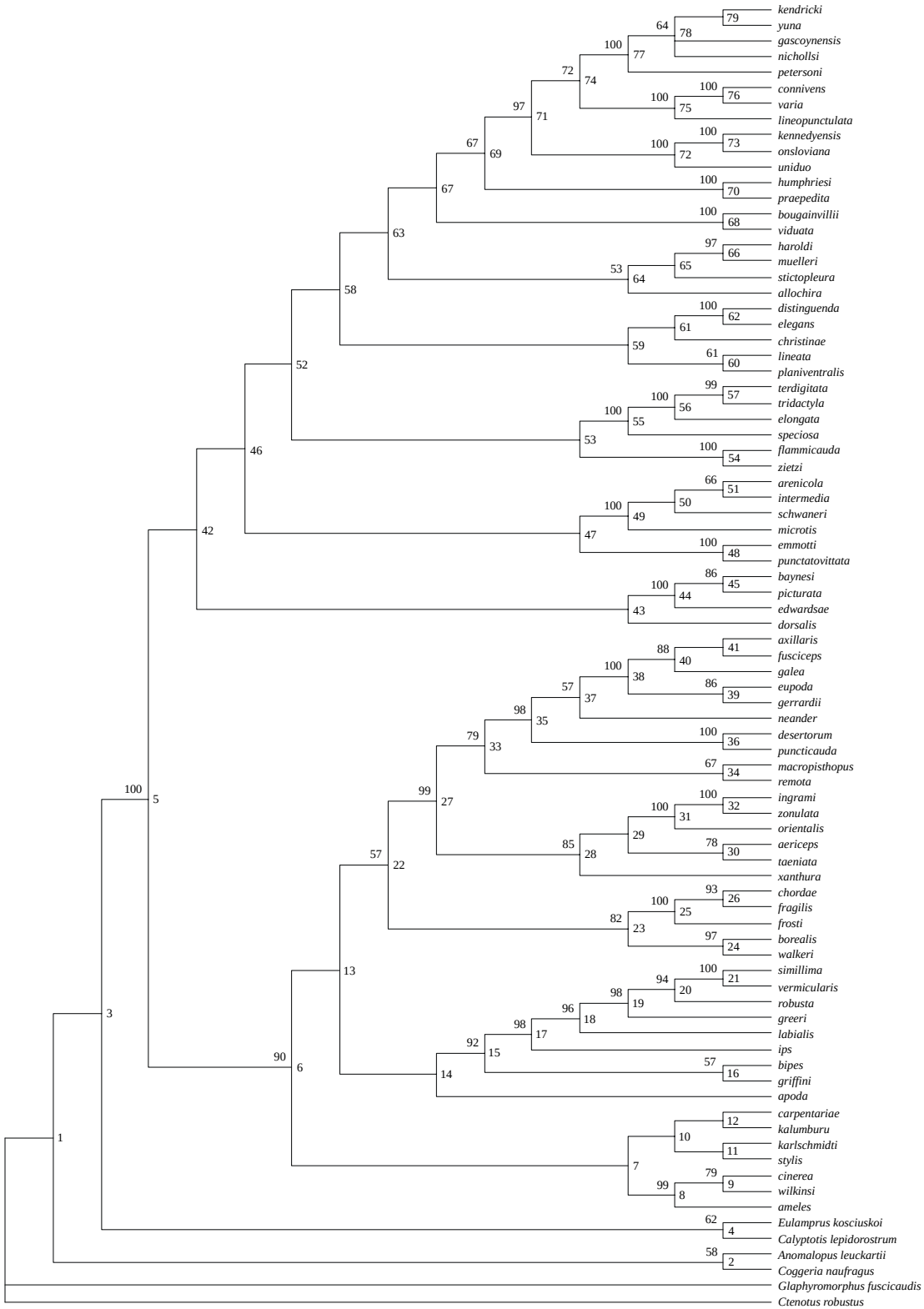

Figure 4.3. Parsimony strict consensus for the combined sequence data. Bootstrap values ≥50 are shown to the left of nodes. Node numbers, shown to the right, correspond with those in Table 4.5.

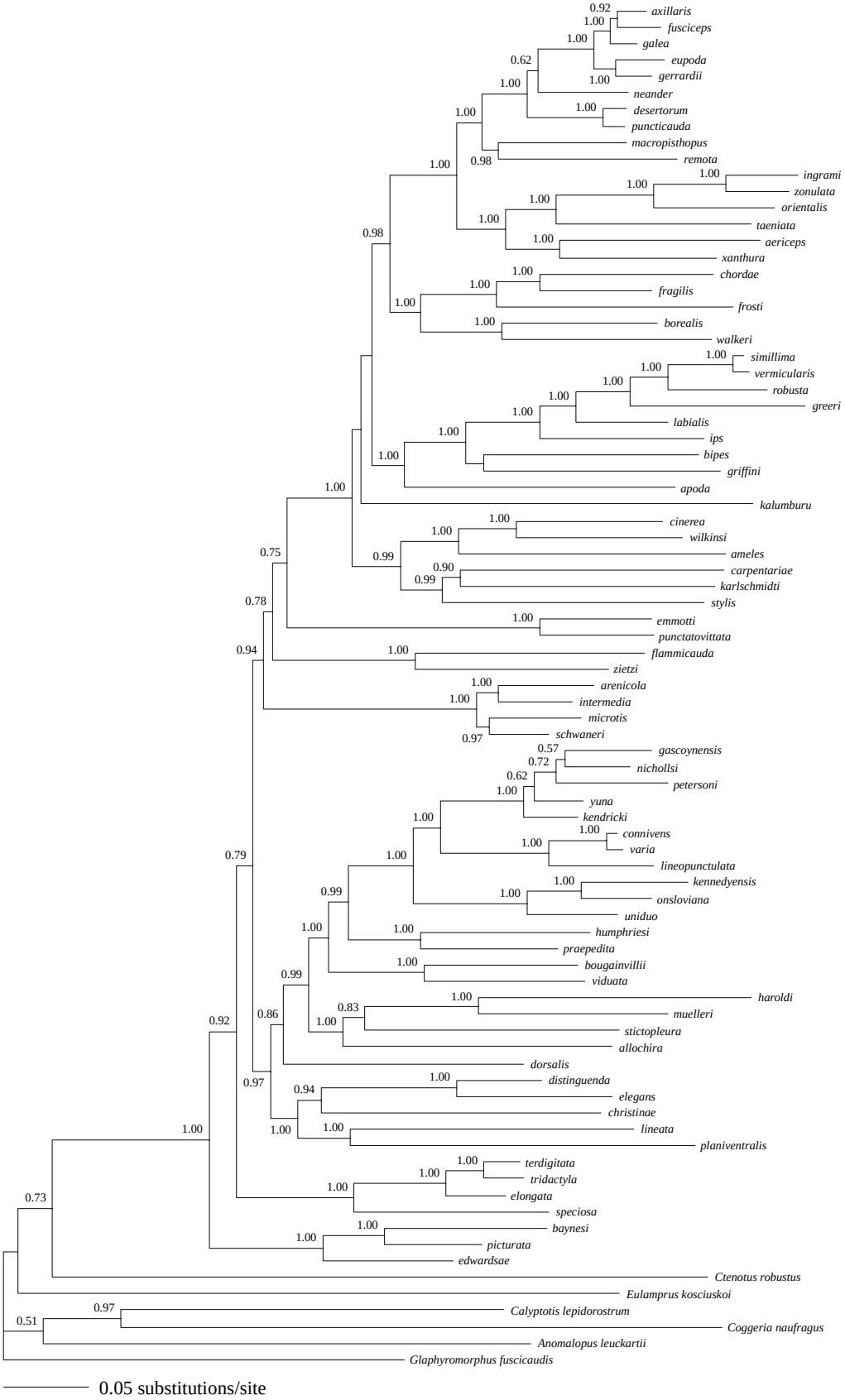

Figure 4.4. Bayesian majority-rule consensus for the combined sequence data. Posterior probabilities ≥0.50 are shown adjacent to nodes.

Table 4.5

Partitioned branch support values for clades present in the parsimony strict consensus for the combined sequence data (see Fig. 4.3). Node numbers correspond with those in Figure 4.3.

Node	12S rRNA	16S rRNA	ND4, 1st position	ND4, 2nd position	ND4, 3rd position	tRNAs	Mitochondrial DNA (total)	ATP synthetase-β subunit	All partitions (total)
1	3	2	1	0	0	-3	3	-2	1
2	3.7	0.7	0.3	0.7	1.7	-0.7	6.4	0.7	7.1
3	3	2	1	0	0	-3	3	-2	1
4	2	-4	0.7	0	4.7	2	5.4	1.7	7.1
5	11	10	0	2	2	-1	24	0	24
6	5.5	7	2.5	2	-10.5	3.2	9.7	0.2	9.9
7	-1	0.5	2.5	-0.5	-5.5	0	-4	6	2
8	5.5	2.9	3	-0.3	-8.2	2	4.9	9	13.9
9	8	-5	0	2	1	1	7	0	7
10	-1	0.5	2.5	-0.5	-5.5	0	-4	6	2
11	3.1	5	1.7	1.2	-5.6	-4.3	1.1	1.9	3
12	2.4	6.2	1.3	1.1	-5.9	-3.6	1.5	1.5	3
13	7	9	2	2	-9	-8	3	0	3
14	7	9	2	2	-9	-8	3	0	3
15	5.1	5.1	-3.2	0.8	5.8	-4.2	9.4	-0.2	9.2
16	7	9	2	2	-9	-8	3	0	3
17	3	0	2	1	6	2	14	-1	13
18	8.8	1.8	0.5	0.5	-2.8	-1.8	7	2	9
19	5	0	1	0	3	1	10	3	13
20	1	-1	3	0	3	2	8	0	8
21	6	3	3	1	13	1	27	0	27
22	4.3	0.9	1.2	0.8	-4.6	2.6	5.2	-0.1	5.1
23	9.3	9.4	-0.4	0.9	-3.5	-8.4	7.3	1.7	9
24	5	12	-1	0	-2	-3	11	5	16
25	0.5	3	2	0.5	-1	2	7	9	16
26	2	3	5	0	3	-2	11	1	12
27	7.7	6.4	0.7	0.5	-5.4	-1.2	8.7	3.3	12
28	2	0	0	0	-1	0	1	2	3
29	-1	-1	-1	0	3	0	0	1	1
30	6	3	1	0	12	2	24	-19	5
31	13	2	1	0	8	1	25	3	28
32	11	6	-1	0	7	0	23	1	24
33	2	2.5	-2	0.5	-2	3.5	4.5	2.5	7
34	-2	1	-2	0	2	0	-1	3	2
35	5.5	-2	0	0	2	0	5.5	4.5	10
36	15	4	1	1	7	1	29	0	29
37	-1.5	0	1	0	1	0	0.5	0.5	1
38	4.7	1.7	2	0	7	0	15.4	0.7	16.1
39	0	0	0	0	5	0	5	-1	4
40	-0.5	0	1	0	3	0	3.5	0.5	4
41	-1.5	0	0.5	0	1	0	0	1	1
42	3.3	6.1	0.9	1.6	-3.5	-4.2	4.2	-2.2	2
43	1	2.1	1.4	1	-4.6	0.5	1.4	-0.4	1
44	15	6	5	1	-5	0	22	2	24
45	4	-1	2	1	-14.8	-0.2	-9	14	5

46	5.3	1.3	2.7	1	-9.7	1	1.6	-0.7	0.9
47	-3.5	3.5	3	1.5	-1.5	0.5	3.5	-1.5	2
48	16.5	11	6	2.5	10	4.5	50.5	2.5	53
49	17	14	11	3	0	-3	42	1	43
50	-0.3	5.3	0.3	1	4	-5.3	5	-2	3
51	-2	1.5	1	0.5	0	0	1	3	4
52	2.2	1.4	1.6	0.8	-5.2	0.6	1.4	-0.4	1
53	3	1.7	1.9	1	-6.9	0.6	1.3	-0.4	0.9
54	11.5	7.5	2	2	-6	4	21	3	24
55	9	3	1	1	7	-5	16	3	19
56	12	3	4	1	5	-4	21	2	23
57	11.3	2.3	3.7	1	-10.7	3	10.6	-0.7	9.9
58	5.3	1.3	2.7	1	-9.7	1	1.6	-0.7	0.9
59	5.3	1.3	2.7	1	-9.7	1	1.6	-0.7	0.9
60	4.2	3.5	0.7	0.2	-4	-4.8	-0.2	3.3	3.1
61	5.3	1.3	2.7	1	-9.7	1	1.6	-0.7	0.9
62	9.8	3.5	7.7	0.8	-3.4	1.2	19.6	9.4	29
63	7	0	3	1	-9.5	-0.5	1	0	1
64	1	5	3	1	-8	6	8	-3	5
65	-1	2	0	0	2	-2	1	0	1
66	1	0	0	0	8	2	11	0	11
67	7	0	3	1	-9.5	-0.5	1	0	1
68	5.9	6.5	2.5	1.4	-1.4	1.8	16.7	4.4	21.1
69	4.3	2.4	-0.3	0	-2.9	-3.5	0	2.9	2.9
70	7.5	3	-0.5	0	6	-2	14	3	17
71	6.1	4.3	0.7	0.5	-4.1	-0.5	7	1	8
72	10.3	1.5	4.5	1.5	2.8	1	21.6	8.4	30
73	2.3	3.3	0.7	1	2.7	1	11	2	13
74	1.3	-2.7	-2.3	0	0.7	0	-3	5	2
75	7.8	5.8	0.2	2	4.2	3	23	0	23
76	9.8	0.8	1.2	1	10.2	1	24	0	24
77	7.3	0.3	-0.3	0	5.7	0	13	1	14
78	-0.2	0.3	4.2	0	-0.8	-1.5	2	0	2
79	0.3	0.3	0.7	0	-0.3	0	1	0	1

4.4. Discussion

Miyamoto and Fitch (1995) have argued that congruence among phylogenies for independent data partitions affords among the most convincing evidence for inferred phylogenetic relationships (see also Swofford, 1991). Data partitions that are potentially subject to disparate modes or patterns of evolution as a consequence of, for example, differing phylogenetic histories (as may be the case for unlinked genes), nucleotide substitution rates, or functions ('process partitions' as defined by Miyamoto and Fitch [1995]), may be expected

to often produce significantly different estimates of phylogeny and, accordingly, can (to a varying extent) be considered evidentially independent. Agreement among phylogenies inferred from such data partitions may be far more readily explained by a shared underlying history than causes such as lineage sorting of ancestral polymorphism, horizontal gene transfer, or error in estimating phylogenetic relationships independently yielding similar topologies. There is thus considerable support for clades recovered in both the mitochondrial DNA and ATP synthetase-β subunit intron sequence analyses, including the *terdigitata* species group and the *L. ameles* + *L. cinerea* + *L. wilkinsi*, *L. borealis* + *L. walkeri*, *L. bougainvillii* + *L. viduata*, *L. carpentariae* + *L. karlschmidtii*, *L. distinguenda* + *L. elegans*, *L. emmotti* + *L. punctatovittata*, *L. haroldi* + *L. muelleri*, and *L. humphriesi* + *L. praepedita* clades.

Although several clades strongly supported in the separate analyses of the mitochondrial DNA and intron sequence data are incongruent (cf. Figs. 4.1 and 4.2, and see Table 4.4), partitioned branch support values reveal minimal antagonism between these data partitions in the combined parsimony analysis (see Table 4.5). Moreover, (total) branch support and bootstrap values are generally higher in the combined analysis than in the separate analysis of the mitochondrial DNA sequence data (which yields a similar tree topology), indicating that the intron sequence data provide additional support for clades recovered in the mitochondrial DNA sequence analysis when the two data partitions are combined (nearly invariably, posterior probabilities for clades strongly supported by the mitochondrial DNA sequence data are very close to unity for the combined data, so that the intron sequence data at least do not conflict noticeably with the mitochondrial DNA sequence data in the combined Bayesian analysis). Many authors have noted that data partitions yielding discordant trees when analysed separately may contribute substantially to support for (perhaps novel) clades inferred in a combined analysis (e.g., Barrett *et al*., 1991; Baker and DeSalle, 1997; Gatesy *et al*., 1999; Gatesy and Baker, 2005); 'In these cases, true but weak

phylogenetic signal may be ... amplified over the noise when data are combined' (Baker and DeSalle, 1997, p. 665). Considering that differing phylogenetic histories constitute a primary potential cause of incongruence for data partitions representing unlinked genes (see Avise, 2000, pp. 323-327), evidence for concordant phylogenetic signal from a combined analysis of these partitions may be as cogent (or nearly so) as that from separate analyses (this argument assumes that the influence of noise, but not conflicting phylogenetic signal, will be reduced by combining the partitions). Accordingly, there is substantial support for clades that are strongly supported in the combined analyses and exhibit positive partitioned branch support values for the mitochondrial DNA and intron sequence data; these include the *macropisthopus*, *nichollsi*, and *orientalis* species groups, the *L. arenicola* + *L. microtis intermedia* + *L. m. microtis* + *L. m. schwaneri*, *L. baynesi* + *L. edwardsae* + *L. picturata*, *L. chordae* + *L. fragilis* + *L. frosti*, and *L. flammicauda* + *L. zietzi* clades, monophyletic groups comprising the *macropisthopus* and *orientalis* species groups, the *nichollsi* species group and the *L. humphriesi* + *L. praepedita* clade, and the *L. borealis* + *L. walkeri* and *L. chordae* + *L. fragilis* + *L. frosti* clades, and a large clade composed of the *bipes*, *macropisthopus*, and *orientalis* species groups, the *L. ameles* + *L. cinerea* + *L. wilkinsi*, *L. borealis* + *L. walkeri*, *L. carpentariae* + *L. karlschmidti*, and *L. chordae* + *L. fragilis* + *L. frosti* clades, *L. apoda*, *L. kalumburu*, and *L. stylis*.

Aside from those clades supported by both the mitochondrial DNA and intron sequence data in the separate or combined analyses, there are several monophyletic groups that are moderately to strongly supported by the mitochondrial DNA and combined sequence data that do not significantly conflict with the intron sequence data, being consistent with a strict consensus of equally parsimonious trees obtained in the parsimony analysis and one or more trees of the 95% credible set of trees derived from the Bayesian analysis, or exhibiting partitioned branch support values that are equal to zero or only slightly negative (greater than -1). Following Wiens (1998), these monophyletic groups are also regarded as well supported and include the *bipes* species group, the *L. allochira* + *L. haroldi* + *L. muelleri* + *L.*

stictopleura clade, and clades comprising the *bipes* species group and *L. apoda*, the *macropisthopus* and *orientalis* species groups and the *L. borealis* + *L. walkeri* and *L. chordae* + *L. fragilis* + *L. frosti* clades, the *nichollsi* species group and the *L. bougainvillii* + *L. viduata* and *L. humphriesi* + *L. praepedita* clades, this clade and the *L. allochira* + *L. haroldi* + *L. muelleri* + *L. stictopleura* clade, and the *L. distinguenda* + *L. elegans* clade, *L. christinae*, *L. lineata*, and *L. planiventralis*.

The above conclusions are largely consistent with those of previous authors. Greer (1986) presented an extensive list of apomorphic character states diagnosing a putative clade of nine small, elongate species possessing extremely reduced (externally imperceptible) forelimbs and didactyl hindlimbs (*L. bipes*, *L. greeri*, *L. griffini*, *L. ips*, *L. labialis*, *L. praefrontalis*, *L. simillima*, and *L. vermicularis*; *L. robusta* was described subsequently by Storr [1990]) that he designated the *bipes* species group. Among these character states, a reduced number of cervical vertebrae (seven, as opposed to the usual eight for scincids) was considered by Greer (1986, p. 122) to be 'especially significant in identifying the *bipes* group as monophyletic because it is not known to occur elsewhere in the family except in the African scincine lineage *Melanoseps – Typhlacontias – Scolecoseps – Feylinia*, in the African lygosomine *Eumecia*, and in the Australian lygosomine *Anomalopus brevicollis*'. Monophyly of the *bipes* species group, as conceived of by Greer (1986), is strongly supported by the separate analyses of the mitochondrial DNA sequence data and the combined analyses. Although this group does not appear in the 95% credible set of trees for the intron sequence data (see Table 4.4), a partitioned branch support value of -0.2 obtained in the combined parsimony analysis indicates only minor conflict between the mitochondrial DNA and intron data partitions (indeed, greater incongruence is observed among partitions of the mitochondrial DNA sequence data, which are known to have the same phylogenetic history; see Table 4.5).

As noted by Greer (1986), Storr's (1984) diagnosis of the *nichollsi* species group, erected to accommodate four small to moderately large, elongate species having highly reduced forelimbs (lacking digits) and didactyl hindlimbs (*L. connivens*, *L. nichollsi* [including *L. petersoni* as a subspecies], *L. onsloviana*, and *L. uniduo*), consists only of plesiomorphic character states (possession of prefrontals and a forelimb groove). Nonetheless, Greer (1986, p. 122) observed that these species 'share an unusual character which may be indicative of their close relationship', namely very loosely attached, or 'tear-away', scales, which were noted to 'occur otherwise in skinks only in a few *Ctenotus*'. A monophyletic group including *L. connivens*, *L. nichollsi*, *L. petersoni* (considered by Storr [1991a] and succeeding authors as a species), *L. onsloviana*, and *L. uniduo*, an additional seven species (*L. gascoynensis*, *L. kendricki*, *L. kennedyensis*, *L. maculosa*, *L. talpina*, *L. varia*, and *L. yuna*), described by Storr (1986, 1991a) and Kendrick (1989) and referred to the *nichollsi* species group, and *L. lineopunctulata* is strongly supported by the analyses presented here. *Lerista lineopunctulata*, a large, elongate species with greatly reduced forelimbs (without digits) and mono- or didactyl hindlimbs, was not included in any of the species groups recognised by Storr (1971), and was considered as the sole representative of Storr *et al*.'s (1999) *lineopunctulata* group. Interestingly, Storr (1986) noted that many specimens of *L. varia* were referred to *L. lineopunctulata* prior to the recognition of the former species (which was confidently placed in the *nichollsi* species group). The position of *L. lineopunctulata* within a subclade of the *nichollsi* species group is strongly supported in all of my analyses, indicating that Storr's (1984) and Greer's (1986) conception of this group must be modified (although only slightly) if it is to be rendered consistent with phylogeny.

Greer (1990b) recognised a putatively monophyletic group of four small species possessing tetra- or tridactyl limbs and a spectacle (*L. muelleri*, *L. orientalis*, *L. taeniata*, and *L. xanthura* [regarded by Greer as incorporating *L. aericeps*]; Storr [1991b] subsequently described *L. ingrami* and *L. zonulata*), designated the *orientalis* species group. Many of the proposed apomorphies diagnosing this group are also present in *L. christinae*, *L.*

distinguenda, *L. elegans*, *L. haroldi*, *L. lineata*, *L. separanda*, and *L. stictopleura* (characters states were apparently polarised with respect to a hypothetical ancestor of *Lerista*), however, these species, which Greer (1990b) referred to collectively as the *elegans* group, were noted to differ from those of the *orientalis* species group in having the first two supraciliaries fused (an apomorphic character state) and exhibiting a less reduced (and presumably less derived) phalangeal configuration. Accordingly, Greer (1990b, p. 444) proposed that the *elegans* and *orientalis* species groups 'can be distinguished as lineages'. The analyses presented here strongly support a clade that largely conforms with Greer's (1990b) *orientalis* species group, differing only in excluding *L. muelleri*. As Storr (1971) noted, the number of supraciliaries varies among *L. muelleri* specimens, and the first and second supraciliaries are frequently unfused (Skinner, unpubl. data; Storr [1991b] reported similar variability for this character in *L. ingrami*). Additionally, *L. muelleri* is tridactyl, and has a more reduced phalangeal configuration than the remaining species of Greer's (1990b) *orientalis* species group (which are tetradactyl) and several (although not all) *elegans* group species (see Greer, 1987, 1990a). Thus, the character states considered by Greer (1990b) to diagnose the *elegans* and *orientalis* species groups do not serve to place *L. muelleri* unequivocally in either group. A sister group relationship of *L. haroldi* and *L. muelleri* is strongly supported by the mitochondrial DNA and intron sequence data, indicating that *L. muelleri* is more closely related to at least some species of Greer's (1990b) *elegans* group than to species of the *orientalis* species group. Although monophyly of the *elegans* group is not supported in the analyses presented here (irrespective of the placement of *L. muelleri*), the Bayesian analyses of the mitochondrial DNA and combined sequence data strongly support a clade that is largely consistent with this group, comprising *L. christinae*, *L. distinguenda*, *L. elegans*, *L. lineata*, and *L. planiventralis*.

Greer *et al*. (1983) identified numerous apomorphic character states differentiating a group of seven highly elongate, limb-reduced species (*L. ameles*, *L. apoda*, *L. cinerea*, *L. storri*, *L. stylis*, *L. vittata*, and *L. wilkinsi*), referred to as the *wilkinsi* species group. Although the majority of these character states are observed elsewhere within *Lerista*, Greer *et al*.

(1983) considered the fusion of the first and second supraciliaries, 'highlighted by the loss of the first supraocular', as a 'unique feature of the group' (pp. 254-255). The Bayesian analyses of the mitochondrial DNA and combined sequence data strongly support a clade not dissimilar to Greer *et al*.'s (1983) *wilkinsi* species group, incorporating *L. ameles*, *L. carpentariae*, *L. cinerea*, *L. karlschmidti*, *L. stylis*, and *L. wilkinsi*. A similar clade, differing only in including *L. kalumburu*, is strongly supported in the Bayesian analysis of the ATP synthetase-β subunit intron sequences. As Greer (1983, p. 53) noted, *L. carpentariae* 'retains the first supraocular, and has the first two supraciliaries fused to it'; 'It is difficult to hypothesize *L. carpentariae* as being closely related to any member of the *wilkinsi* group, therefore, without also hypothesizing parallel evolution of this group's unique scale arrangements'. Accordingly, despite several shared apomorphies, Greer (1983) excluded *L. carpentariae* from the *wilkinsi* species group, positing instead that this species is the sister lineage of either *L. karlschmidti* or *L. praepedita*. Although phylogenetic propinquity of *L. carpentariae* and *L. karlschmidti* is well supported by the analyses presented here, moderate support for a clade incorporating these species, *L. stylis*, and perhaps *L. kalumburu*, in conjunction with the relatively distant relationship of *L. apoda* and the remaining species of Greer *et al*.'s (1983) *wilikinsi* species group, indicates that evolution of the anterior supraocular and supraciliaries has been more complicated than Greer (1983) envisaged.

Among the species groups identified by Storr (1971) is an assemblage of five large, elongate species possessing mono- or didactyl forelimbs and di- or tridactyl hindlimbs (*L. desertorum*, *L. gerrardii*, *L. macropisthopus*, *L. neander*, and *L. picturata* [considered by Storr to include *L. baynesi* as a subspecies]), referred to as the *macropisthopus* group. Although Storr (1971) was not evidently concerned that his species groups should be monophyletic, this group is largely consistent with a well-supported clade comprising *L. desertorum*, *L. gerrardii*, *L. macropisthopus*, *L. neander*, and an additional three species (*L. axillaris*, *L. eupoda*, and *L. puncticauda*) described by Storr (1991c) and Smith (1996).

Monophyly of Storr *et al*.'s (1999) *terdigitata* group, erected for four small to moderately large, tridactyl species (*L. elongata*, *L. terdigitata*, *L. tridactyla*, and *L. speciosa*), similarly, is strongly supported by my analyses.

Storr (1991c) recognised four subspecies of *L. macropisthopus* (*L. m. fusciceps*, *L. m. galea*, *L. m. macropisthopus*, and *L. m. remota*), differing primarily in colouration and limb morphology. The phylogenetic analyses presented here reveal that these subspecies do not compose a clade; *L. m. macropisthopus* and *L. m. remota* are placed basally within the *macropisthopus* species group, distant from *L. m. fusciceps* and *L. m. galea*, indicating that *L. macropisthopus* presently includes more than one historically-independent lineage (i.e., species). Similarly, the three subspecies of *L. microtis* (*L. m. intermedia*, *L. m. microtis*, and *L. m. schwaneri*) compose a paraphyletic group. Storr (1991d) reported that these subspecies differ consistently in colouration, body size, and number of midbody dorsal rows, and it is probable that future study will confirm that *L. microtis* also constitutes an assemblage of distinct species. Additional species displaying notable phenotypic variability or discontinuous geographical distributions that may manifest the presence of unrecognised lineages (e.g., *L. karlschmidti L. lineopunctulata*, *L. planiventralis*) further emphasise the need for thorough phylogeographic and taxonomic study of several clades within *Lerista*.

Chapter 5

Correlated Progression and the Evolution of Body Form in *Lerista*

5.1. Introduction

The mode of origination of clades traditionally designated as higher taxa has been the focus of prolonged debate in evolutionary biology (e.g., Gould, 2002; Levinton, 2001). The primary issue inciting discussion is the efficacy of the neo-Darwinian model of gradual phenotypic change mediated by natural selection in explaining the substantial phenotypic differences separating such clades. Although large phenotypic discontinuities among contemporary species may conceivably be produced by gradual divergence in conjunction with extinction of intermediate forms, there are at least two potential difficulties for neo-Darwinian accounts of the emergence of higher taxa. Firstly, organismal integration must be maintained throughout major phenotypic transitions, however, functional intermediary stages may be difficult to envisage, raising the possibility that novel phenotypes often arise by saltation. And secondly, specification of selection pressures driving phenotypic transformations may be problematic. Kemp (1999, 2007) has argued that the origination of many higher taxa can be conceptualised as a trend, consisting of a series of directional changes in phenotype. Where such trends occur over geologically extended periods (as may be usual), the explanation of a continuous, unidirectional selection pressure may become implausible considering the temporal scale of environmental fluctuation (Gould, 2002; Kemp, 2007).

Levinton (2001) discerned two models of gradual phenotypic change that enable substantial alteration of body form without significant disruption of organismal integration and, accordingly, afford a possible solution to the first of the above difficulties. The

independent blocks model asserts that phenotypes are composed of functionally autonomous blocks of integrated characters that evolve independently; the dissociation of blocks decreases the probability that particular phenotypic modifications, which effectively have to be accommodated only within a block (as opposed to the entire phenotype), will compromise the viability of an organism. The correlated progression model, by contrast, assumes that phenotypes are sufficiently integrated that alteration of any single character may affect the functionality of all other characters (thus, phenotypes are not readily dissoluble into independent blocks of characters). The functionality of an organism may exhibit some resilience to small alterations, however, so that major phenotypic transitions can be achieved via a series of slight character changes, each followed by compensating changes in other characters that permit further slight changes (see Thomson, 1966; Kemp, 1982, 1999, 2007).

The independent blocks and correlated progression models may be differentiated empirically on the basis of patterns of character change. Under the independent blocks model, character changes associated with the origination of a higher taxon can occur independently (across blocks) and, consequently, may be predicted to exhibit no significant temporal correlation. Correlated progression, conversely, predicts the interdependence, and thus temporal coincidence, of substantial character changes. Although direct evidence for patterns of character change is typically available only from the fossil record, ancestral character state reconstruction may be employed to infer such patterns indirectly. In this chapter, I apply the latter, indirect approach to investigate the evolution of body form in *Lerista*, a clade of more than 75 species of scincid lizards, distributed in arid, semi-arid, and seasonally dry habitats throughout Australia (Greer, 1989; Cogger, 2000). My primary goal is to evaluate the ability of the independent blocks and correlated progression models to account for the considerable morphological divergence that has occurred within this clade, which includes several species that possess pentadactyl limbs and resemble typical non-fossorial scincids in body proportions, as well as many species exhibiting varying degrees of limb reduction and body elongation, including two that are highly elongate and entirely limbless

(see Fig. 5.1). Additionally, I consider the selection pressures that may have driven this divergence and potential causes of directional change.

5.2. Materials and Methods

Aside from the evident reduction and loss of limbs, a suite of phenotypic alterations may accompany the evolution of a limbless, elongate body form (inferred to be apomorphic; see below), including an increase in the relative length of the body (achieved, for example, by augmenting the number of presacral vertebrae), a decrease in the relative diameter of the body, an increase in the relative length of the tail, relative lengthening of the viscera, and unilateral reduction of paired organs (Gans, 1975). I examined five morphometric variables, recorded for 69 species of *Lerista* and one outgroup taxon (*Ctenotus robustus*): snout-vent length, fore- and hindlimb length (measured from the axilla and groin, respectively, to the tip of the longest digit), head width (a measure of body diameter, recorded at the widest point of the head), and tail length. Specimen registration and collection locality data are provided in Appendix 3. All measurements were divided by head length (measured from the tip of the snout to the anterior margin of the auricular opening) to negate the effect of varying absolute body size (see Lande, 1978; Greer and Wadsworth, 2003). As a means of reducing any influence of allometric growth, only the largest available specimens were measured. Mean values calculated for each species were employed in reconstructing ancestral states.

Ancestral states for each variable were reconstructed using weighted squared-change parsimony (Maddison, 1991), implemented in Mesquite (Maddison and Maddison, 2003), assuming a phylogeny for *Lerista* inferred from nucleotide sequences for six mitochondrial genes and a nuclear intron (see Skinner *et al.*, 2007; Fig. 3.1). The amount of change occurring along each branch of the phylogeny was then calculated assuming the inferred ancestral values (see Huey and Bennett, 1987; Losos, 1990; Appendix 7). As a means of assessing the extent of correlated change among characters, I calculated the gradient of a linear regression line (b) and the coefficient of determination (r^2) for all pairs of variables,

Fig. 5.1. Selected species of *Lerista* illustrating the considerable divergence of body form within this clade; from top to bottom, *L. microtis*, *L. punctatovittata*, and *L. ameles*.

considering inferred amounts of change for individual branches as variates (*sensu* Sokal and Rohlf, 1995).

The significance of observed values of b and r^2 was assessed by comparison with values derived from data simulated under a Brownian motion model. Mesquite was employed to simulate 1000 data sets for each variable (each data set consisting of a set of states for terminal nodes), assuming the same phylogeny used in inferring ancestral states and a rate parameter value estimated from the empirical data. Ancestral states reconstructed for each data set were used to calculate the amount of change occurring along each branch of the phylogeny, as described above. Values of b and r^2 were then calculated for all pairs of variables (again, considering amounts of change for individual branches as variates) for each simulation replicate (i.e., the first simulated data sets for all variables were compared, then the second simulated data sets, etc.). As data were simulated for each variable independently, frequency distributions for these values approximate probability distributions under the independent blocks model of phenotypic change (assuming characters evolve according to a Brownian motion model); observed values in the tails of these frequency distributions (I accepted a probability of type I error of 0.05) were regarded as evidence for interdependence of character changes and, accordingly, correlated progression.

5.3. Results and Discussion

Significant inverse relationships, indicated by values of both b and r^2, exist between changes in relative snout-vent length (i.e., snout-vent length divided by head length) and relative forelimb length, and relative snout-vent length and relative hindlimb length (Fig. 5.2), consistent with the correlated progression model of phenotypic transformation. An association of limb reduction and body elongation in squamates has been noted by many authors (e.g., Gans, 1975; Lande, 1978; Greer, 1987; Greer *et al*., 1998; Wiens and Slingluff, 2001), and may be ascribed to the complementary relationship of limb-mediated locomotion and locomotion by lateral undulation; as lateral undulation, facilitated by body elongation,

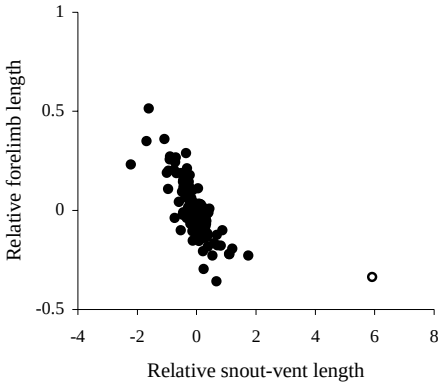

b = -0.1327* (-0.20858*), r^2 = 0.5004* (0.6466*)

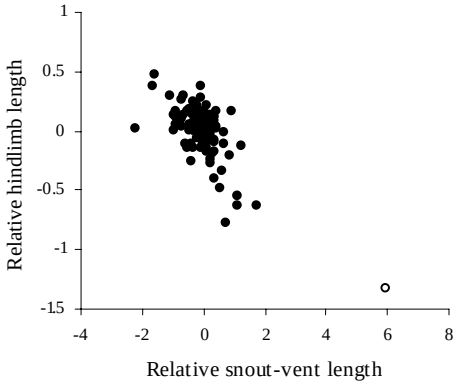

b = -0.2108* (-0.1976*), r^2 = 0.5088* (0.3129*)

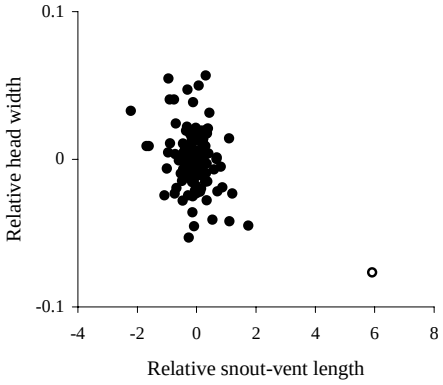

b = -0.0109 (-0.0088), r^2 = 0.1559 (0.0569)

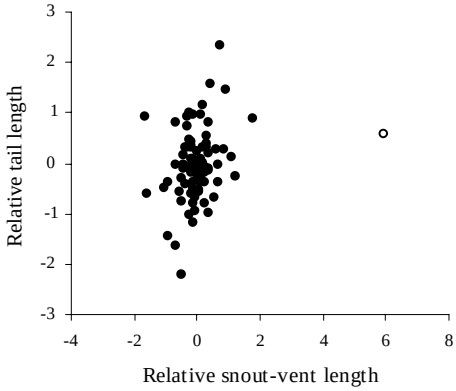

b = 0.2089 (0.3668*), r^2 = 0.0619 (0.0775)

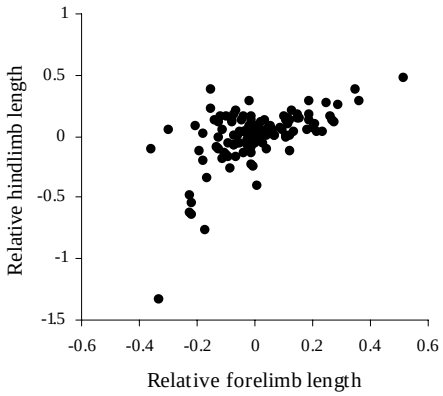

b = 0.8921*, r^2 = 0.3204*

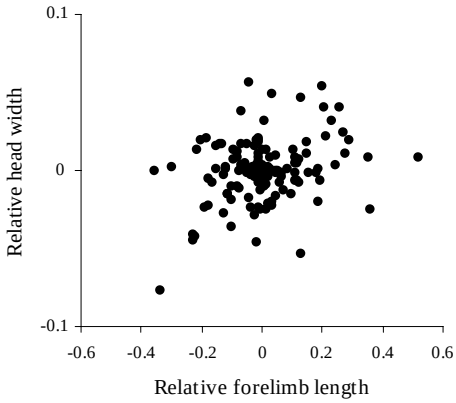

b = 0.0425, r^2 = 0.0836

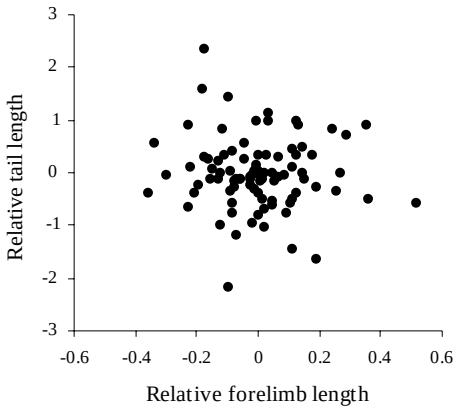

b = -0.3319, r^2 = 0.0055

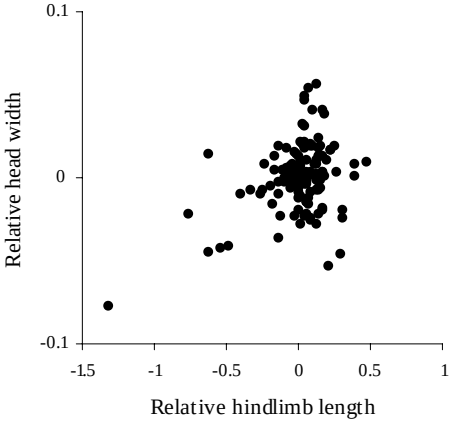

b = 0.0346, r^2 = 0.1377

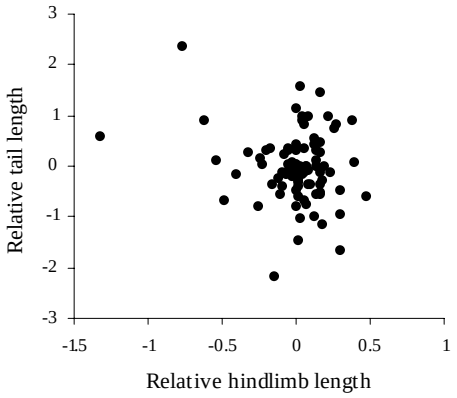

b = -0.5109, r^2 = 0.0340

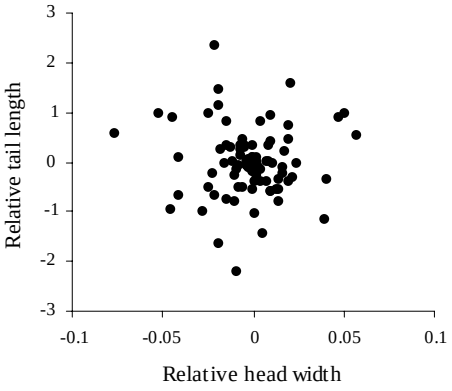

b = -0.6442, r^2 = 0.0004

Figure 5.2. Relationships between the extent of changes in morphometric variables along branches in a phylogeny for *Lerista*. Points represent the inferred amount of change occurring along a single branch. The gradient of a linear regression line (b) and the coefficient of determination (r^2) are presented, with significant values (see text) indicated by an asterisk. Values in parentheses are those obtained when data for the extremely divergent *L. apoda* (shown as open circles) are excluded.

increases in significance, reliance on limb-mediated locomotion decreases and, consequently, the limbs are reduced (Greer and Wadsworth, 2003). Accepting this interpretation, there is minimal difficulty in envisaging the evolution of a limbless, elongate body form by correlated progression. An initial increase in the relative length of the body enables more efficient movement by lateral undulation, prompting (or permitting) greater reliance on this locomotory mode. This increased reliance on undulatory locomotion is followed by reduction in the relative length of the fore- and hindlimbs; such reduction could be passive, resulting from an absence of selection against alteration of disused structures, or actively selected for (as a means of decreasing the effective diameter of the body, for example). Reduction of the limbs, in turn, places increased emphasis on undulatory locomotion, leading to selection for further body elongation.

The explanation of significant relationships between changes in relative snout-vent length and relative fore- and hindlimb length as a consequence of correlated progression implies that limb reduction and body elongation are restricted by functional constraints. As Greer and Wadsworth (2003) have discussed, a stout body supporting diminutive limbs would be unable to perform either limb-mediated or undulatory locomotion, imposing an evident constraint on limb reduction in the absence of body elongation. A highly elongate body bearing unreduced limbs similarly may be poorly suited for efficient locomotion, constraining body elongation in the absence of limb reduction (see Greer and Wadsworth, 2003). As elongation (and hence attenuation) proceeds, the body may become insufficiently strong to provide support as lever base or muscular anchor point for limbs large enough to generate effective propulsive forces. Moreover, the delivery of these forces (primarily by the hindlimbs) increasingly far from the centre of mass would reduce locomotory control. At the same time, the presence of unreduced limbs could impede subsurface undulatory locomotion by increasing the effective diameter of the body (Gans, 1975). Nonetheless, there is evidently some capacity for at least minor limb reduction in the absence of body elongation, and vice versa, considering the imperfect (although significant) relationships between relative snout-

vent length and relative fore- and hindlimb length among extant species of *Lerista* (see Appendix 8). Thus, although substantial, independent alteration of relative limb length and relative body length may be prohibited by functional constraints, there is evidence for the potential independence of slight changes required for correlated progression.

Aside from significant relationships between changes in relative snout-vent length and relative fore- and hindlimb length, there is a significant relationship (again, indicated by values of both *b* and r^2) between changes in relative forelimb length and relative hindlimb length (Fig. 5.2). It is probable that this relationship reflects the correlation of changes in both variables with changes in relative snout-vent length, as opposed to a causal association; nonetheless, the pattern of relationship may provide insight into the mode of limb reduction in *Lerista*. Although decreases (i.e., negative changes) in relative forelimb length are associated with both increases and decreases in relative hindlimb length, decreases in relative hindlimb length are nearly invariably accompanied by decreases in forelimb length (Fig. 5.2). Thus, forelimb reduction may proceed without hindlimb reduction, however, hindlimb reduction generally occurs in conjunction with forelimb reduction. This is consistent with a more significant role of the hindlimb in limb-mediated locomotion and selection in several lineages for preserving some ability to employ limb-mediated locomotion as limb reduction and body elongation progress, a conclusion also indicated by patterns of digit loss (see Skinner *et al.*, 2007). An ability in these lineages to fold the hindlimbs against the sides of the tail during undulatory locomotion would serve to decrease the effective diameter of the body, enabling body elongation with minimal limb reduction. Nevertheless, some hindlimb reduction is evident in all lineages experiencing substantial body elongation (including those in which presumably functional hindlimbs are conserved).

There are no significant correlations between changes in either relative head width or relative tail length and the remaining variables (Fig. 5.2). Accordingly, the relative diameter of the body and relative length of the tail may be considered to have evolved independently of

the extensive alterations to the relative length of the limbs and body. The dissociation of changes in relative tail length may be a consequence of caudal autotomy in *Lerista*. Although increasing the relative length of the tail affords an efficient means of attaining an elongate body form (Gans, 1975), potential tail loss may have emphasised elongation through an increase in relative snout-vent length, moderating functional constraints on changes to relative tail length. Alterations to the relative diameter of the body may be more severely constrained, permitting negligible directional change. As the body becomes increasingly attenuate, the effectiveness of locomotory forces produced by lateral undulation will eventually decrease (due to the increasing ratio of the surface and cross-sectional areas of the body), establishing a lower limit on relative body diameter (see Greer and Wadsworth, 2003). An upper limit on relative body diameter could result from the decreasing efficiency of movement through substrates such as loose soil or sand as the cross-sectional area of the body increases (Gans, 1975). Among extant species of *Lerista*, relative head width varies considerably less than the other variables, deviating from the mean by no more than 16% (the corresponding values for relative snout-vent length, relative fore- and hindlimb length, and relative tail length are 85%, 162%, 100%, and 42%, respectively). Thus, the insignificant relationships between changes in relative head width and relative limb and body length are perhaps attributable to minimal modification of the relative diameter of the body (i.e., there is no substantial phenotypic divergence to be explained by the independent blocks or correlated progression models).

All highly elongate species of *Lerista* have evolved from a comparatively non-elongate ancestor via a series of directional changes in relative snout-vent length; successive changes along direct paths from the root node to these species are nearly all positive, with negative changes occurring along single branches and representing no more than a 9% decrease in relative snout-vent length (for comparison, positive changes occurring along all of the 10 consecutive branches separating *L. apoda* from the ancestor of *Lerista* produce an increase in relative snout-vent length of 102%). Furthermore, there is meagre evidence for the reverse trend of non-elongate species evolving from elongate species; the greatest inferred

negative change occurs along four consecutive branches and represents a decrease in relative snout-vent length of 24%. Almost certainly, the recurring evolution of a limb reduced, elongate body form in *Lerista* is a consequence of adaptation to increasingly fossorial habits (Gans, 1975; Greer, 1989). The expansion of seasonally dry and arid habitats in Australia from the late Miocene (Archer *et al*., 2000; Martin, 2006) provides a suitable environmental context for the evolution of fossoriality (*Lerista* is estimated to be of late mid-Miocene age; see Skinner *et al*., 2007; Appendix 5), however, this alone does not account for the predominance of limb reduction and body elongation. Such habitats sustain both fossorial and surface-active species of *Lerista* and, accordingly, it is not evident that aridification should bias the direction of evolutionary change. The paucity of trends toward a non-elongate body form may perhaps be explained by the improbability of re-elaborating reduced limbs. Skinner *et al*. (2007) found no cogent evidence for increases in the number of manual or pedal digits in *Lerista*, consistent with the generally (although often implicitly) accepted view that limb reduction is rarely (perhaps never) reversed (e.g., Presch 1975; Greer 1987, 1990, 1991; see, however, Kohlsdorf & Wagner 2006). Although increases in the relative length of the fore- and hindlimbs may be possible (indeed, these are inferred; see Fig. 5.2), the re-acquisition of functional limbs could be inhibited by effective irreversibility of structural reduction (i.e., the loss of limb bones). Thus, the transition from an elongate to a non-elongate body form via correlated progression, although conceivable, may be prevented by the absence of necessary changes to the limbs.

The substantial divergence of relative limb and body length evident within *Lerista* is readily explained by the correlated progression model of phenotypic transformation. At each step in the attainment of a limb-reduced, elongate body form, alterations to the relative length of the limbs are accompanied by changes in relative snout-vent length (or vice versa) enabling the maintenance of locomotory ability. Nonetheless, some dissociation of hindlimb reduction and body elongation is possible, emphasising the potentially variable intensity of functional constraints and, accordingly, that the independent blocks model and correlated progression

are extremes of a continuum of models (each invoking a different degree of functional integration) and do not describe discrete categories of phenotypic change. An increase in the extent of seasonally dry and arid habitats coincident with the origination of *Lerista* would have facilitated limb reduction and body elongation by furnishing an environment conducive to the adoption of fossorial habits, however, trends toward a limbless, highly elongate body form may be attributed primarily to the very low probability of re-elaborating reduced limbs. Such asymmetry in the probabilities of possible phenotypic changes may be a significant cause of evolutionary trends resulting in the emergence of higher taxa.

References

Alberch, P., Gale, E. A., 1983. Size dependence during the development of the amphibian foot. Colchicine-induced digital loss and reduction. J. Embryol. Exp. Morph. 76, 177-197.

Alberch, P., Gale, E. A., 1985. A developmental analysis of an evolutionary trend: digital reduction in amphibians. Evolution 39, 8-23.

Archer M., Hand, S. J., Godthelp, H., 2000. Australia's Lost World. Reed New Holland, Sydney.

Arévalo, E., Davis, S. K., Sites, Jr., J. W., 1994. Mitochondrial DNA sequence divergence and phylogenetic relationships among eight chromosome races of the *Sceloporus grammicus* complex (Phrynosomatidae) in central Mexico. Syst. Biol. 43, 387-418.

Avise, J. C., 2000. Phylogeography: the History and Formation of Species. Harvard University Press, Cambridge.

Baker, R. H., DeSalle, R., 1997. Multiple sources of character information and the phylogeny of Hawaiian drosophilids. Syst. Biol. 46, 654-673.

Barraclough, T. G., Vogler, A. P., 2000. Detecting the geographical pattern of speciation from species-level phylogenies. Am. Nat. 155, 419-434.

Barrett, M., Donoghue, M. J., Sober, E., 1991. Against consensus. Syst. Zool. 40, 486-493.

Bremer, K., 1988. The limits of amino acid sequence data in angiosperm phylogenetic reconstruction. Evolution 42, 795-803.

Bremer, K., 1994. Branch support and tree stability. Cladistics 10, 295-304.

Buckley, T. R., Arensburger, P., Simon, C., Chambers, G. K., 2002. Combined data, Bayesian phylogenetics, and the origin of the New Zealand cicada genera. Syst. Biol. 51, 4-18.

Choquenot, D., Greer, A. E., 1989. Intrapopulational and interspecific variation in digital limb bones and presacral vertebrae of the genus *Hemiergis* (Lacertilia, Scincidae). J. Herpetol. 23, 274-281.

Cogger, H. G., 2000. Reptiles and Amphibians of Australia. Reed New Holland, Sydney.

Felsenstein, J., 1985. Phylogenies and the comparative method. Am. Nat. 125, 1-15.

Forstner, M. R. J., Davis, S. K., Arévalo, E., 1995. Support for the hypothesis of anguimorph ancestry for the suborder Serpentes from phylogenetic analysis of mitochondrial DNA sequences. Mol. Phylogenet. Evol. 4, 93-102.

Gans, C., 1975. Tetrapod limblessness: evolution and functional corollaries. Amer. Zool. 15, 455-467.

Gatesy, J., Baker, R. H., 2005. Hidden likelihood support in genomic data: can forty-five wrongs make a right? Syst. Biol. 54, 483-492.

Gatesy, J., O'Grady, P., Baker, R. H., 1999. Corroboration among data sets in simultaneous analysis: hidden support for phylogenetic relationships among higher level artiodactyl taxa. Cladistics 15, 271-313.

Goldman, N., Whelan, S., 2000. Statistical tests of gamma-distributed rate heterogeneity in models of sequence evolution in phylogenetics. Mol. Biol. Evol. 17, 975-978.

Gould, S. J., 2002. The Structure of Evolutionary Theory. Belknap Press of Harvard University Press, Cambridge.

Greer, A. E., 1979a. A phylogenetic subdivision of Australian skinks. Rec. Aust. Mus. 32, 339-371.

Greer, A. E., 1979b. *Eremiascincus*, a new generic name for some Australian sand swimming skinks (Lacertilia: Scincidae). Rec. Aust. Mus. 32, 321-338.

Greer, A. E., 1983a. The Australian scincid lizard genus *Calyptotis* De Vis: resurrection of the name, description of four new species, and discussion of relationships. Rec. Aust. Mus. 35, 29-59.

Greer, A. E., 1983b. A new species of *Lerista* from Groote Eylandt and the Sir Edward Pellew Group in northern Australia. J. Herpetol. 17, 48-53.

Greer, A. E., 1986. Diagnosis of the *Lerista bipes* species-group (Lacertilia: Scincidae), with a description of a new species and an updated diagnosis of the genus. Rec. West. Aust. Mus. 13, 121-127.

Greer, A. E., 1987. Limb reduction in the lizard genus *Lerista*. 1. Variation in the number of phalanges and presacral vertebrae. J. Herpetol. 21, 267-276.

Greer, A. E., 1989. The Biology and Evolution of Australian Lizards. Surrey Beatty and Sons, Chipping Norton.

Greer, A. E., 1990a. Limb reduction in the lizard genus *Lerista*. 2. Variation in the bone complements of the front and rear limbs and the number of postsacral vertebrae. J. Herpetol. 24, 142-150.

Greer, A. E., 1990b. The *Glaphyromorphus isolepis* species group (Lacertilia: Scincidae): diagnosis of the taxon and description of a new species from Timor. J. Herpetol. 24, 372-377.

Greer, A. E., 1990c. The taxonomic status of *Lerista aericeps* Storr 1986 with a diagnosis of the *Lerista orientalis* species group. Rec. West. Aust. Mus. 14, 443-448.

Greer, A. E., 1991. Limb reduction in squamates: identification of the lineages and discussion of the trends. J. Herpetol. 25, 166-173.

Greer, A. E., 1992. Revision of the species previously associated with the Australian scincid lizard *Eulamprus tenuis*. Rec. Aust. Mus. 44, 7-19.

Greer, A. E., Caputo, V., Lanza, B., Palmieri, R., 1998. Observations on limb reduction in the scincid lizard genus *Chalcides*. J. Herpetol. 32, 244-252.

Greer, A. E., Cogger, H. G., 1985. Systematics of the reduced-limbed and limbless skinks currently assigned to the genus *Anomalopus* (Lacertilia: Scincidae). Rec. Aust. Mus. 37, 11-54.

Greer, A. E., McDonald, K. R., Lawrie, B. C., 1983. Three new species of *Lerista* (Scincidae) from northern Queensland with a diagnosis of the *wilkinsi* species group. J. Herpetol. 17, 247-255.

Greer, A. E., Parker, F., 1967. A new scincid lizard from the northern Solomon Islands. Breviora 275, 1-20.

Greer, A. E., Parker, F., 1974. The *fasciatus* species group of *Sphenomorphus* (Lacertilia: Scincidae): notes on eight previously described species and description of three new species. Papua New Guin. Sci. Soc. Proc. 25, 31-61.

Greer, A. E., Shea, G., 2004. A new character within the taxonomically difficult *Sphenomorphus* group of lygosomine skinks, with a description of a new species from New Guinea. J. Herpetol. 38, 79-87.

Greer, A. E., Wadsworth, L., 2003. Body shape in skinks: the relationship between relative hind limb length and relative snout-vent length. J. Herpetol. 37, 554-559.

Harvey, P. H., Holmes, E. C., Mooers A. Ø., Nee, S., 1994. Inferring evolutionary processes from molecular phylogenies. In: Scotland, R. W., Siebert, D. J., Williams, D. M. (Eds.), Models in Phylogeny Reconstruction. Clarendon Press, Oxford, pp. 313-333.

Harvey, P. H., May, R. M., Nee, S., 1994. Phylogenies without fossils. Evolution 48, 523-529.

Harvey, P. H., Nee, S., 1994. Phylogenetic epidemiology lives. Trends Ecol. Evol. 12, 16-22.

Harvey, P. H., Pagel, M. D., 1991. The Comparative Method in Evolutionary Biology. Oxford University Press, Oxford.

Helm-Bychowski, K., Cracraft, J., 1993. Recovering phylogenetic signal from DNA sequences: relationships within the corvine assemblage (class Aves) as inferred from complete sequences of the mitochondrial DNA cytochrome-*b* gene. Mol. Biol. Evol. 10, 1196-1214.

Honda, M., Ota, H., Kobayashi, M., Nabhitabhata, J., Yong, H., Hikida, T., 2000. Phylogenetic relationships, character evolution, and biogeography of the subfamily Lygosominae (Reptilia: Scincidae) inferred from mitochondrial DNA sequences. Mol. Phylogenet. Evol. 15, 452-461.

Hubbell, S. P., 2001. The Unified Neutral Theory of Biodiversity and Biogeography. Princeton University Press, Princeton.

Huey, R. B., Bennett, A. F., 1987. Phylogenetic studies of coadaptation: preferred temperatures versus optimal performance temperatures of lizards. Evolution 41, 1098-1115.

Jackman, T. R., Larson, A., de Queiroz, K., Losos, J. B., 1999. Phylogenetic relationships and tempo of early diversification in *Anolis* lizards. Syst. Biol. 48, 254-285.

Jarman, S. N., Ward, R. D., Elliott, N. G., 2002. Oligonucleotide primers for PCR amplification of coelomate introns. Mar. Biotechnol. 4, 347-355.

Kemp, T. S., 1982. Mammal-like Reptiles and the Origin of Mammals. Academic Press, London.

Kemp, T. S., 1999. Fossils and Evolution. Oxford University Press, Oxford.

Kemp, T. S., 2007. The origin of higher taxa: macroevolutionary processes, and the case of the mammals. Acta Zool. 88, 3-22.

Kendrick, P. G., 1989. Two new species of *Lerista* (Lacertilia: Scincidae) from the Cape Range and Kennedy Range of Western Australia. J. Herpetol. 23, 350-355.

Kohlsdorf, T., Wagner, G. P., 2006. Evidence for the reversibility of digit loss: a phylogenetic study of limb evolution in *Bachia* (Gymnophthalmidae: Squamata). Evolution 60, 1896-1912.

Kraus, F., Miyamoto, M., 1991. Rapid cladogenesis among the pecoran ruminants: evidence from mitochondrial DNA sequences. Syst. Zool. 40, 117-130.

Lande, R., 1978. Evolutionary mechanisms of limb loss in tetrapods. Evolution 32, 73-92.

Lessa, E. P., Cook, J. A., 1998. The molecular phylogenetics of tuco-tucos (genus *Ctenomys*, Rodentia: Octodontidae) suggests an early burst of speciation. Mol. Phylogenet. Evol. 9, 88-99.

Levinton, J. S., 2001. Genetics, Paleontology, and Macroevolution. Cambridge University Press, Cambridge.

Lomolino, M. V., Riddle, B. R., Brown, J. H., 2006. Biogeography. Sinauer, Sunderland.

Losos, J. B., 1990. Ecomorphology, performance capability, and scaling of West Indian *Anolis* lizards: an evolutionary analysis. Ecol. Monogr. 60, 369-388.

Lutzoni, F., Pagel, M., Reeb, V., 2001. Major fungal lineages are derived from lichen symbiotic ancestors. Nature 411, 937-940.

Macey, J. R., Verma, A., 1997. Homology in phylogenetic analysis: alignment of transfer RNA genes and the phylogenetic position of snakes. Mol. Phylogenet. Evol. 7, 272-279.

Maddison, W., 1989. Reconstructing character evolution on polytomous cladograms. Cladistics 5, 365-377.

Maddison, W. P., 1991. Squared-change parsimony reconstructions of ancestral states for continuous-valued characters on a phylogenetic tree. Syst. Zool. 40, 304-314.

Maddison, W. P., Maddison, D. R., 2003. Mesquite: a Modular System for Evolutionary Analysis, Vers. 1.0. http://mesquiteproject.org.

Martin, H. A., 2006. Cenozoic climatic change and the development of the arid vegetation in Australia. J. Arid Environ. 66, 533-563.

Miyamoto, M. M., Fictch, W. M., 1995. Testing species phylogenies and phylogenetic methods with congruence. Syst. Biol. 44, 64-76.

Mooers, A. Ø., Vamosi, S. M., Schluter, D., 1999. Using phylogenies to test macroevolutionary hypotheses of trait evolution in cranes (Gruinae). Am. Nat. 154, 249-259.

Nylander, J. A. A., 2002. MrModeltest, Vers. 1.0b. http://www.ebc.uu.se/systzoo/staff/nylander.html.

O'Connor, D., Moritz, C., 2003. A molecular phylogeny of the Australian skink genera *Eulamprus*, *Gnypetoscincus* and *Nangura*. Aust. J. Zool. 51, 317-330.

Pagel, M., Meade, A., Barker, D., 2004. Bayesian estimation of ancestral character states on phylogenies. Syst. Biol. 53, 673-684.

Poe, S., Chubb, A. L., 2004. Birds in a bush: five genes indicate explosive evolution of avian orders. Evolution 58, 404-415.

Posada, D., Crandall, K. A., 1998. Modeltest: testing the model of DNA substitution. Bioinformatics 14, 817-818.

Presch, W., 1975. The evolution of limb reduction in the teiid lizard genus *Bachia*. Bull. S. California Acad. Sci. 74, 113-121.

Purvis, A., Gittleman, J. L., Brooks, T. (Eds.), 2005. Phylogeny and Conservation. Cambridge University Press, Cambridge.

Reeder, T. W., 1995. Phylogenetic relationships among phrynosomatid lizards as inferred from mitochondrial ribosomal DNA sequences: substitutional bias and information content of transitions relative to transversions. Mol. Phylogenet. Evol. 4, 203-222.

Reeder, T. W., 2003. A phylogeny of the Australian *Sphenomorphus* group (Scincidae: Squamata) and the phylogenetic placement of the crocodile skinks (*Tribolonotus*): Bayesian

approaches to assessing congruence and obtaining confidence in maximum likelihood inferred relationships. Mol. Phylogenet. Evol. 27, 384-397.

Ronquist, F., Huelsenbeck, J. P., 2003. MrBayes 3: Bayesian phylogenetic inference under mixed models. Bioinformatics 19, 1572-1574.

Rosenzweig, M. L., 1975. On continental steady states of species diversity. In: Cody, M. L., Diamond, J. M. (Eds.), Ecology and Evolution of Communities. Belknap Press of Harvard University Press, Cambridge.

Rosenzweig, M. L., 1995. Species Diversity in Space and Time. Cambridge University Press, Cambridge.

Sadlier, R. A., 1998. Recognition of *Eulamprus tryoni* (Longman), a scincid lizard endemic to the McPherson Ranges of eastern Australia. Mem. Queensl. Mus. 42, 573-578.

Sanderson, M. J., 2002. Estimating absolute rates of molecular evolution and divergence times: a penalized likelihood approach. Mol. Biol. Evol. 19, 101-109.

Sanderson, M. J., 2003. r8s: inferring absolute rates of molecular evolution and divergence times in the absence of a molecular clock. Bioinformatics 19, 301-302.

Schluter, D., Price, T., Mooers, A. Ø., Ludwig, D., 1997. Likelihood of ancestor states in adaptive radiation. Evolution 51, 1699-1711.

Simpson, G. G., 1953. The Major Features of Evolution. Columbia University Press, New York.

Skinner, A., 2007. Phylogenetic relationships and rate of early diversification of Australian *Sphenomorphus* group scincids (Scincoidea, Squamata). Biol. J. Linn. Soc. 92, 347-366.

Skinner, A., Donnellan, S. C., Hutchinson, M. N., Hutchinson, R. G., 2005. A phylogenetic analysis of *Pseudonaja* (Hydrophiinae, Elapidae, Serpentes) based on mitochondrial DNA sequences. Mol. Phylogenet. Evol. 37, 558-571.

Skinner, A., Lee, M. S. Y., Hutchinson, M. N., 2007. Rapid and repeated limb reduction in *Lerista* (Scincidae, Squamata). In review.

Slowinski, J. B., 2001. Molecular polytomies. Mol. Phylogenet. Evol. 19, 114-120.

Smith, L. A., 1996. A new *lerista* (Lacertilia: Scincidae) from Western Australia, *Lerista eupoda*. J. Proc. R. Soc. West. Aust. 79, 161-164.

Sokal, R. R., Rohlf, F. J., 1995. Biometry. W. H. Freeman and Company, New York.

Sorenson, M. D., 1999. TreeRot, Vers. 2. Boston University, Boston.

Storr, G. M., 1964. *Ctenotus*, a new generic name for a group of Australian skinks. West. Aust. Nat. 9, 84-85.

Storr, G. M., 1971. The genus *Lerista* (Lacertilia, Scincidae) in Western Australia. J. R. Soc. West. Aust. 54, 59-75.

Storr, G. M., 1984. Revision of the *Lerista nichollsi* complex (Lacertilis: Scincidae). Rec. West. Aus. Mus. 11, 109-118.

Storr, G. M., 1986. Two new members of the *Lerista nichollsi* complex (Lacertilia: Scincidae). Rec. West. Aust. Mus. 13, 47-52.

Storr, G. M., 1990. A new member of the *Lerista bipes* group (Lacertilia: Scincidae) from the Kimberley. Rec. West. Aus. Mus. 14, 439-442.

Storr, G. M., 1991a. Four new members of the *Lerista nichollsi* complex (Lacertilia: Scincidae). Rec. West. Aust. Mus. 15, 139-147.

Storr, G. M., 1991b. Revision of *Lerista orientalis* (Lacertilia: Scincidae) of northern Australia. Rec. West. Aust. Mus. 15, 413-417.

Storr, G. M., 1991c. Partial revision of the *Lerista macropisthopus* group (Lacertilia: Scincidae). Rec. West. Aust. Mus. 15, 149-161.

Storr, G. M., 1991d. Revision of *Lerista microtis* (Lacertilia: Scincidae). Rec. West. Aust. Mus. 15, 469-476.

Storr, G. M., Smith, L. A., Johnstone, R. E., 1999. Lizards of Western Australia. I. Skinks. Western Australian Museum, Perth.

Swofford, D. L., 1991. When are phylogeny estimates from molecular and morphological data incongruent? In: Miyamoto, M. M., Cracraft, J. (Eds.), Phylogenetic Analysis of DNA Sequences. Oxford University Press, New York, pp. 295-333.

Swofford, D. L., 1999. PAUP*: Phylogenetic Analysis Using Parsimony (* and other methods), Vers. 4.0. Sinauer, Sunderland.

Thompson, J. D., Gibson, T. J., Plewniak, F., Jeanmougin, F., Higgins, D. G., 1997. The ClustalX windows interface: flexible strategies for multiple sequence alignment aided by quality analysis tools. Nuc. Acids Res. 24, 4876-4882.

Thomson, K. S., 1966. The evolution of the tetrapod middle ear in the rhipidistian-amphibian transition. Amer. Zool. 6, 379-397.

Walsh, H. E., Kidd, M. G., Moum, T., Friesen, V. L., 1999. Polytomies and the power of phylogenetic inference. Evolution 53, 932-937.

Webb, C. O., Ackerly, D. D., McPeek, M. A., Donoghue, M. J., 2002. Phylogenies and community ecology. Annu. Rev. Ecol. Syst. 33, 475-505.

Wiens, J. J., 1998. Combining data sets with different phylogenetic histories. Syst. Biol. 47, 568-581.

Wiens, J. J., Reeder, T. W., Montes de Oca, A. N., 1999. Molecular phylogenetics and evolution of sexual dichromatism among populations of the Yarrow's spiny lizard (*Sceloporus jarrovii*). Evolution 53, 1884-1897.

Wiens, J. J., and Slingluff, J. L., 2001. How lizards turn into snakes: a phylogenetic analysis of body-form evolution in anguid lizards. Evolution 55, 2303-2318.

Wilgenbusch, J. C., Warren, D. L., Swofford, D. L., 2004. AWTY: a system for graphical exploration of MCMC convergence in Bayesian phylogenetic inference. http://ceb.csit.fsu.edu/awty.

Wuyts, J., De Rijk, P., Van de Peer, Y., Winkelmans, T., De Wachter, R., 2001. The European large subunit ribosomal RNA database. Nuc. Acids Res. 29, 175-177.

Wuyts, J., Van de Peer, Y., Winkelmans, T., De Wachter, R., 2002. The European database on small subunit ribosomal RNA. Nuc. Acids Res. 30, 183-185.

Appendix 1

Specimens included in the analyses presented in Chapter 2. Abbreviations are: ABTC, Australian Biological Tissue Collection, South Australian Museum, Adelaide; AMS, Australian Museum, Sydney; NTM, Northern Territory Museum, Darwin; QM, Queensland Museum, Brisbane; SAMA, South Australian Museum, Adelaide; TNHC, Texas Natural History Collection, University of Texas at Austin; WAM, Western Australian Museum, Perth; m-R, mitochondrial DNA sequences from Reeder (2003); m-p, mitochondrial DNA sequences acquired in the present study; i, ATP synthetase-β subunit intron sequence acquired in the present study. Collection localities for specimens included in Reeder's (2003) analysis are provided in his Appendix A.3.

Species	Registration number	Collection locality	Sequence source
Outgroup			
Egernia whitii	SAMA R34781		m-R
Eugongylus rufescens	AMS R122480		m-R
Lamprolepis smaragdina	TNHC 55655		m-R
Mabuya longicaudata	SAMA R38916		m-R
Ingroup			
Anomalopus leuckartii	ABTC 3713	5 km E Tooraweenah, NSW	m-p, i
Anomalopus mackayi	NR 6054		m-R
Anomalopus swansoni	SAMA R33731		m-R, i
Calyptotis lepidorostrum	ABTC 3903	Mary Cairncross Park, Qld	m-p, i
Calyptotis ruficauda	ABTC 3989	Cairncross State Forest, NSW	m-p, i
Calyptotis scutirostrum	SAMA R33887		m-R, i
Coeranoscincus frontalis	ABTC 16213	Walter Hill Range, Qld	m-p, i
Coeranoscincus reticulatus	SAMA R37800		m-R, i
Coggeria naufragus	ABTC 32113	Fraser Island, Qld	m-p, i
Ctenotus leonhardii	WAM R97180		m-R, i
Ctenotus pantherinus	ABTC 57950	4 km SSW Mt Cuthbert, SA	m-p, i
Ctenotus robustus	SAMA R36579		m-R
	ABTC 17100	Esdale, NSW	i
Eremiascincus richardsonii	SAMA R40946		m-R, i
Eulamprus amplus	AMS field no. 32592		m-R
	ABTC 10873	Finch Hatton National Park, Qld	i
Eulamprus kosciuskoi	ABTC 1169	Gloucester Falls, NSW	m-p, i
Eulamprus luteilateralis	ABTC 10871	Eungella, Qld	m-p, i
Eulamprus murrayi	SAMA R33699		m-R, i
Eulamprus quoyii	QM J56099		m-R
	ABTC 3960	Whian Whian State Forest, NSW	i
Eulamprus tenuis	ABTC 14173	Eungella, Qld	m-p, i
Glaphyromorphus cracens	ABTC 77143	35 km E Mt Surprise, Qld	m-p, i
Glaphyromorphus crassicaudis	NTM R19119		m-R, i
Glaphyromorphus darwiniensis	ABTC 29653	Litchfield National Park, NT	m-p, i
Glaphyromorphus douglasi	ABTC 29631	Litchfield National Park, NT	m-p

Glaphyromorphus isolepis	SAMA R34105		m-R
Glaphyromorphus fuscicaudis	ABTC 32148	Mt Hartley, Qld	m-p, i
Glaphyromorphus gracilipes	SAMA R23027		m-R, i
Glaphyromorphus mjobergi	ABTC 16212	Majors Mount, Qld	m-p, i
Glaphyromorphus pardalis	ABTC 32201	Wakooka Outstation, Qld	m-p
Glaphyromorphus pumilus	ABTC 11368	nr Mareeba, Qld	m-p, i
Glaphyromorphus punctulatus	ABTC 10857	Mt Morgan, Qld	m-p, i
Gnypetoscincus queenslandiae	QM J51015		m-R
	ABTC 1126	Millaa Millaa Falls, Qld	i
Hemiergis initialis	ABTC 73302	Denton's Dump, start of Goog's Track, SA	m-p, i
Hemiergis peronii	SAMA R45326		m-R, i
Lerista bipes	ABTC 41733	9 km SE Maryinna Hill, SA	m-p, i
Lerista bougainvillii	ABTC 68814	South Para Gorge, SA	m-p, i
Nangura spinosa	QM J57246		m-R
	ABTC 31885	Nangur State Forest, Qld	i
Notoscincus ornatus	NTM R14923		m-R, i
Ophioscincus ophioscincus	QM J46126		m-R
	ABTC 3934	Mt Glorious, Qld	i
Ophioscincus truncatus	ABTC 3971	nr Alstonville, NSW	m-p, i
Papuascincus sp.	ABTC 48281	Nokopo, PNG	m-p, i
Prasinohaema virens	AMS R129721		m-R, i
Saiphos equalis	SAMA R33627		m-R, i
Scincella lateralis	DCC 2842		m-R
Sphenomorphus jobiensis	ABTC 48822	Usino, PNG	m-p, i
Sphenomorphus muelleri	AMS R122684		m-R, i
Sphenomorphus solomonis	ABTC 48124	Siar plantation, PNG	m-p, i

Appendix 2

Specimens included in the phylogenetic analysis presented in Chapter 3. Abbreviations as for Appendix 1.

Species	Registration number	Locality
aericeps	SAMA R35983	Mokari, SA
allochira	WAM R116698	Vlaming Head, WA
ameles	SAMA R55815	35 km E Mt Surprise, Qld
apoda	WAM R114243	Coulomb Point Nature Reserve, WA
arenicola	SAMA R50095	Talia Beach, S Venus Bay, SA
axillaris	WAM R97212	21 km S Kalbarri, WA
baynesi	SAMA R26475	Near Border Village, SA
bipes	SAMA R53899	63 km N Broome, WA
borealis	SAMA R51132	El Questro Stn, WA
bougainvillii	SAMA R52630	South Para Gorge, SA
carpentariae	NTM R14161	Sir Edward Pellew Island, NT
chordae	SAMA R54482	22 km S Torrens Creek, Qld
christinae	WAM R115299	Ellenbrook, WA
cinerea	SAMA R54520	3 km N Lolworth Homestead, Qld
connivens	SAMA R29286	Carnarvon, WA
desertorum	WAM R92030	67 km SE Blue Robin Hill, WA
distinguenda	SAMA R20805	Eyre Peninsula, SA
dorsalis	SAMA R48848	Arcoona Stn, SA
edwardsae	SAMA R37941	10 km SE Moonabie Homestead, SA
elegans	WAM R90275	75 km SSW Karridale, WA
elongata	SAMA R42424	Dog fence, near Coober Pedy, SA
emmotti	ABTC 31973	Noonbah Stn, Qld
eupoda	WAM R135101	Cue, WA
flammicauda	WAM R151177	Tom Price, WA
fragilis	SAMA R55885	69 km S Alpha, Qld
frosti	SAMA R53312	Trephina Gorge, NT
gascoynensis	WAM R116790	Gascoyne Junction, WA
gerrardii	SAMA R22901	Northampton, WA
greeri[1]	WAM R108753	30 km SE Gordon Downs, WA
greeri[2]	WAM R114424	Derby, WA
griffini	NTM R22909	Spirit Hills, Keep River, NT
haroldi	WAM R116653	Gnaraloo Homestead, WA
humphriesi	WAM R116872	Carrollgouda Well, WA
ingrami	QM J62430	Cape Flattery, Qld
ips	WAM R131074	Kiwirrkurra, WA
kalumburu	WAM R113949	Carson Escarpment, WA
karlschmidti	NTM R23965	Ramingining area, NT
kendricki	WAM R116264	Kalbarri, WA
kennedyensis	WAM R99638	Merlinleigh Homestead, WA
labialis	SAMA R48727	4 km W Mt Lindsay, SA
lineata	WAM R144983	Jandakot Airport, WA
lineopunctulata	SAMA R 29778	Scarborough Beach, Perth, WA
macropisthopus	SAMA R29294	One Tree Point, Carnarvon, WA
microtis	WAM R90186	35 km NE Augusta, WA
muelleri	SAMA R54734	Wirraminna Stn, SA

neander	WAM R104362	11 km SSW Capricorn Roadhouse, WA
nichollsi	AMS R123100	Kalli Homestead, WA
onsloviana	WAM R116826	Onslow, WA
orientalis	NTM R21731	Litchfield National Park, NT
petersoni	WAM R99637	Merlinleigh Homestead, WA
picturata	SAMA R22997	32 km S Norseman, WA
planiventralis	WAM R141463	Faure Island, WA
praepedita	SAMA R29419	Scarborough Beach, Perth, WA
punctatovittata	SAMA R42016	Morgan Mail Road, SA
puncticauda	WAM R117169	Queen Victoria Spring, WA
robusta	WAM R108783	Cherrabun Homestead, WA
simillima	WAM R100874	6 km NW Fitzroy Crossing, WA
speciosa	SAMA R58029	Sentinel Hill, SA
stictopleura	WAM R116825	Mt Augustus, WA
stylis	NTM R21679	Kakadu National Park, NT
taeniata	SAMA R32057	55 km S Immarna Siding, SA
terdigitata	SAMA R38568	Middleback Ranges, SA
tridactyla	WAM R112650	Ponier Rock, WA
uniduo	SAMA R29291	One Tree Point, Carnarvon, WA
varia[2]	SAMA R29388	Nanga Dunes, WA
varia[1]	WAM R141494	Faure Island, WA
vermicularis	WAM R108778	6 km WNW Fitzroy Crossing, WA
viduata	WAM R116535	Kundip, WA
walkeri	WAM R96954	29 km WSW Mt French, WA
wilkinsi	SAMA R55679	40 km S Torrens Creek, Qld
xanthura	WAM R135156	Telfer Dome, WA
yuna	WAM R100846	Yuna, WA
zietzi	WAM R114563	53 km WNW Newman, WA
zonulata	SAMA R55820	Einasleigh Road, Qld
Outgroup		
Ctenotus robustus[3]	SAMA R36579	Esdale, NSW
Ctenotus robustus[1]	SAMA R36603	Esdale, NSW
Eulamprus kosciuskoi	ABTC 1169	Gloucester Falls, NSW
Glaphyromorphus fuscicaudis	ABTC 32148	Mt Hartley, Qld

[1]ATP synthetase-β subunit intron only; [2]Mitochondrial genes only; [3]Mitochondrial gene sequences from Reeder (2003).

Appendix 3

Specimens measured for the analyses presented in Chapters 3 and 5. Abbreviations as for Appendix 1.

Species	Registration numbers
aericeps	SAMA R35984, SAMA R35985, SAMA R38349, SAMA R40510, SAMA R57102
allochira	WAM R132457, WAM R132460
ameles	SAMA R55807, SAMA R55813, SAMA R55815
apoda	WAM R114221, WAM R114222, WAM R114233
arenicola	SAMA R50095, SAMA R53771, SAMA R57756
axillaris	WAM R129857
baynesi	SAMA R59595, SAMA R59597, SAMA R59609, WAM R137697
bipes	SAMA R36116, SAMA R46145, SAMA R48590, SAMA R48819, SAMA R56468
borealis	SAMA R51132, SAMA R51133
bougainvillii	SAMA R54815, SAMA R55069, SAMA R56435, SAMA R58289, SAMA R58833
christinae	WAM R115088, WAM R68395, WAM R94518
cinerea	SAMA R54519, SAMA R54520, SAMA R54521
connivens	SAMA R22862, SAMA R22864, SAMA R29286
desertorum	SAMA R40424, SAMA R44332, SAMA R44334, SAMA R44418, SAMA R46517
distinguenda	SAMA R57693, SAMA R58494, WAM R152938, WAM R154677, WAM R157728
dorsalis	SAMA R58510, SAMA R59225, SAMA R59233, SAMA R59680, SAMA R59706
edwardsae	SAMA R42286, SAMA R44342, SAMA R57662, SAMA R58491, SAMA R59727
elegans	WAM R129790, WAM R129947, WAM R137471, WAM R140888, WAM R140893
elongata	SAMA R40736, SAMA R42266, SAMA R42424, SAMA R46415
eupoda	WAM R108854, WAM R135010
flammicauda	WAM R151177
fragilis	SAMA R54557, SAMA R54558, SAMA R55654, SAMA R55885
frosti	SAMA R1571A, SAMA R18492, SAMA R37077, SAMA R53312
gascoynensis	WAM R124939, WAM R126577
gerrardii	SAMA R22901, WAM R136434, WAM R141835
greeri	WAM R103405, WAM R114399
griffini	WAM R114398, WAM R114403, WAM R141581
haroldi	WAM R116654
humphriesi	WAM R123586, WAM R66348
ips	WAM R108919, WAM R131075, WAM R135152, WAM R139053
kalumburu	WAM R129939
kendricki	WAM R116264, WAM R119182, WAM R146398
kennedyensis	WAM R108627, WAM R125883, WAM R95769
labialis	SAMA R50900, SAMA R51418, SAMA R52835, SAMA R52854, SAMA R53337
lineata	WAM R63062, WAM R63067
lineopunctulata	SAMA R29415, SAMA R29420, SAMA R29777, SAMA R29778
macropisthopus	SAMA R22859, SAMA R22860, SAMA R29282, SAMA R29294, SAMA R29295
microtis	SAMA R45855, SAMA R45924, SAMA R45925, SAMA R52648
muelleri	SAMA R57108, SAMA R57361, SAMA R57365, SAMA R58172, SAMA R58374
neander	WAM R117334, WAM R87730
nichollsi	WAM R127532, WAM R127533, WAM R132289
onsloviana	WAM R116830
orientalis	SAMA R5391, SAMA R5394A
petersoni	WAM R116712, WAM R99632

picturata	SAMA R22997, SAMA R23062, WAM R146441
planiventralis	WAM R127526, WAM R140858, WAM R141608, WAM R151191
praepedita	SAMA R29419, WAM R115314, WAM R116881, WAM R121920
punctatovittata	SAMA R41230, SAMA R42011, SAMA R42015, SAMA R48266, SAMA R51873
puncticauda	WAM R145938
robusta	WAM R108784
simillima	WAM R100878, WAM R101336, WAM R108778
speciosa	SAMA R58029, SAMA R59098, SAMA R59099
stictopleura	WAM R116814, WAM R116815, WAM R138081, WAM R138083
stylis	SAMA R3511A, SAMA R3511B
taeniata	SAMA R32057, SAMA R38569, SAMA R45535, SAMA R57648, SAMA R57724
terdigitata	SAMA R37539, SAMA R44446, SAMA R57639, SAMA R58466, SAMA R59753
tridactyla	WAM R112651, WAM R117165, WAM R137817
uniduo	SAMA R29292, SAMA R29293
varia	SAMA R29387, SAMA R29388
vermicularis	WAM R108921, WAM R137925, WAM R60157
viduata	WAM R114160, WAM R114164, WAM R116535
walkeri	WAM R117938, WAM R158787, WAM R46727, WAM R61662
wilkinsi	SAMA R55679
xanthura	WAM R108922, WAM R135156, WAM R140439
yuna	WAM R119190, WAM R125967
zietzi	WAM R145729, WAM R145738
zonulata	SAMA R54499, SAMA R55820, SAMA R55821, SAMA R55822
Outgroup	
Ctenotus robustus	SAMA R52344, SAMA R52654, SAMA R53222
Eulamprus kosciuskoi	SAMA R33634
Glaphyromorphus fuscicaudis	SAMA R22383

Appendix 4

Bayesian majority-rule consensus (as in Fig. 3.1) with maximum likelihood numbers of digits for the manus and pes (inferred assuming maximum likelihood rates of digit gain and loss) shown adjacent to internal nodes.

Appendix 5

Estimation of the absolute age of *Lerista*

Although no fossil record exists for *Lerista*, fossil scincids from the Oligo-Miocene to Pliocene limestone deposits of Riversleigh enabled the calibration of a phylogeny for lygosomines from which an absolute divergence time for two species of *Lerista* (*bipes* and *bougainvillii*) could be derived and used to calibrate the ultrametric tree presented in Figure 3.1. The lygosomine phylogeny was inferred from published 12S rRNA, 16S rRNA, and ND4 and adjacent tRNA-His, tRNA-Ser, and tRNA-Leu nucleotide sequences (2356 aligned sites) for 59 species (12S and 16S rRNA sequences for *Corucia zebrata* are from Honda *et al*. [1999]; the remaining sequences are from Reeder [2003] and Skinner [2007]). A majority rule consensus of trees sampled in a Bayesian analysis of the combined sequence data is presented below. Penalised likelihood rate smoothing (Sanderson, 2002) was used to produce an ultrametric tree from this consensus (with mean branch lengths) that was assumed in calculating node ages.

The fossils employed in calibrating the lygosomine phylogeny include a partial mandible and several mandible fragments referred to the *Egernia striolata* and *Egernia frerei* species groups (Hutchinson, 1992) and two partial dentaries described as *Tiliqua pusilla* (Shea and Hutchinson, 1992), all present in deposits of early Middle Miocence age (*c*. 15 million years [Archer *et al*., 1989]). The synchronous occurrence of *Tiliqua pusilla* and species of *Egernia* establishes a minimum age for the node immediately below *Egernia whitii* and *Tiliqua adelaidensis* in the figure below (labelled with an asterisk). Specifying an age of 15 million years for this node implies that *Lerista bipes* and *Lerista bougainvillii* diverged 12.1 million years ago, yielding an age of 13.4 million years for *Lerista*. This value is very similar to an estimate of 13.9 million years obtained assuming a rate of sequence divergence

of 1.3% per million years (Macey *et al*., 1998) (the estimated age of 13.9 million years is based on a maximum uncorrected sequence divergence within *Lerista* of 18.114% for ND4 and the adjacent tRNAs).

References

Archer, M., Godthelp, H., Hand, S. J., Megirian, D., 1989. Fossil mammals of Riversleigh, northwestern Queensland: preliminary overview of biostratigraphy, correlation and environmental change. Aust. Zool. 25, 29-65.

Honda, M., Ota, H., Kobayashi, M., Hikida, T., 1999. Phylogenetic relationships of Australian skinks of the *Mabuya* group (Reptilia: Scincidae) inferred from mitochondrial DNA sequences. Genes Genet. Syst. 74, 135-139.

Hutchinson, M. N., 1992. Origins of the Australian scincid lizards: a preliminary report on the skinks of Riversleigh. Rec. North. Terr. Mus. (The Beagle) 9, 61-70.

Macey, J. R., Schulte II, J. A., Ananjeva, N. B., Larson, A., Rastegar-Pouyani, N., Shammakov, M., Papenfuss, T. J., 1998. Phylogenetic relationships among agamid lizards of the *Laudakia caucasia* species group: testing hypotheses of biogeographic fragmentation and an area cladogram for the Iranian plateau. Mol. Phylogenet. Evol. 10, 118-131.

Reeder, T. W., 2003. A phylogeny of the Australian *Sphenomorphus* group (Scincidae: Squamata) and the phylogenetic placement of the crocodile skinks (*Tribolonotus*): Bayesian approaches to assessing congruence and obtaining confidence in maximum likelihood inferred relationships. Mol. Phylogenet. Evol. 27, 384-397.

Sanderson, M. J., 2002. Estimating absolute rates of molecular evolution and divergence times: a penalized likelihood approach. Mol. Biol. Evol. 19, 101-109.

Shea, G. M., Hutchinson, M. N., 1992. A new species of lizard (*Tiliqua*) from the Miocene of Riversleigh, Queensland. Mem. Queensl. Mus. 32, 303-310.

Skinner, A., 2007. Phylogenetic relationships and rate of early diversification of Australian *Sphenomorphus* group scincids (Scincoidea, Squamata). Biol. J. Linn. Soc. 92, 347-366.

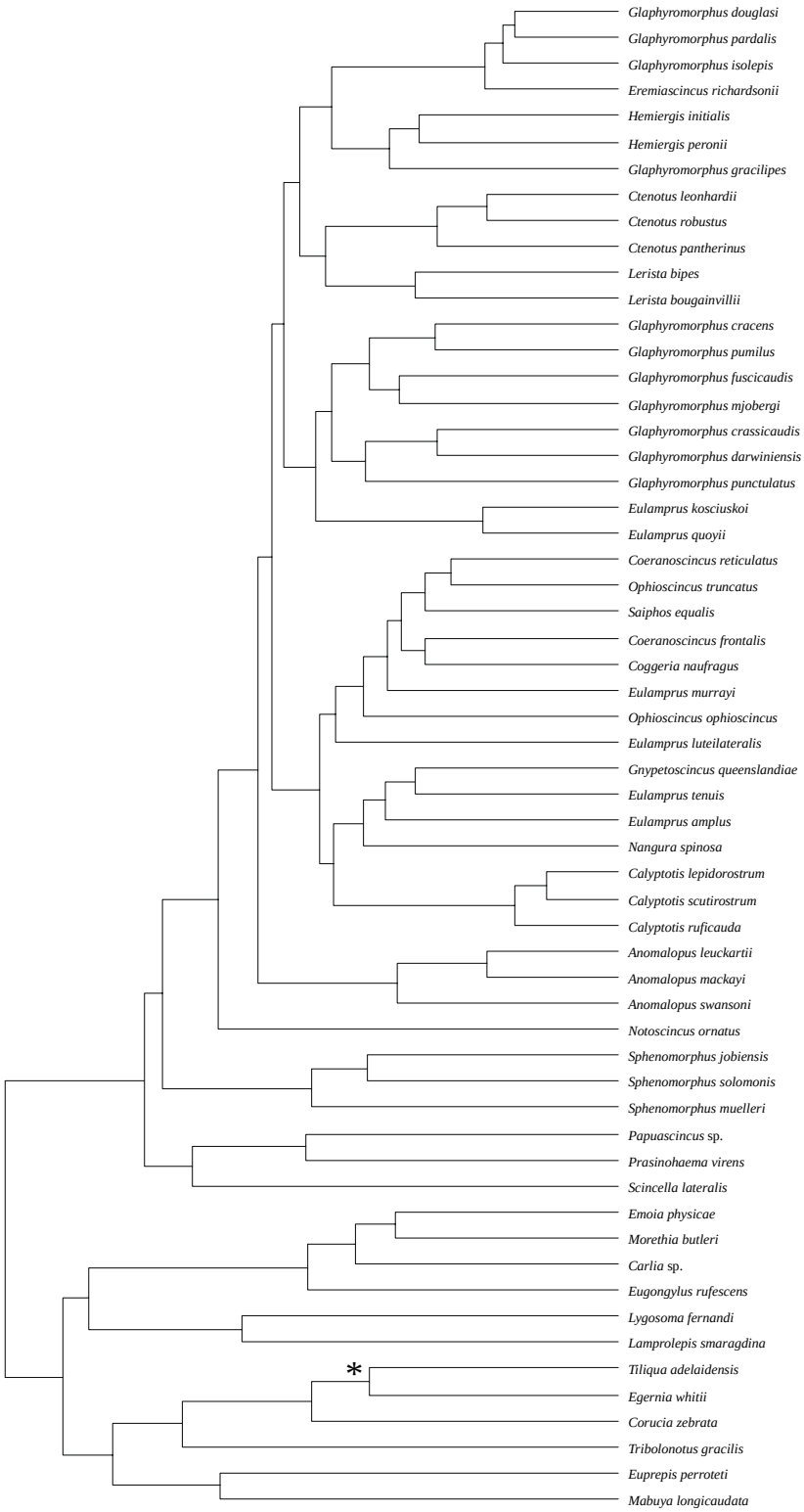

Majority-rule consensus of trees sampled in a Bayesian analysis of lygosomine nucleotide sequences. Mean branch lengths from the Bayesian analysis have been modified via penalised likelihood rate smoothing to produce an ultrametric tree. A minimum age of 15 million years can be ascribed to the node indicated by an asterisk on the basis of fossil evidence.

Appendix 6

Specimens included in the phylogenetic analyses presented in Chapter 4. Abbreviations as for Appendix 1.

Species	Registration number	Locality
aericeps	SAMA R35983	Mokari, SA
allochira	WAM R116698	Vlaming Head, WA
ameles	SAMA R55815	35 km E Mt Surprise, Qld
apoda	WAM R114243	Coulomb Point Nature Reserve, WA
arenicola	SAMA R50095	Talia Beach, S Venus Bay, SA
axillaris	WAM R97212	21 km S Kalbarri, WA
baynesi	SAMA R26475	Near Border Village, SA
bipes	SAMA R53899	63 km N Broome, WA
borealis	SAMA R51132	El Questro Stn, WA
bougainvillii	SAMA R52630	South Para Gorge, SA
carpentariae	NTM R14161	Sir Edward Pellew Island, NT
chordae	SAMA R54482	22 km S Torrens Creek, Qld
christinae	WAM R115299	Ellenbrook, WA
cinerea	SAMA R54520	3 km N Lolworth Homestead, Qld
connivens	SAMA R29286	Carnarvon, WA
desertorum	WAM R92030	67 km SE Blue Robin Hill, WA
distinguenda	SAMA R20805	Eyre Peninsula, SA
dorsalis	SAMA R48848	Arcoona Stn, SA
edwardsae	SAMA R37941	10 km SE Moonabie Homestead, SA
elegans	WAM R90275	75 km SSW Karridale, WA
elongata	SAMA R42424	Dog fence, near Coober Pedy, SA
emmotti	ABTC 31973	Noonbah Stn, Qld
eupoda	WAM R135101	Cue, WA
flammicauda	WAM R151177	Tom Price, WA
fragilis	SAMA R55885	69 km S Alpha, Qld
frosti	SAMA R53312	Trephina Gorge, NT
gascoynensis	WAM R116790	Gascoyne Junction, WA
gerrardii	SAMA R22901	Northampton, WA
greeri[1]	WAM R108753	30 km SE Gordon Downs, WA
greeri[2]	WAM R114424	Derby, WA
griffini	NTM R22909	Spirit Hills, Keep River, NT
haroldi	WAM R116653	Gnaraloo Homestead, WA
humphriesi	WAM R116872	Carrollgouda Well, WA
ingrami	QM J62430	Cape Flattery, Qld
ips	WAM R131074	Kiwirrkurra, WA
kalumburu	WAM R113949	Carson Escarpment, WA
karlschmidti	NTM R23965	Ramingining area, NT
kendricki	WAM R116264	Kalbarri, WA
kennedyensis	WAM R99638	Merlinleigh Homestead, WA
labialis	SAMA R48727	4 km W Mt Lindsay, SA
lineata	WAM R144983	Jandakot Airport, WA
lineopunctulata	SAMA R 29778	Scarborough Beach, Perth, WA
macropisthopus fusciceps	SAMA R29294	One Tree Point, Carnarvon, WA
macropisthopus galea	WAM R115194	Eurardy Stn, WA

macropisthopus macropisthopus	WAM R103912	4 km N Comet Vale, WA
macropisthopus remota	WAM R102636	Little Sandy Desert, WA
microtis intermedia	WAM R129702	Quagi Beach, WA
microtis microtis	WAM R90186	35 km NE Augusta, WA
microtis schwaneri	SAMA R45924	Wedge Island, SA
muelleri	SAMA R54734	Wirraminna Stn, SA
neander	WAM R104362	11 km SSW Capricorn Roadhouse, WA
nichollsi	AMS R123100	Kalli Homestead, WA
onsloviana	WAM R116826	Onslow, WA
orientalis	NTM R21731	Litchfield National Park, NT
petersoni	WAM R99637	Merlinleigh Homestead, WA
picturata	SAMA R22997	32 km S Norseman, WA
planiventralis	WAM R141463	Faure Island, WA
praepedita	SAMA R29419	Scarborough Beach, Perth, WA
punctatovittata	SAMA R42016	Morgan Mail Road, SA
puncticauda	WAM R117169	Queen Victoria Spring, WA
robusta	WAM R108783	Cherrabun Homestead, WA
simillima	WAM R100874	6 km NW Fitzroy Crossing, WA
speciosa	SAMA R58029	Sentinel Hill, SA
stictopleura	WAM R116825	Mt Augustus, WA
stylis	NTM R21679	Kakadu National Park, NT
taeniata	SAMA R32057	55 km S Immarna Siding, SA
terdigitata	SAMA R38568	Middleback Ranges, SA
tridactyla	WAM R112650	Ponier Rock, WA
uniduo	SAMA R29291	One Tree Point, Carnarvon, WA
varia[2]	SAMA R29388	Nanga Dunes, WA
varia[1]	WAM R141494	Faure Island, WA
vermicularis	WAM R108778	6 km WNW Fitzroy Crossing, WA
viduata	WAM R116535	Kundip, WA
walkeri	WAM R96954	29 km WSW Mt French, WA
wilkinsi	SAMA R55679	40 km S Torrens Creek, Qld
xanthura	WAM R135156	Telfer Dome, WA
yuna	WAM R100846	Yuna, WA
zietzi	WAM R114563	53 km WNW Newman, WA
zonulata	SAMA R55820	Einasleigh Road, Qld
Outgroup		
Anomalopus leuckartii	ABTC 3713	5 km E Tooraweenah, NSW
Calyptotis lepidorostrum	ABTC 3903	Mary Cairncross Park, Qld
Coggeria naufragus	ABTC 32113	Fraser Island, Qld
Ctenotus robustus[3]	SAMA R36579	Esdale, NSW
Ctenotus robustus[1]	SAMA R36603	Esdale, NSW
Eulamprus kosciuskoi	ABTC 1169	Gloucester Falls, NSW
Glaphyromorphus fuscicaudis	ABTC 32148	Mt Hartley, Qld

[1]ATP synthetase-β subunit intron only; [2]Mitochondrial genes only; [3]Mitochondrial gene sequences from Reeder (2003).

Appendix 7

Bayesian majority-rule consensus (as in Fig. 3.1) assumed in the analyses presented in Chapter 5. Node numbers correspond with those in the table below.

Ancestral states inferred for the morphometric variables examined in Chapter 5; entries for species are means of observed values. Node numbers correspond with those in the phylogeny above.

Node	Snout-vent length/head length	Forelimb length/head length	Hindlimb length/head length	Head width/head length	Tail length/head length
Root node	6.581	0.914	1.743	0.680	-
4	6.634	0.902	1.739	0.677	-
6	6.763	0.885	1.735	0.674	8.768
8	7.962	0.691	1.612	0.651	8.530
9	8.632	0.332	1.515	0.651	8.152
11	8.873	0.256	1.451	0.650	7.988
14	8.069	0.712	1.606	0.647	8.545
15	7.683	0.833	1.620	0.653	8.154
17	7.462	0.875	1.636	0.663	7.553
19	7.306	0.876	1.641	0.676	6.755
22	8.163	0.712	1.601	0.644	8.589
23	8.111	0.726	1.643	0.641	8.488
24	7.922	0.782	1.728	0.633	8.411
25	7.886	0.777	1.791	0.621	8.419
28	7.744	0.843	1.783	0.631	8.324
30	7.216	1.031	1.962	0.632	8.049
33	8.171	0.707	1.629	0.643	8.459
35	8.315	0.649	1.582	0.645	8.351
36	8.182	0.693	1.630	0.645	-
38	8.138	0.709	1.663	0.645	8.379
40	7.840	0.819	1.773	0.654	-
43	8.509	0.577	1.516	0.647	8.251
44	7.814	0.844	1.651	0.671	8.244
47	8.849	0.449	1.421	0.644	8.146
48	9.955	0.227	0.882	0.602	8.265
51	9.058	0.243	1.509	0.663	7.783
52	9.298	0.105	1.647	0.681	-
54	9.437	0.089	1.746	0.700	7.537
57	9.093	0.184	1.514	0.668	7.660
58	9.172	0.091	1.349	0.681	7.313
60	8.961	0.023	1.569	0.698	-
63	9.142	0.064	1.677	0.671	-
65	9.227	0.054	1.691	0.673	7.540
67	9.335	0.046	1.711	0.675	-
69	9.359	0.044	1.714	0.673	-
72	8.268	0.705	1.572	0.643	8.682
73	6.654	1.220	2.047	0.652	8.104
76	8.401	0.682	1.534	0.643	-
77	7.501	0.954	1.653	0.653	-
80	8.641	0.632	1.477	0.641	8.888
81	-	-	-	-	-
84	9.461	0.454	1.279	0.636	9.191
85	10.054	0.288	0.950	0.629	9.466
86	10.343	0.176	0.768	0.614	9.805
88	10.470	0.101	0.777	0.603	9.536
91	10.374	0.220	0.787	0.633	-

93	-	-	-	-	-
96	9.484	0.455	1.303	0.636	9.190
98	9.505	0.460	1.335	0.637	9.164
99	10.182	0.336	1.322	0.639	9.164
101	10.261	0.182	1.547	0.655	9.053
103	10.259	0.153	1.604	0.658	8.928
105	10.284	0.070	1.742	0.671	8.371
107	10.318	0.043	1.776	0.670	8.312
109	10.360	0.024	1.773	0.673	-
111	10.403	0.013	1.782	0.677	-
113	10.401	0.001	1.912	0.670	7.833
116	9.127	0.546	1.403	0.638	9.115
117	8.748	0.612	1.420	0.635	9.045
118	8.148	0.655	1.318	0.634	8.495
121	8.386	0.733	1.552	0.627	9.377
123	8.234	0.777	1.622	0.612	9.370
126	8.666	0.690	1.593	0.649	9.099
127	8.216	0.842	1.749	0.648	8.989
128	8.010	0.952	1.881	0.647	9.090
131	7.986	0.891	1.787	0.648	8.827
133	7.780	0.916	1.739	0.656	9.185
135	-	-	-	-	-
138	9.010	0.556	1.514	0.667	9.324
139	9.109	0.552	1.512	0.668	9.361
141	9.515	0.541	1.679	0.672	-
144	8.892	0.464	1.458	0.674	9.358
145	8.831	0.451	1.377	0.680	-
148	8.911	0.446	1.516	0.670	-
fuscicaudis	5.637	1.113	1.809	0.735	-
kosciuskoi	4.419	1.134	1.773	0.710	-
robustus	5.082	1.235	2.120	0.683	9.694
aericeps	8.061	1.064	2.039	0.641	8.585
allochira	7.742	0.810	1.519	0.650	-
ameles	11.040	-	-	0.592	12.160
apoda	16.098	-	-	0.562	9.749
arenicola	6.164	1.314	2.109	0.638	7.354
axillaris	8.491	0.413	1.238	0.677	-
baynesi	9.106	0.170	1.188	0.640	7.209
bipes	10.131	-	1.992	0.660	9.018
borealis	7.185	0.764	1.329	0.639	7.049
bougainvillii	7.585	1.022	1.704	0.670	8.581
carpentariae	11.326	-	0.371	0.646	-
chordae	7.968	0.901	1.832	0.559	10.365
christinae	6.663	1.203	2.082	0.606	7.837
cinerea	9.939	-	0.634	0.594	7.356
connivens	9.390	0.032	1.605	0.729	-
desertorum	9.483	0.516	1.607	0.671	9.596
distinguenda	7.089	1.133	2.123	0.646	7.487
dorsalis	7.819	0.996	1.883	0.662	9.190
edwardsae	8.872	0.035	1.575	0.653	8.106
elegans	6.865	1.099	1.964	0.620	8.363
elongata	7.614	0.905	1.640	0.643	8.709
emmotti	-	-	-	-	-
eupoda	8.622	0.461	1.601	0.646	-
flammicauda	6.500	1.143	1.786	0.647	-
fragilis	7.988	0.799	1.647	0.612	8.349
frosti	8.086	0.864	1.597	0.674	10.296
gascoynensis	9.586	0.034	1.773	0.684	-

gerrardii	9.240	0.393	1.553	0.688	9.468
greeri	10.345	-	1.736	0.669	-
griffini	10.645	-	1.571	0.676	10.651
haroldi	7.082	1.024	1.877	0.695	-
humphriesi	10.487	-	0.401	0.561	7.607
ingrami	-	-	-	-	-
ips	10.163	-	1.921	0.710	7.210
kalumburu	9.847	0.340	1.358	0.621	10.017
karlschmidti	-	-	-	-	-
kendricki	8.401	0.025	1.725	0.647	-
kennedyensis	9.385	0.108	1.802	0.679	6.853
labialis	10.293	-	1.944	0.652	8.569
lineata	7.759	0.767	1.876	0.596	9.407
lineopunctulata	9.492	0.097	0.947	0.672	7.165
macropisthopus	9.055	0.465	1.363	0.693	9.282
microtis	6.395	1.364	2.204	0.671	8.587
muelleri	7.958	0.852	1.906	0.632	9.502
neander	9.293	0.537	1.282	0.677	9.394
nichollsi	9.359	0.031	1.679	0.650	7.656
onsloviana	9.745	0.042	1.874	0.757	8.096
orientalis	7.854	0.949	1.775	0.706	10.178
petersoni	9.685	0.027	1.795	0.695	-
picturata	9.168	0.174	1.572	0.659	8.406
planiventralis	7.795	0.755	2.082	0.575	7.483
praepedita	11.691	-	0.261	0.557	9.168
punctatovittata	10.050	0.389	1.144	0.626	10.311
puncticauda	9.663	0.562	1.798	0.675	-
robusta	10.512	-	1.645	0.697	-
simillima	10.557	-	1.857	0.665	8.161
speciosa	7.481	0.941	1.613	0.648	8.600
stictopleura	8.473	0.582	1.784	0.618	7.394
stylis	11.474	-	0.156	0.647	9.539
taeniata	7.313	1.079	2.087	0.629	7.186
terdigitata	7.173	0.887	1.635	0.668	6.271
tridactyla	7.284	0.865	1.650	0.698	6.447
uniduo	9.163	-	1.514	0.645	-
varia	8.488	-	1.580	0.670	7.175
vermicularis	10.245	-	1.993	0.674	7.459
viduata	6.905	1.101	1.816	0.711	7.895
walkeri	7.702	0.646	1.068	0.627	8.652
wilkinsi	11.340	-	0.945	0.584	10.997
xanthura	7.291	1.196	2.151	0.651	9.920
yuna	9.226	0.029	1.668	0.689	7.323
zietzi	7.173	1.166	1.696	0.676	-
zonulata	7.434	0.916	1.640	0.617	8.663

Appendix 8

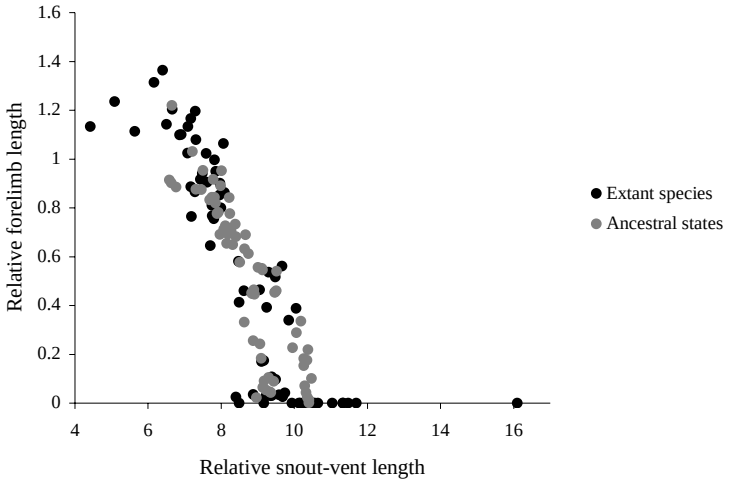

Relationship between relative snout-vent length and relative forelimb length; $r^2 = 0.7030$.

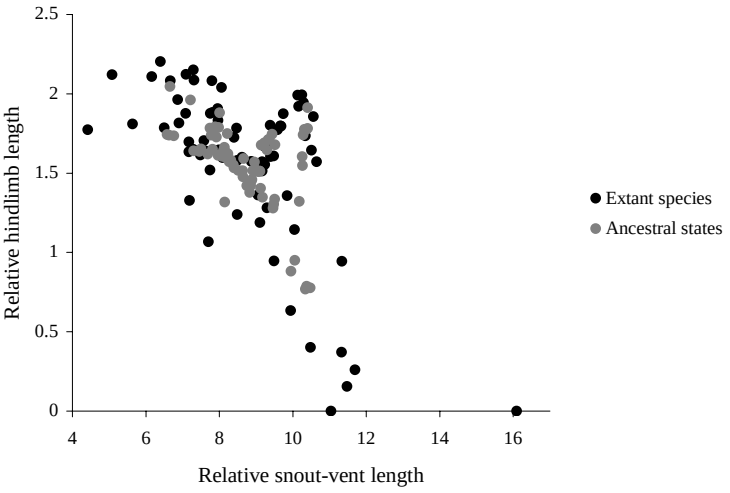

Relationship between relative snout-vent length and relative hindlimb length; $r^2 = 0.3741$.